# NOTE TO USERS

# DESIGNING HYDROGEL MICROSPHERES FROM LIQUID-LIQUID PHASE TRANSITIONS OF AQUEOUS POLYMER SOLUTIONS

By

XIANGCHUN YIN, M.Sc.

A Thesis

Submitted to the School of Graduate Studies

in Partial Fulfillment of the Requirement

For the Degree

Doctor of Philosophy in Chemistry

McMaster University

# MICROSPHERES FROM PHASE TRANSITIONS OF POLYMER SOLUTIONS

DOCTOR OF PHILOSOPHY (2004) McMaster University

(Chemistry) Hamilton, Ontario

TITLE: Designing Hydrogel Microspheres from Liquid-Liquid Phase Transitions of Aqueous Polymer Solutions

AUTHOR: Xiangchun Yin, M.Sc. (Zhongshan University, China)

SUPERVISOR: Professor Harald D. H. Stöver

NUMBER OF PAGES: xxii; 158

## Abstract

This thesis focuses on reactive water-soluble polymers suitable for forming liquid-liquid phase transitions from both polyelectrolyte complexation and thermal induction. Novel hydrogel microspheres are formed by liquid-liquid phase transition followed by crosslinking reactions. Besides studying the properties of polymers and hydrogel microspheres formed, the mechanism of liquid-liquid phase transitions as well as potential applications of these systems in protein separation and encapsulation are discussed.

Chapter 1 describes the background of liquid-liquid phase transitions of aqueous polymer solutions, including polyelectrolyte complexation, thermally induced phase transition and their application in designing hydrogel microspheres.

Chapter 2 describes the thermo-responsive properties of fully MPEG-grafted maleic anhydride copolymers in aqueous solutions. The phase transitions are ascribed to the cooperative effects of intra/intermolecular hydrogen bonding and hydrophobic interactions. Chapter 3 describes the use of analogous partially MPEG-grafted maleic anhydride copolymers as reactive polyanions to form phase-separated liquid polyelectrolyte complexes with polycations, and to prepare hydrogel microspheres by crosslinking the polyelectrolyte complexes with polyamines.

Chapter 4 and Chapter 5 extend this two-stage approach of liquid-liquid phase transition followed by crosslinking reaction to thermally induced phase transitions. Thermally induced liquid-liquid phase transitions of poly(*N,N*-dimethacrylamide-*co*-

glycidyl methacrylate) and poly(*N,N*-dimethylacrylamide-*co*-allyl methacrylate) aqueous solutions are thus used to prepare hydrogel microspheres. The morphology of the resulting microspheres is studied by electron microscopy.

The mechanism of thermally induced liquid-liquid phase transitions of poly(*N,N*-dimethacrylamide) copolymer solutions is discussed in Chapter 6, together with the preparation of well-defined model copolymers using atom transfer radical polymerization.

## Acknowledgements

I would like to thank my supervisor, Professor Harald D. H. Stöver, for his guidance and friendship, which helped me find myself in a different world that I had never experienced before. They will continue to be a motivation for my future work.

I would also like to thank my supervisory committee members, Professor Alex Adronov and Professor Robert Pelton, for their help and their critical comments to keep my research focused on chemistry studies.

Also, in grateful appreciation to Dr. Nicholas Burke, who I respect for his intelligence and generosity as much as anyone I have ever worked with.

Many thanks go to the following, who helped me enormously during the graduate studies:

Members of Dr. Stöver's research group during my stay: Wenhui, Mukkaram, Yan, Erica, Jafar, Lisa, Guodong, and Anna.

Klaus Schultes (ESEM facility); George Timmins, Brian Sayer, and Don Hughes (NMR facility); and Dr. Paul Berti's group for using the UV-vis spectrometer.

Carol Dada and the entire Chemistry Department Staff.

This research is supported by NSERC and 3M Company.

Finally, a big thank you to my understanding and caring wife, Xiyan Chang.

## Table of Contents

## Table of Contents (continued)

**Table of Contents (continued)**

## Table of Contents (continued)

## Table of Contents (continued)

**Table of Contents (continued)**

## Table of Contents (continued)

## List of Figures

## List of Figures (continued)

## List of Figures (continued)

## List of Figures (continued)

## List of Figures (continued)

## List of Tables

## List of Abbreviations

**AIBN** – 2,2'-Azobisisobutyronitrile

**AMA** – Allyl Methacrylate

**ATRP** – Atom Transfer Radical Polymerization

**DMA** – *N, N*-dimethylacrylamide

**ESEM** – Environmental Scanning Electron Microscope

**FT-IR** – Fourier Transform Infrared

**GMA** – Glycidyl Methacrylate

**GPC** – Gel Permeation Chromatography

**LCST** – Lower Critical Solution Temperature

**$Me_6$TREN** – Tris(2-(dimethylamino)ethyl)amine

**MPEG** – Methoxy Poly(ethylene glycol)

**NIPAM** – *N*-isopropylacrylamide

**NMR** – Nuclear Magnetic Resonance

**pDADMAC** – Polydiallyldimethylammonium Chloride

**PEI** – Polyethylenimine

**SMA** – Poly(Styrene-*alt*-Maleic Anhydride)

**TEM** – Transmission Electron Microscope

**THF** – Tetrahydrofuran

# Preface — Thesis Outline

This thesis is prepared in a "sandwich" style. It starts with a general introduction to liquid-liquid phase transitions of aqueous polymer solutions and their application in designing hydrogel microspheres. Each subsequent chapter consists of a published paper or a manuscript. The last chapter summarizes the results and outlines the future work based on the completed research.

## Chapter 1 Introduction to Liquid-Liquid Phase Transitions of Aqueous Polymer Solutions

The aim of Chapter 1 is to review the background of liquid-liquid phase transitions of aqueous polymer solutions. It includes polyelectrolyte complexation, thermally induced phase transition and their application in designing hydrogel microspheres.

## Chapter 2 Thermosensitive and pH-Sensitive Polymers Based on Maleic Anhydride Copolymers

### Research Objective

The aim of Chapter 2 is to study the thermo and pH responsive properties of MPEG-grafted maleic anhydride copolymers. It provides a platform for us to understand

the thermally induced phase transition of aqueous polymer solutions and to develop new materials with thermoresponsive properties.

## Synopsis

Amphiphilic copolymers with thermosensitive and pH-sensitive properties were prepared by grafting methoxy poly(ethylene glycol) (MPEG) of different molecular weights, onto maleic anhydride copolymers. Aqueous solutions of these graft copolymers were thermo-responsive with phase transition temperatures highly sensitive to changes in pH and salinity, and to the presence of hydrophobic and hydrogen bonding additives. The phase transitions were attributed to the cooperative effects of hydrophobic interactions and intra/intermolecular hydrogen-bonding interactions.

## Associated Publication

Yin, X.; Stöver, H. D. H. "Thermosensitive and pH-Sensitive Polymers Based on Maleic Anhydride Copolymers", *Macromolecules* **2002**, *35*, 10178-10181.

# Chapter 3 Hydrogel Microspheres Formed by Complex Coacervation of Partially MPEG-Grafted Poly(Styrene-*alt*-Maleic Anhydride) with pDADMAC and Crosslinking with Polyamines

## Research Objective

The objective of Chapter 3 is to develop novel hydrogel microspheres through complex coacervation of synthetic polyelectrolytes followed by crosslinking reactions. Compared to natural polymers, synthetic polymers have defined structures, and can hence give a clear picture for the phase behaviour of coacervation, and in turn provide guidance in developing new polymer systems showing coacervation.

## Synopsis

Poly(styrene-*alt*-maleic anhydride) partially grafted with methoxy poly(ethylene glycol) (SMA-*g*-MPEG) was prepared by reacting poly(styrene-*alt*-maleic anhydride) with a stoichiometric amount of MPEG lithium alcoholate. Aqueous solutions of the resulting SMA-*g*-MPEG formed complex coacervates with polydiallyldimethylammonium chloride (pDADMAC). These phase-separated liquid polyelectrolyte complexes were subsequently crosslinked by the addition of two different polyamines to prepare crosslinked hydrogel microspheres. Chitosan served as an effective crosslinker at pH 7.0, while polyethylenimine (PEI) was used as crosslinker under basic conditions (pH 10.5). The resulting coacervate microspheres swelled with increasing salinity, which was attributed mainly to the shielding of the electrostatic

association within the polyelectrolyte complexes. The morphology of the coacervate microspheres was investigated by environmental scanning electron microscopy.

**Associated Publication**

Yin, X.; Stöver, H. D. H. "Hydrogel Microspheres Formed by Complex Coacervation of Partially MPEG-Grafted Poly(Styrene-*alt*-Maleic Anhydride) with pDADMAC and Crosslinking with Polyamines", *Macromolecules* **2003**, *36*, 8773-8779.

## Chapter 4 Hydrogel Microspheres by Thermally Induced Coacervation of Poly(*N,N*-Dimethylacrylamide-*co*-Glycidyl Methacrylate) Aqueous Solutions

**Research Objective**

The objective of Chapter 4 is to design hydrogel microspheres through thermally induced liquid-liquid phase transitions of aqueous polymer solutions followed by crosslinking reactions.

**Synopsis**

Aqueous solutions of poly(*N,N*-dimethacrylamide-*co*-glycidyl methacrylate) (DMA-*co*-GMA) were shown to undergo liquid-liquid phase separation upon heating. The phase transition temperatures as measured by the cloud point method decreased with increasing levels of the hydrophobic GMA comonomer. The initially formed coacervate

microdroplets could be crosslinked by addition of polyamines. The morphology of the resulting hydrogel microspheres depended on both coacervation conditions and crosslinking conditions. Specifically, colloidally stable microspheres were formed at temperatures slightly above the phase transition temperatures, while agglomeration took place at higher temperatures. Low molecular weight polyamines were effective internal crosslinkers for the coacervate droplets, while higher molecular weight polyamines resulted in agglomeration. Addition of sodium dodecyl sulfate increased the phase transition temperatures of polymer solutions dramatically, while addition of poly(vinylpyrrolidone) did not affect the phase separation temperatures, and could be used as a steric stabilizer.

**Associated Publication**

Yin, X.; Stöver, H. D. H. "Hydrogel Microspheres by Thermally Induced Coacervation of Poly(*N,N*-Dimethylacrylamide-*co*-Glycidyl Methacrylate) Aqueous Solutions", *Macromolecules* **2003**, *36*, 9817-9822.

# Chapter 5 Temperature-Sensitive Hydrogel Microspheres Formed by Liquid-Liquid Phase Transitions of Aqueous Solutions of Poly(*N*,*N*-Dimethylacrylamide-*co*-Allyl Methacrylate)

## Research Objective

The objective of Chapter 5 is to further extend the preparation of hydrogel microspheres based on thermally induced liquid-liquid phase transitions of aqueous DMA copolymer solutions to form thermoresponsive hydrogel microspheres that might find applications in protein separation and purification.

## Synopsis

Poly(*N*,*N*-dimethylacrylamide-*co*-allyl methacrylate) (DMA-*co*-AMA) copolymers were prepared by copolymerizing DMA with the hydrophobic comonomer AMA. The methacryloyl group of AMA reacted preferentially, resulting in pendant allyl groups along the copolymer chains. Aqueous solutions of these DMA-*co*-AMA copolymers were thermo-responsive, and showed liquid-liquid phase transitions at temperatures depending on the AMA content. Hydrogel microspheres were prepared from these thermally phase-separated liquid microdroplets by free radical crosslinking of the pendant allyl groups. The resulting microspheres retained some of the thermo-responsive properties of their precursor polymers. The morphologies of microspheres as a function of reaction temperature and amount of initiator were described.

**Associated Publication**

Yin, X.; Stöver, H. D. H. "Temperature-Sensitive Hydrogel Microspheres Formed by Liquid-Liquid Phase Transitions of Aqueous Solutions of Poly(*N, N*-Dimethylacrylamide-*co*-Allyl Methacrylate) ", *J. Polym. Sci., Part A: Polym. Chem.* Submitted.

## Chapter 6 Probing The Influence of Polymer Architecture on Liquid-Liquid Phase Transitions of Aqueous Poly(*N,N*-Dimethylacrylamide) Copolymer Solutions

**Research Objective**

The objective of Chapter 6 is to study the mechanism of thermally induced liquid-liquid phase transitions using well-defined copolymers prepared by atom transfer radical polymerization.

**Synopsis**

Thermosensitive poly(*N,N*-dimethylacrylamide-*co*-*N*-phenylacrylamide) (DMA-*co*-PhAm) copolymers were prepared by atom transfer radical polymerization (ATRP) in methanol/water mixtures at room temperature with methyl 2-chloropropionate as the initiator and CuCl/$Me_6$TREN as the catalyst. The resultant DMA-*co*-PhAm copolymers had tailored compositions and controlled molecular weights, and their aqueous solutions underwent liquid-liquid phase separations upon heating. These phase transition

temperatures, measured by the cloud point method, were dependent on polymer concentrations, compositions and molecular weights. The efficiency of the thermally induced liquid-liquid phase transitions, i.e. the yield of phase-separated polymer, increased with increasing solution temperature. This suggested that the thermally induced liquid-liquid phase transition was a continuous equilibrium process, and that the solubility of polymers in the equilibrium phase decreased with increasing temperatures beyond the onset of phase separation. The efficiency of phase separation could be enhanced by adding NaCl to the solution.

**Associated Publication**

Yin, X.; Stöver, H. D. H. "Probing The Influence of Polymer Architecture on Liquid-Liquid Phase Transitions of Aqueous Poly(*N,N*-Dimethylacrylamide) Copolymer Solutions", *Macromolecules.* Submitted.

## Chapter 7 Summary and Future Work for Liquid-Liquid Phase Transitions of Aqueous Polymer Solutions

The aim of Chapter 7 is to summarize the results and outline the future work based on the completed research.

# Chapter 1 Introduction to Liquid-Liquid Phase Transitions of Aqueous Polymer Solutions

## 1.0 Background

Reversible phase transitions of aqueous polymer solutions induced by stimuli such as temperature, pH, electrostatic interaction, and light, remain one of the most intriguing phenomena in polymer science as well as in other fields, including biotechnology, biochemistry, separation science and robotics,[1-5] because they can form a basis for molecular switch systems. The polymers involved are frequently referred to as smart or environmentally responsive materials.[6]

The driving force for phase transitions of aqueous polymer solutions lies in the balance of hydrophilic and hydrophobic components in the polymer-water, polymer-polymer or water-water interactions. At conditions below the critical point, water is a good solvent for the polymer, the polymer-water interactions are stronger than the polymer-polymer interactions, and the polymer is hence soluble. At the θ condition, the polymer-polymer interactions are equal to the polymer-solvent interactions. When the conditions cross over the θ condition, water becomes a poor solvent for the polymer, and phase separation takes place.

The interactions present in aqueous polymer solutions can be divided into four main categories: van der Waals forces, hydrogen bonding interactions, electrostatic interactions and hydrophobic interactions. Due to the presence of water, the van der Waals force is usually negligible as compared to other interactions.

The hydrogen bonding arises from the interaction between electron-deficient hydrogen atoms and atoms of high electron density, such as N, O etc.[7] Water molecules can also form hydrogen bonds, which has significant implications for hydrogen bonding interactions between polymer chains in the solution. Hydrogen bond formation between polymers requires breaking the hydrogen bonds between polymer and water. Hydrogen bond formation is usually associated with negative $\Delta H$ and $\Delta S$, indicating that the hydrogen bonding interaction is generally favoured by lower temperatures.

Favourable electrostatic interactions between polymers are formed by mixing oppositely charged polyelectrolytes. This process is mainly driven by the entropy gain associated with the release of small counterions into the solution.[8]

Hydrophobic interactions denote the tendency of non-polar groups to aggregate in aqueous solutions.[9] The hydration of non-polar groups leads to water molecules forming a highly oriented structure around them, which destabilizes the solution by decreasing the entropy of these water molecules. Hence, the hydrophobic interaction is primarily entropy driven.

Phase transitions induced by these secondary forces are usually reversible. Depending on the water content in the separated polymer phase, the phase transitions of aqueous polymer solutions can be divided into liquid-solid (gel) precipitation and liquid-liquid phase transition. The liquid-liquid phase transition is also called coacervation, which is generally subdivided further into two classes: complex coacervation and simple coacervation. Complex coacervation is induced by polyelectrolyte complexation, while simple coacervation is induced by changing solution conditions such as the temperature

or the solvent compositions.[10] Both coacervation processes have been widely used for protein separation and for preparation of hydrogel microspheres and microcapsules.

In the following section of this introduction, the process of liquid-liquid phase transitions of aqueous polymer solutions will be discussed in detail, with emphasis on polyelectrolyte complexation, thermally induced phase transition, and the application of liquid-liquid phase transitions in designing hydrogel microspheres.

## 1.1 Liquid-Liquid Phase Transitions in Polyelectrolyte Complexation

When two oppositely charged polyelectrolytes are mixed together, the polyelectrolyte complexes formed have three possible states:[11] solid (gel) precipitates, liquid coacervate and soluble complexes. The factors influencing the states of polyelectrolyte complexes are complicated and include both the structures of polycation and polyanion, such as molecular geometry, charge density, and molecular weight; and solution conditions, such as stoichiometry of polycation/polyanion, polyelectrolyte concentration, ionic strength and pH of the solutions.

Early research on polyelectrolyte complexation mainly focussed on the solution properties of soluble complexes using light scattering and viscometry.[11] The soluble complexes are usually formed using very dilute polyelectrolyte solutions or nonstoichiometric polyanion/polycation ratios. During these studies, a two-step mechanism was proposed to describe the formation of polyelectrolyte complexes: small primary complexes were first formed due to electrostatic interactions, and then these

small primary complexes grown into bigger aggregates via polyelectrolyte bridging and hydrophobic interaction.

In recent years, the alternating adsorption of oppositely charged polyelectrolytes on a solid surface, which is mainly based on the precipitation of polyelectrolyte complexation, has evolved as a facile method to fabricate thin polymer films.[12] The electrostatic interaction between polyelectrolytes and oppositely charged solid surfaces causes adsorption of the polyelectrolyte from aqueous solution and leads to charge reversal at the substrate surface, which enables further alternate adsorption of positively and negatively charged polyelectrolytes. By replacing one of the polyelectrolytes with a similarly charged species, the incorporation of proteins, inorganic nanoparticles, or multivalent dyes in the multilayers can be studied.[13,14]

The liquid-liquid coacervation of polyelectrolyte complexation is an intermediate phase transition process between soluble complexation and solid (gel) precipitation. The term coacervation was introduced in 1930 by Bungenberg de Jong for the complexation of gelatin and arabic gum aqueous solutions.[15] It has at times been confused with the concepts of gelation and polyelectrolyte complexation in the literature. According to the original concept used by Bungenberg, the coacervate is a concentrated but fluid polymer solution, whereas the gel is non-flowing on the experimental time scale. A simple test-tube inverting experiment can be used to determine the boundary between coacervate and gel. When a test tube containing two separated phases is tilted, the concentrated polymer phase is defined as a coacervate if the solution deforms by flowing immediately, and as a gel if the solution does not obviously flow.

The liquid-liquid phase transition can be obtained by tailoring polymer-solvent and polymer-polymer interactions, which includes the hydrophilic-hydrophobic balance of polyelectrolytes, the strength of electrostatic interaction, and the salt concentration. The following examples are intended to show the effect of polymer structures on the state of polyelectrolyte complexes. Polyelectrolyte complexes formed from poly(diallydimethylammonium chloride) and poly(sodium styrenesulfonate) are solid precipitates under all circumstances due to the strong electrostatic interaction[13,14] On the other hand, complexation of poly(diallydimethylammonium chloride) and poly(methacrylic acid) over a wide range of conditions (pH, molecular weights of polymers, and salt concentrations) results in liquid-liquid coacervation.[16] The weak acid, which partially dissociates, forms a relatively weak electrostatic interaction and the formation of only partially desolvated coacervates. In addition, soluble polyelectrolyte complexes are obtained when poly(diallydimethylammonium chloride) is complexed with poly(methacrylic acid-*g*-polyethylene glycol).[17] The hydrophilicity of polyelectrolyte complexes increases with the incorporation of polyethylene glycol chains, leading to favourable polymer-water interaction and soluble polyelectrolyte complexes.

Burgess evaluated two main theoretical models proposed to elucidate complex coacervation:[15] the Voorn-Overbeek theory and the Veis-Aranyi "dilute phase aggregate model". According to the Voorn-Overbeek theory, spontaneous coacervation occurs as a result of competition between the electrostatic attractive forces, which tend to accumulate oppositely charged polyelectrolytes, and the entropy effects, which tend to disperse them. Coacervation hence only takes place at the charge neutralization point. The Voorn-

Overbeek theory ignores the importance of releasing salt ions during the polyelectrolyte complexation, which is an entropic driving process. It also neglects polymer-solvent interactions, which play an important role for entrapping water during the phase transition process.

The Veis-Aranyi "dilute phase aggregate model" proposes that complex coacervation occurs in two steps.[18] First, oppositely charged polyelectrolytes aggregate by electrostatic interactions to form primary polyelectrolyte complexes, and then these primary polyelectrolyte complexes further aggregate to form the coacervate phase by polyelectrolyte bridging and hydrophobic interactions. The polymer-solvent interaction determines the phase transition of the primary aggregates, and the coacervation can take place over a wide range depending on the solubility of the primary coacervates. The Veis-Aranyi "dilute phase aggregate model" has been confirmed by the fact that the formation of primary aggregates could be observed using dynamic light scattering and electrophoretic measurements.[19]

Complex coacervation has been studied for use in protein separation because the coacervate phase has a high water content and hence permits protein retention without denaturation. Dubin et al. studied the selectivity of protein separation via polyelectrolyte-protein coacervation by controlling the pH and ionic strength of the solution.[20,21] The flow chart of batchwise protein purification with complex coacervation is shown in Figure 1.1.

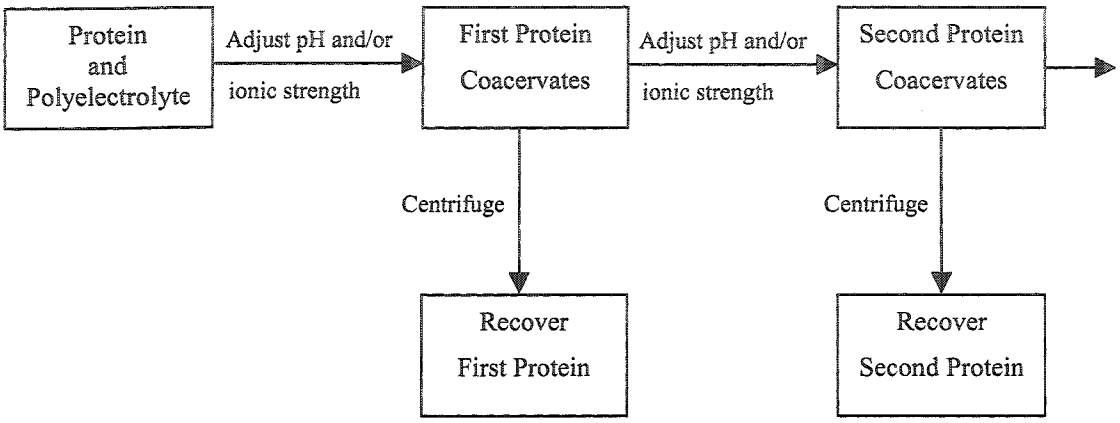


**Figure 1.1** Flow chart for protein purification with complex coacervation.

## 1.2 Thermally Induced Phase Transitions

The most studied thermosensitive polymer is poly(*N*-isopropylacrylamide) (pNIPAM), which undergoes a sharp coil-globule transition at temperatures above its lower critical solution temperature (LCST) of around 32°C, and precipitates from solution in the form of a solid.[3] Most fundamental studies of thermosensitive polymers have been based on pNIPAM solutions. Hence, the thermally induced phase transition of aqueous pNIPAM solutions is discussed first in this section.

### 1.2.1 Thermally Induced Liquid-Solid Phase Transitions of Poly(*N*-isopropylacrylamide) Solutions

The thermoreversible phase transition property of aqueous pNIPAM solution was first reported by Heskins and Guillet.[22] Since then, extensive applications of this behaviour have been described. For example, pNIPAM has been used to prepare macrogels,[23] microgels,[24] and to modify surface properties of substrates.[25]

The phase transition of aqueous pNIPAM solution has been investigated by a variety of techniques, including UV-vis turbidimetry, calorimetry, light scattering, fluorescence, IR, $^{1}$H-NMR, and viscometry, etc. UV-vis turbidimetry is a classical method to detect the macroscopic phase transition, and the phase transition temperature thus obtained is called the cloud point. Calorimetry not only provides the phase transition temperature but also supplies information about the heat of phase transition.[26] In dilute pNIPAM solution, the collapse of individual polymer chains upon heating can be followed using light scattering and valuable information about the coil-to-globule

transition can be obtained.[27] The transition of pNIPAM chains from hydrophilic state to hydrophobic state upon raising temperature can also be observed by tracing the emission of fluorescent labels.[28] IR provides information on the molecular level about the change in the hydration state of groups on the polymer chain upon phase transition.[29]

It is generally accepted that the thermally induced phase transition of aqueous pNIPAM solution is an entropically driven process. However, there has been much debate as to the dominant factors leading to positive entropy change upon phase separations. It has been ascribed to the formation of hydrogen bonds between water molecules and amide group of pNIPAM,[3] the hydrophobic interaction between the polymer side chains,[3,30] the disruption of specific hydrogen-bonded cyclic structures involving alkyl amide units and water,[31] and a combination of hydrogen-bonding and hydrophobic interactions.[28]

Because the amide groups in pNIPAM can form strong hydrogen bonds with water, and the endothermicity of the phase separation is in the range of the enthalpy of hydrogen bonding, it was originally believed that the LCST of aqueous pNIPAM solution is mainly due to strong hydrogen bonding interactions, which lead to the immobilization of water around the polymer chains and hence to an entropy penalty in solution.[3]

Recently, much support has been gathered for the notion that the lower critical solution temperature of aqueous pNIPAM solution is mainly due to the hydrophobic interactions, and that cleaving hydrogen bonds between the polymer and water plays only a minor role in driving the phase separation. For example, results from laser light scattering experiments show that only a small portion of the water molecules bound to

amide groups of pNIPAM is removed during the phase separation,[32-34] and FT-IR spectra show that C-H stretching bands of isopropyl groups in pNIPAM are clearly red-shifted during the phase transition indicating the dehydration of the isopropyl groups.[29]

At low temperatures, strong H-bonding interactions between hydrophilic groups and water lead to good solubility of the polymer, which results in the hydration of hydrophobic groups. The water surrounding the hydrophobic groups is highly organized, leading to a high entropic penalty. Above the phase transition temperature, the unfavourable entropic contribution dominates, leading to a negative free energy change upon de-mixing. The positive enthalpy change detected by calorimetry during phase transition is associated with the breakage of the hydration layers of water molecules surrounding the hydrophobic groups.

Any factor affecting polymer-polymer interactions and polymer-solvent interactions will change the phase transition temperature. For example, Feil et al found that the phase transition temperature of aqueous pNIPAM solution increased with incorporation of hydrophilic monomers, and decreased with incorporation of hydrophobic monomers.[35]

The presence of additives such as inorganic salts can also change the polymer and/or water structures and substantially change the polymer-polymer and polymer-water interactions.

The effect of inorganic salts on the phase transition temperature depends on the nature of ions. There are two possible manifestations: 1) direct interaction between the ions and the polymer chain, and 2) changes of water structure.

Changes in the water structure by the added salts are the most plausible reasons. Frank proposed a model, which was derived from numerical analyses of the entropy of hydration around ionic solutes.[36] According to the model, the ionic solute is surrounded by three concentric regions. The innermost region is composed of water molecules immobilized through ion-dipole interactions. This water layer is more ordered than normal water. The second region is composed of water with less ordered structures than normal water. Water in the third region has order similar to that of normal water. In general, an ion with a large innermost region is referred to as "water-structure maker", while an ion that has a small innermost region and a large second region is referred to as "water-structure breaker". Salts such as NaCl acting as water-structure makers increase the polarity of water as a solvent and subsequently enhance the polymer-polymer hydrophobic interaction, resulting in a lowering of the phase separation temperature. The effect of decreasing the phase transition temperature by adding salts is referred to as "salting-out". On the other hand, salts such as NaI functioning as water-structure breakers weaken water-water hydrogen bonds and enhance polymer-solvent interactions, resulting in an increase in the phase transition temperature. The phenomenon of salt increasing the phase transition temperature is termed "salting-in".

### 1.2.2 Thermally Induced Liquid-Liquid Phase Transitions of Aqueous Polymer Solutions.

The thermally induced liquid-liquid phase transitions are commonly seen in biomacromolecules, such as elastin-like proteins.[37] Elastins are proteins that are

responsible for elastic properties of tissues such as arterial walls, lungs, ligaments, and skins. Below the phase transition temperature, the elastin-like protein chains are in a relatively extended conformation in solution with tightly bound water molecules on the hydrophobic portions. The polymer chain folds into an ordered β-spiral structure upon raising the temperature.[37,38] Similar to pNIPAM solutions, the thermally induced phase transition of elastin-like protein solutions is also mainly ascribed to hydrophobic interactions. The phase transition process is demonstrated in Figure 1.2, where the elastin-like protein is soluble in water at temperatures below the critical point, but aggregation occurs upon heating, and a viscous polymer phase is formed upon settling.

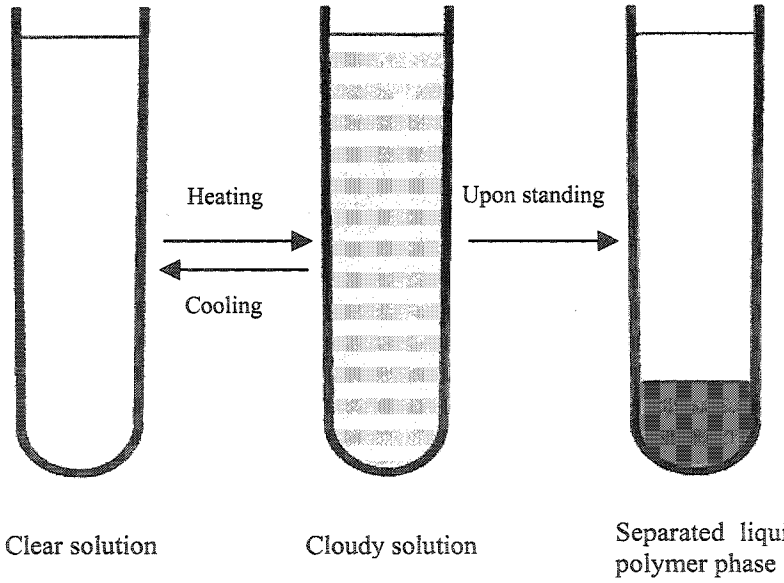


**Figure 1.2** Illustration of thermally induced liquid-liquid phase transition of elastin-like proteins.

The phase transition temperature of elastin-like proteins is sensitive to the peptide structures including the type and sequence of primary amino acids, and the peptide chain length. It is also influenced by solution condition such as pH and small ion concentrations.[38] The thermally induced liquid-liquid phase transition of elastin-like proteins has been investigated by various techniques including calorimetry, light scattering, and NMR.

Elastin-like proteins have been used to prepare thermosensitive hydrogels and to modify the surface properties of substrates.[39] The thermally reversible liquid-liquid phase transition has been used to purify cells.[40]

Compared to biomacromolecules, only a few studies have been reported on the thermally induced liquid-liquid phase transition of aqueous synthetic polymer solutions. One example is the thermally induced phase transition of aqueous poly(*N,N*-dimethylacrylamide) (pDMA) copolymer solutions.

As described above, the phase separation of aqueous pNIPAM solution above its LCST is mainly due to the hydrophobic interaction of isopropyl groups. In contrast to pNIPAM, aqueous solutions of pDMA homopolymers do not have LCST, since the two methyl groups in DMA contribute less hydrophobicity than the isopropyl group of NIPAM. However, aqueous solutions of DMA copolymers containing hydrophobic groups, which can enhance the polymer-polymer interactions, are thermo-responsive. Unlike pNIPAM, many DMA copolymer solutions undergo liquid-liquid phase transitions, with the phase transition temperature depending on the amount of hydrophobic comonomer.[41,42] More recently, Akashi et al. described similar composition-

controlled liquid-liquid phase transitions of linear and crosslinked copolymers comprised of *N*-vinylformamide or *N*-vinylacetamide, and vinyl acetate, as respectively the hydrophilic and hydrophobic components.[43]

The thermally induced liquid-liquid phase transitions of aqueous polymer solutions may potentially replace the traditional aqueous two-phase system (ATPS) of dextran/poly(ethylene glycol) for protein separation and purification, since the "one component" phase transition can avoid additional separation steps.[44]

## 1.3 Hydrogel Microspheres from Liquid-Liquid Phase Transitions of Aqueous Polymer Solutions

Hydrogels are hydrophilic polymer networks, which can absorb and retain large amounts of water. Microspheres are broadly defined as spherically shaped particles in the range of 20 nm to 2,000 μm. Since the swelling-deswelling properties of hydrogels are influenced by their dimensions and interfaces,[45] particular attention has been paid to developing hydrogel microspheres due to their relatively fast response properties. In addition, hydrogel microspheres have gained interest as delivery vehicles for protein-based vaccines since their spherical shapes can enhance the response of immune systems.[46] Hydrogel microspheres have been studied for uses in drug delivery, chemical separation, catalysis and enzyme immobilization.[47,48]

Hydrogel microspheres can be prepared by suspension, emulsion, dispersion and precipitation polymerizations.[49,50] Among them, suspension polymerization, which involves dispersing two immisible phases - organic phase and water phase, is mostly used. However, a major challenge in these polymerization methods is that the use of organic solvents and the unreacted monomer remaining in the final microspheres are undesirable for some applications. Such challenge can be addressed by designing hydrogel microspheres based on preformed water-soluble polymers.

The liquid-liquid phase transition of aqueous polymer solutions (coacervation) is a water-based process, and hence offers interesting new routes to hydrogel microspheres. As illustrated in Figure 1.3, coacervates can be dispersed as microdroplets in the equilibrium phase. These microdroplets are not colloidally stable and tend to coalesce,

but can be crosslinked by covalent bonds or by physical gelation into stable hydrogel microspheres.

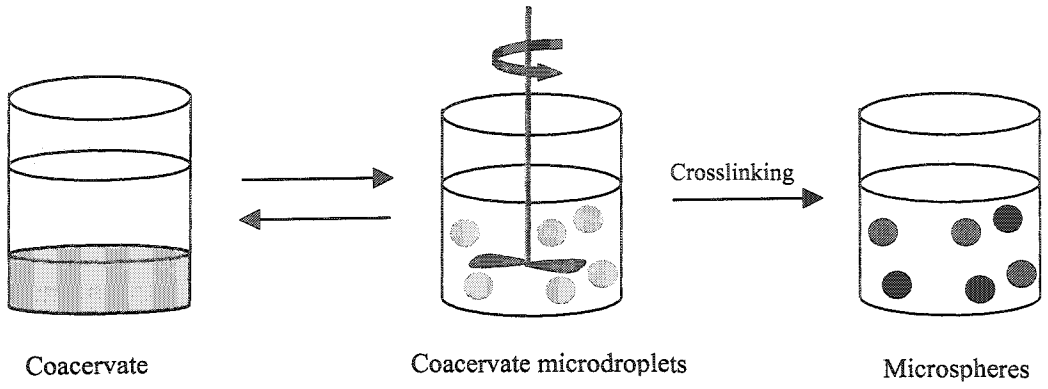


**Figure 1.3** Preparation of microspheres through coacervation.

Until now, natural products, such as gelatin/acacia, chitosan/alginate, were the main materials used for preparing microparticles through coacervation,[51] and only a few studies have been carried out using synthetic polymers.[52] The gelatin/acacia complex coacervates are typically covalently crosslinked with formaldehyde or glutaraldehyde. In contrast, the ionically crosslinked chitosan/alginate systems, where alginate/calcium gel beads are subsequently coated with the positively charged chitosan, are usually not stable under high salt concentrations.

## 1.4 Research Objectives

As discussed above, coacervation is an intriguing method to prepare hydrogel microspheres. However, the coacervation method currently has some limitations: only natural materials are used in this process. Due to the complicated structural characteristics of natural materials, a clear understanding of their coacervation process is missing. There is no clear picture of the relationship between the microstructure of the polymer, and the properties of the final microspheres prepared. No fundamental study has been performed on the effect of polymer properties on the morphology of coacervate microspheres.

At this point, the main objectives of this research are to develop well-defined synthetic polymers for coacervation, both to obtain a clearer picture of the phase behavior of coacervation, and to provide guidance for finding new systems showing coacervation. In addition, we want to make use of the formed novel coacervates to prepare microspheres and to carry out fundamental research on the physicochemical properties of these microspheres. Finally, we also explore the potential applications of the obtained coacervate hydrogel microspheres in protein separation and protein encapsulation.

The systems designed for coacervation include both polyelectrolyte complexation and thermally induced liquid-liquid phase transitions. The obtained coacervates will be chemically crosslinked to form hydrogel microspheres using polymer-bound reactive groups.

**References**


1. Gehrke, S. H. *Adv. Polym. Sci.* **1993**, *110*, 81-144.
2. Osada, Y.; Gong, J. P. *Adv. Mater.* **1998**, *10*, 827-837.
3. Schild, H. G. *Prog. Polym. Sci.* **1992**, *17*, 163-249.
4. Freitas, R. F. S.; Cussler, E. L. *Chem. Eng. Sci.* **1987**, *42*, 97-103.
5. Dong, L. C.; Hoffman, A. S. *J. Controlled Release* **1990**, *13*, 21-31.
6. Galaev, I. *Russ. Chem. Rev.* **1995**, *64*, 471- 489.
7. Prins, L. J.; Reinhoudt, D. N.; Timmerman, P. *Angew. Chem. Int. Ed. Engl.* **2001**, *40*, 2382-2426.
8. Tsuchida, E.; Abe, K. *Adv. Polym. Sci.* **1982**, *45*, 1-124.
9. Lazaridis, T. *Acc. Chem. Res.* **2001**, *34*, 931-937.
10. Menger, F. M.; Peresypkin, A. V.; Caran, K. L.; Apkarian, R. P. *Langmuir* **2000**, *16*, 9113-9116.
11. Philipp, B.; Dautzenberg, H.; Linow, K. J.; Kotz, J.; Dawydoff, W. *Prog. Polym. Sci.* **1989**, *14*, 91-172.
12. Decher, G. *Science* **1997**, *277*, 1232-1237.
13. Ariga, K.; Lvov, Y.; Kunitake, T. *J. Am. Chem. Soc.* **1997**, *119*, 2224-2231.
14. Caruso, F.; Caruso, R. A.; Möhwald, H. *Science* **1998**, *282*, 1111-1114.
15. Burgess, D. J. *J. Colloid Interface Sci.,* 1990, **140**, 227-238.
16. Private communication from Dr. Nicholas Burke: Department of Chemistry, McMaster University.
17. Dautzenberg, H. *Macromol. Chem. Phys.* **2000**, *201*, 1765-1773.

18. Veis, A.; Aranyi, C.J., *J. Phys. Chem.* 1960, **64**,1203-1210.

19. Xia, J.; Dubin, P. L.; Kim, Y.; Muhoberac, B.; Klimkowski, V. J. *J. Phys. Chem.* **1993**, *97*, 4528-4534.

20. Dubin, P.L.; Gao, J.; Mattison, K. *Sep. Purif. Methods* **1994**, *23*, 1-16.

21. Wang, Y.; Gao, J. Y.; Dubin, P.L. *Biotechnol. Prog.* **1996** *12*, 356-362.

22. Huskins, M.; Guillet, J. E. *J. Macromol. Sci. Chem.* **1968**, *A2*, 1441-1455.

23. Shibayama, M.; Tanaka, T. *Adv. Polym. Sci.* **1993**, *109*, 1-62.

24. Pelton R. *Adv. Colloid Interface Sci.* **2000**, *85*, 1-33.

25. Kikuchi, A.; Okano, T. *Prog. Polym. Sci.* **2002**, *27*, 1165-1193.

26. Schild, H. G.; Tirrell, D. A. *J. Phys. Chem.* **1990**, *94*, 4352-4356.

27. Qiu, X.; Kwan, C. M. S.; Wu, Q. *Macromolecules* **1997**, *30*, 6090-6094.

28. Winnik, F. M. *Macromolecules* **1990**, *23*, 233-242.

29. Maeda, Y.; Higuchi, T.; Ikeda, I. *Langmuir* **2000**, *16*, 7503-7509.

30. Fujishige, S.; Kubota, K.; Ando, I. *J. Phys. Chem.* **1989**, *93*, 3311-3313.

31. Platé, N. A.; Lebedeva, T. L.; Valuev, L. *Polym. J.* **1999**, *31*, 21-27.

32. Wang, X.; Qiu, X.; Wu, C. *Macromolecules* **1998**, *31*, 2972-2976.

33. Lele, A. K.; Hirve, M. M.; Badiger, M. V. *Macromolecules* **1997**, *30*,157-159.

34. Tamai, Y.; Tanaka, H.; Nakanishi, K. *Macromolecules* **1996**, *29*,6761-6769.

35. Feil, H.; Bae, Y. H.; Feijen, J. *Macromolecules* **1993**, *26*, 2496-2500.

36. Frank, H. S.; Wen, W. Y. *Discussions Faraday Soc.* 1957, *24*, 133-140.

37. Urry, D. W. *J. Phys. Chem. B* **1997**, *101*, 11007-11028.

38. Urry, D. W. *Angew. Chem. Int. Ed. Engl.* **1993**, *32*, 819-841.

39. Nath, N.; Chilkoti, A. *Adv. Mater.* **2002**, *14*, 1243-1247.

40. Meyer, D. E.; Chilkoti, A. *Nature Biotech.* **1999**, *17*, 1112-1115.

41. Mueller, K. F. *Polymer* **1992**, *33*, 3470-3476.

42. Miyazaki, H.; Kataoka, K. *Polymer* **1996**, *37*, 681-685.

43. Yamamoto, K.; Serizawa, T.; Akashi, M. *Macromol. Chem. Phys.* **2003**, *204*, 1027-1033.

44. Johansson, H. O.; Persson, J.; Tjerneld, F. *Biotechnol. Bioeng.* **1999**, *66*, 247-257.

45. Tanaka, T.; Sato, E.; Hirokawa, Y.; Hirotsu, S.; Peetermans, J. *Phys. Rev. Lett.* **1985**, *55*, 2455-2458.

46. Murthy, N.; Xu, M.; Schuck, S.; Kunisawa, J.; Shastri, N.; Fréchet, J. M. J. *Proc. Natl. Acad. Sci. USA.* **2003**, *100*, 4995-5000.

47. Langer, R. *Acc. Chem. Res.* **2000**, *33*, 94-101.

48. Hoffman, A. S. *Adv.Drug Deliv. Rev.* **2002**, *54*, 3-12.

49. Arshady, R. *Colloid. Polym. Sci.* **1992**, *270*, 1705-1717.

50. Arshady, R. *Polym. Eng. Sci.* **1993**, *33*, 865-875.

51. Prokop, A.; Hunkeler, D.; DiMari, S.; Haralson, M.; Wang, T.G. *Adv. Polym. Sci.* **1998**, *136*, 1-51.

52. Cohen, S.; Baño, M. C.; Visscher, K. B.; Chow, M.; Allcock, H. R.; Langer, R. *J. Am. Chem. Soc.* **1990**, *112*, 7832-7833.

# Chapter 2 Thermosensitive and pH-Sensitive Polymers Based on Maleic Anhydride Copolymers


## Abstract

Amphiphilic copolymers with thermosensitive and pH-sensitive properties were prepared by grafting methoxy poly(ethylene glycol) (MPEG) of different molecular weights, onto alternating copolymers of maleic anhydride with styrene and 4-*tert*-butylstyrene. Aqueous solutions of these graft copolymers were thermo-responsive with phase transition temperatures highly sensitive to changes in pH and salinity, and to the presence of hydrophobic and hydrogen bonding additives. The phase transitions were attributed to the cooperative effects of both hydrophobic interactions and intra/intermolecular hydrogen-bonding interactions. This chapter has been reproduced with permission from *Macromolecules* **2002**, *35*, 10178-10181. Copyright 2002 American Chemical Society.


## 2.0 Introduction

Recently, polymer systems that undergo phase transition in response to external stimuli such as changes in temperature and pH, have attracted much attention.[1] Aqueous solutions of poly(*N*-isopropylacrylamide), pNIPAM, the most well-known temperature responsive polymer, exhibit a lower critical solution temperature (LCST) around 32°C. The reason for this phase transition lies in the balance of hydrophilic and hydrophobic interactions in the system. At low temperature, where water is a good solvent for the

polymer, the polymer-solvent interactions are stronger than the polymer-polymer interactions, and the polymer chains are in the expanded "coil" conformation. The solvent quality decreases with increasing temperature, and the polymer-polymer interactions increase due to the hydrophobic interactions. At the θ-temperature for the system, the polymer-polymer interactions are equal to the polymer-solvent interactions. Above this critical temperature, water becomes a poor solvent for the polymer, and the polymer chains collapse into compact "globules" and phase separation takes place.[2-5] Hence, any factor affecting the polymer-solvent, polymer-polymer or solvent-solvent interactions will influence the phase transition temperature. For example, the LCST of pNIPAM copolymers usually increases with copolymerization of hydrophilic monomers, and decreases with incorporation of hydrophobic monomers.[6] However, Cho *et al.* found that the LCST of poly(*N,N*–dimethylaminoethyl methacrylate) copolymers decreased with increasing hydrophilic comonomer content, which was attributed to the enhanced intra/intermolecular hydrogen bonding.[7,8]

Amphiphilic graft copolymers have been extensively studied due to their wide applications in cosmetics, foods, coatings and pharmaceuticals. They can be used to modify viscosity and interfacial structures, and to encapsulate active compounds in controlled delivery systems. Polymers with hydrophobic backbone and with poly(ethylene oxide) grafts are among the most studied amphiphilic graft copolymers.[9,10] One of the questions in the area of amphiphilic graft copolymers has been the nature of the association of the polymer chains in aqueous solutions, which has been described as monomolecular as well as polymolecular micelles and also higher order aggregates.[11,12]

Particular attention has been given to the solution properties of amphiphilic copolymers based on maleic anhydride copolymers, as these polymers are widely used as surfactants and materials for biomedical applications.[11-18]

In this study, we describe the temperature and pH responsive properties of methoxy poly(ethylene glycol) (MPEG) grafted amphiphilic copolymers based on alternating copolymers of maleic anhydride with styrene and 4-*tert*-butylstyrene, respectively. The phase transitions of the resulting amphiphilic graft copolymers are attributed to the combination of hydrophobic interactions and intra/intermolecular hydrogen bonding. These copolymers have potential applications in developing new types of hydrogel and surfactants with pH/temperature responsive properties.

## 2.1 Experimental Section

### 2.1.1 Materials

Styrene, 4-*tert*-butylstyrene, maleic anhydride, methoxy poly(ethylene glycol) of different molecular weights, and butyllithium (1.60 mol $L^{-1}$ in hexane) were purchased from Aldrich. Maleic anhydride was recrystallized in chloroform before use, others were used as received. 2,2'-Azobis(isobutyronitrile) (AIBN) was obtained from American Polymer Standards Laboratories and recrystallized in methanol. The solvents, methyl ethyl ketone (MEK), tetrahydrofuran (THF), and anhydrous diethyl ether were obtained from Caledon. The THF solvent was dried by refluxing with metallic sodium followed by distillation.

### 2.1.2 Preparation of Maleic Anhydride Copolymer

The styrene-*alt*-maleic anhydride copolymer (SMA) and the 4-*tert*-butylstyrene-*alt*-maleic anhydride copolymer (*t*BSMA) were prepared by solution copolymerization of styrene/maleic anhydride or 4-*t*-butylstyrene/maleic anhydride.

4.91 g of maleic anhydride (0.05 mol) was dissolved in 100 mL of MEK in a 120 mL glass flask. 5.25 g of styrene (99%, 0.05 mol) was added. The solution was deoxygenated with nitrogen, and 0.055 g of AIBN ($3.35 \times 10^{-4}$ mol) was added. The polymerization was carried out at 70°C for 7 h. The polymer product was precipitated in 500 mL of diethyl ether and dried in a vacuum. 6.25 g of product was obtained, in a yield of 62%. *t*-BSMA was prepared by the same procedure.

### 2.1.3 Preparation of Grafted Amphiphilic Copolymers

For a typical procedure, a solution of lithium alcoholate obtained by reacting 1.80g ($5.14 \times 10^{-3}$ mol) of methoxy poly(ethylene glycol) ($M_n$, 350) with 3.2 mL of 1.6 mol $L^{-1}$ butyl lithium ($5.12 \times 10^{-3}$ mol) in 10 mL of THF was added dropwise to a solution of 1.0 g of SMA in 100 mL of THF. The reaction was carried out at room temperature under a nitrogen atmosphere for 24 h. The grafted copolymer was precipitated into 500 mL of diethyl ether and dried in a vacuum oven at 40°C for 48 h. 2.60 g of grafted product was obtained (yield: 95%).

### 2.1.4 Characterization of Polymers

FT-IR spectra were measured on a Bio-RAD FTS-40 spectrometer using KBr pellets. $^1$H NMR spectra were recorded on a Bruker AC 200, using $D_2O$ as the solvent. The molecular weights of the maleic anhydride copolymers were determined using a size

exclusion chromatograph consisting of a Waters 515 HPLC pump, three Ultrastyragel columns and a Waters 2414 refractive index detector, using THF as solvent at a flow rate of 1 mL $min^{-1}$, and narrow disperse polystyrene as calibration standards.

The degree of ionization of the grafted copolymer at different pH's was determined from potentiometric titrations curves. 20 mL of 1 wt % aqueous polymer solutions at pH 2.0 was titrated with 0.1 mol $L^{-1}$ NaOH. The degree of ionization is defined as $\alpha = \alpha_N + [H^+]/C_p$, where $\alpha_N$ is the degree of neutralization, $C_p$ is the equivalent concentration of polymer, and $[H^+]$ is proton concentration and is deducted from the pH of the solution. The titration was performed on an automatic PC-Titrator (Mandel) at room temperature.

### 2.1.5 Measurement of Phase Transition Temperatures

The phase transition temperatures of amphiphilic grafted copolymer solutions were measured using the cloud point method. An automatic PC-Titrator (Mandel) equipped with a temperature probe and with a photometer incorporating a 1 cm path length fiber optics probe (GT-6LD, Mitsubishi) was used to trace the phase transition by monitoring the transmittance of a white light beam. The turbidity of solution was recorded as photoinduced voltage, where a reading of about –220 mV corresponded to a transparent solution below the cloud point, and a reading close to 0 mV for the system above the cloud point. The phase transition temperature was defined as the inflection point of the mV vs temperature curve, as determined by the maximum in the first derivative. The concentration of the polymer solutions was 1.0 wt %, and the heating rate was 1.0°C $min^{-1}$.

## 2.2 Results and Discussion

Wesslén *et al.* have reported the preparation of MPEG grafted maleic anhydride copolymer by the direct reaction of MPEG with succinic anhydride groups.[10-11] In that reaction, the extent of MPEG esterification of anhydride units in SMA was limited to about 20% at most. In the present work, the grafting was carried out by reacting appropriate MPEG lithium alcoholates with maleic anhydride copolymers. Several amphiphilic copolymers with different styrenic units and different MPEG chain lengths were prepared, and their characteristics are summarized in Table 2.1.

**Table 2.1** Composition and phase transition temperatures of graft copolymers.

| Graft copolymer [a] | $M_n$ of MPEG | MPEG/Styrene units [b] (mol/mol) | Phase Transition Temperature [c] (°C) |
|---|---|---|---|
| SMA-*g*-MPEG160 | 164 | 0.96 | not water-soluble [d] |
| SMA-*g*-MPEG350 | 350 | 0.96 | 40.5 |
| SMA-*g*-MPEG550 | 550 | 0.98 | 65.8 |
| SMA-*g*-MPEG750 | 750 | 0.95 | 74.7 |
| *t*BSMA-*g*-MPEG350 | 350 | 0.98 | 33.7 |

[a] $M_n$ (PDI) of SMA, 25,000 (2.1); $M_n$ (PDI) of tBSMA, 63,000 (4.3). [b] Estimated from $^1$H-NMR. [c] Measured at pH 3.0. [d] Below pH 4.5, even at 0°C.

Figure 2.1 shows typical IR spectra of both the starting, and the grafted copolymers. It confirms that the grafting reaction is very efficient. The spectrum of the styrene-*alt*-maleic anhydride (SMA) copolymer displays characteristic anhydride peaks at 1780 and 1850 $cm^{-1}$. In the spectrum of SMA-*g*-MPEG350, the anhydride peaks have disappeared and instead the spectrum shows characteristic absorptions of ester carbonyl at 1730 $cm^{-1}$, ether at 1106 $cm^{-1}$ and carboxylic acid at 1605 $cm^{-1}$.

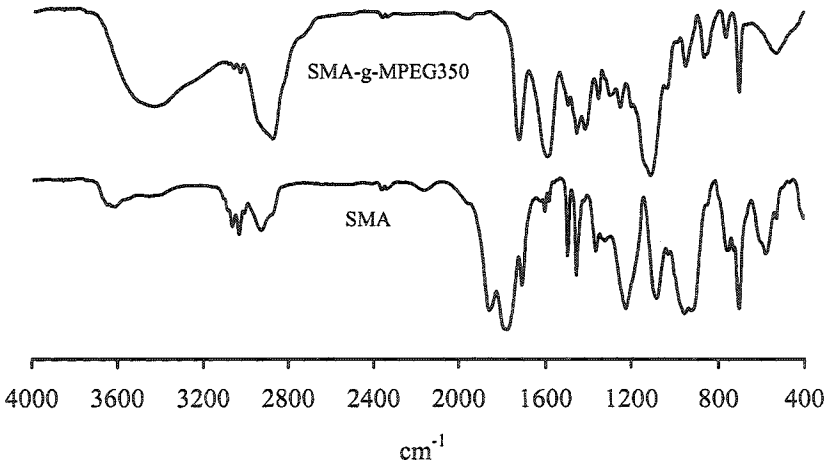


**Figure 2.1** FT-IR spectra of SMA and SMA-*g*-MPEG350.

The amount of MPEG in the grafted copolymer can be estimated from $^{1}H$ NMR spectrum. $^{1}H$-NMR spectra (not shown) of the graft copolymers reveal a broad aromatic resonance at $\delta$ = 7.2 ppm, and peaks at $\delta$ = 3.56 and 3.24 ppm, corresponding to the ethylene oxide and methoxy units of the MPEG grafts, respectively. The extent of MPEG reaction with anhydride units in SMA can be estimated from the ratio of peak areas for

methoxy protons (3H) vs phenyl protons (5 H for SMA and 4 H for *t*BSMA). The results are shown in Table 2.1. For each of the MPEGs studied, nearly complete esterification (≥95%) of anhydride units is achieved. The estimated esterification extent is not 100% only because of the partial hydrolysis of SMA. Thus, there is one MPEG grafted chain almost in each repeating unit of the grafted copolymer.

The phase transition temperatures of the grafted copolymer solutions are dependent on the length of the grafted methoxy poly(ethylene glycol) chains (shown in Table 2.1 and Figure2.2). SMA-*g*-MPEG164 has grafted methoxy poly(ethylene glycol) chains with molecular weight of 164. This graft copolymer is not water-soluble below pH 4.5, even at 0°C. Apparently, the hydrogen bonding between the acid groups and the short PEG side chains reduces the polymer-water interactions, and prevents solvation of the polymer in acidic conditions.

With increasing length of methoxy poly(ethylene glycol), the grafted copolymers become water-soluble even under acidic conditions, and the solutions are thermo-responsive. The phase transition temperatures increase with the increasing MPEG chain length (shown in Figure 2.2), due to the increasing hydrophilicity of the polymer. Therefore, the methoxy poly(ethylene glycol) grafts have two opposing functions: up to the level of carboxylic acid available in the backbone, they form intra/intermolecular hydrogen bonds with the acid groups, while any excess MPEG is free to hydrogen-bond with water. These two functions affect the phase transition temperature in opposite ways, depending on MPEG/acid ratios.

*t*BSMA-*g*-MPEG350 has 4-*tert*-butyl styrene units instead of styrene units. The phase transition temperature of *t*BSMA-*g*-MPEG350 is 33.7°C at acidic conditions, about 7°C lower than that of SMA-*g*-MPEG350 under identical conditions (see Figure 2.2). As expected, the phase transition temperature decreases with increasing hydrophobicity of the polymer.

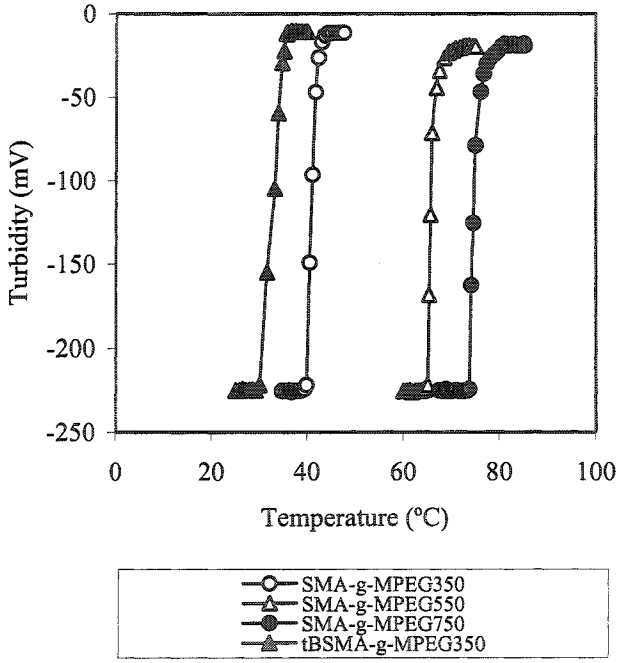


**Figure 2.2** Phase transitions of grafted copolymer solutions at pH 3.0.

Figure 2.3 describes the dependence of the degree of ionization on the pH of the solution for SMA-*g*-MPEG350. The grafted amphiphilic copolymer is completely protonated at pH = 3.0, and fully ionized at pH = 9.0.

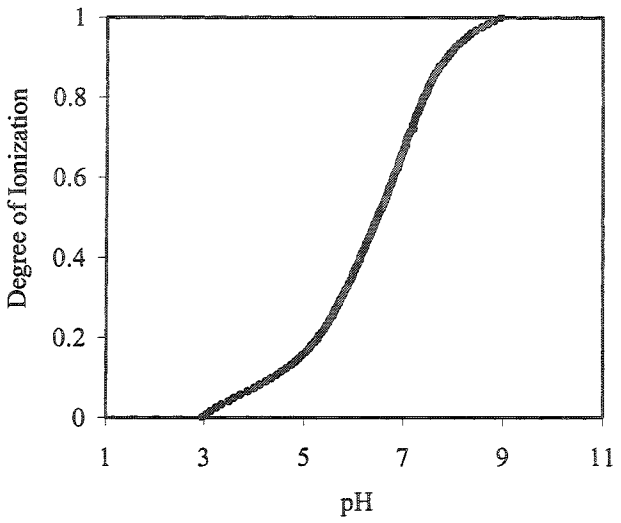


**Figure 2.3** pH dependence of the degree of ionization of SMA-*g*-MPEG350.

The dependence of the phase separation of SMA-*g*-MPEG350 in aqueous solution on pH and degree of ionization is shown in Figures 2.4 and 2.5. At pH 3.0, the phase transition temperature is about 41°C. The phase transition temperature increases rapidly with increasing pH of the solution: it is 51°C at pH 3.5 (about 5% ionization), and 79°C at pH 4.5 (about 10% ionization). The polymer solution does not exhibit a cloud point at pH 5.5 (about 22% ionization). At high pH, the carboxylic acid is ionized, the intra/intermolecular hydrogen bonds are disrupted and the polymer chains expand due to the electrostatic repulsion between charged sites along the polymer chains. As well, polymer-water interactions increase upon ionization. Together, these effects result in a steep increase of phase transition temperature with the degree of ionization. The solid line in Figure 2.5 is a second order polynomial fit to the data points. The dashed line

represents its extrapolation, suggesting a maximum degree of ionization that would still permit an LCST, of about 12%.

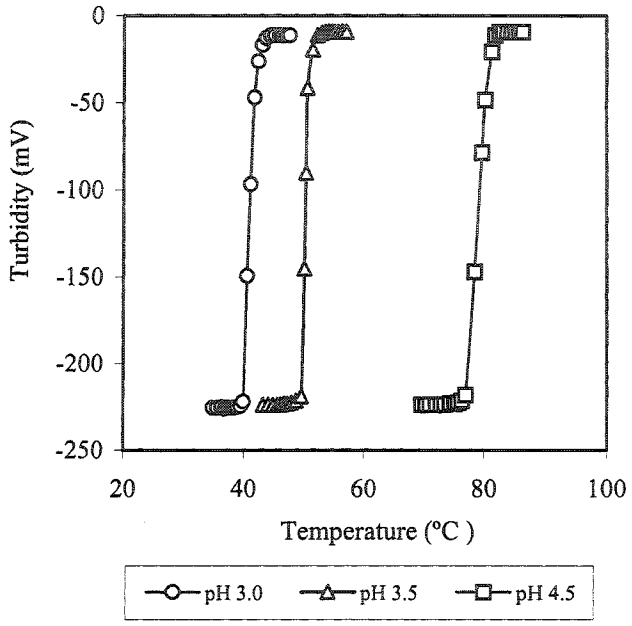


**Figure 2.4** Dependence of the phase transition of SMA-*g*-MPEG350 solution on pH.

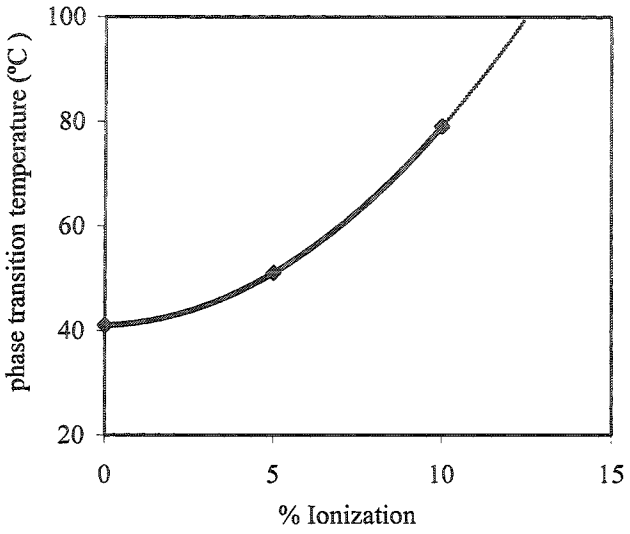


**Figure 2.5** Dependence of the phase transition temperature of SMA-*g*-MPEG350 on the degree of ionization. Trendlines are 2nd order polynomials.

Hoffman compared the phase transition behaviors of analogous random and graft copolymers, poly(acrylic acid-*co*-NIPAM) and poly(acrylic acid-*g*-NIPAM).[19] In the graft copolymer, the hydrophobic and hydrophilic units are separate and behave independently, such that the phase transition temperature of the NIPAM graft was not affected by the amount of hydrophilic acrylic acid units present. The analogous random copolymer, in contrast, showed a strong dependence of the cloud point on the acrylic acid comonomer fraction. For our alternating graft copolymers, the hydrophobic units and hydrophilic units are evenly distributed, such that the effects of incorporating hydrophilic units on the intra/intermolecular interactions should be even larger than that seen in random copolymers. Here, the ionization of the carboxylic groups should not only disrupt

the intra/intermolecular hydrogen bonding, but also suppress the hydrophobic-hydrophobic interaction between styrene units. This will be studied further in future work.

It is well known that the effect of salts on the LCST is mainly due to the changes of the water structure by the added salts.[20] As shown in Figure 2.6, the phase transition temperature decreases with the addition of NaCl. NaCl is considered as a water-structure maker, and hence shows a "salting-out" effect on the phase transition of grafted amphiphilic copolymers. With increasing NaCl concentration, the polymer-polymer interactions increase *via* the hydrophobic interactions of polymers.

Alcohols can disrupt the hydrophobic interactions in the aqueous polymer solutions.[21] With the addition of ethanol, the hydrophobic interactions are suppressed, polymer-water interactions increase, and the phase transition temperature shifts to higher temperature (shown in Figure 2.6).

Urea is known as a hydrogen-bond breaker.[22] With the increase of urea concentration in the solution, the phase transition temperatures of grafted copolymer increase (Figure 2.6). Compared to the pNIPAM system, in which the urea and its concentration have less effect on the phase transition temperature than ethanol, [23-24] the effect of urea on the phase separation temperature of the studied grafted copolymer is obvious. This confirms that the intra/intermolecular hydrogen bonding plays an important role during the phase separation process.

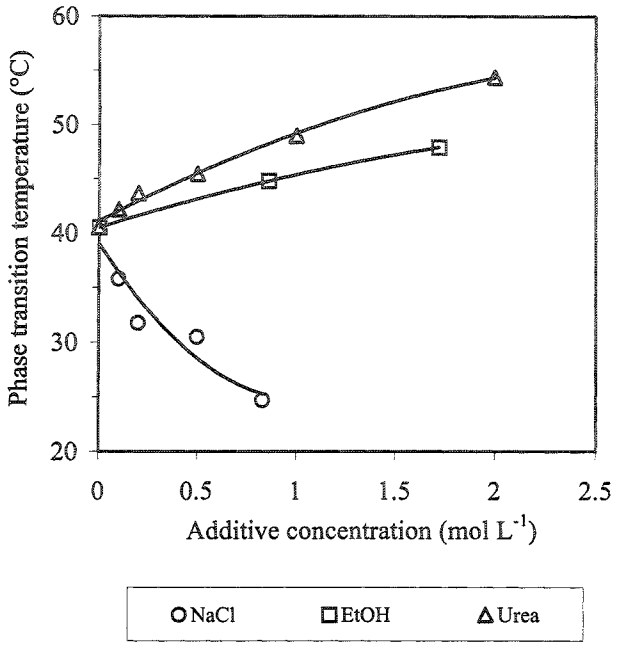


**Figure 2.6** Effects of additives on the phase transition temperature of SMA-g-MPEG350 in aqueous solution at pH 3.0.

Figure 2.7 schematically illustrates the phase transition process of the grafted amphiphilic copolymer solutions. When the temperature is below the phase transition temperature, the polar groups of the polymer strongly interact with water. Although there are hydrophobic and hydrogen-bonding interactions between polymer sections, water is a good solvent for the polymer, and the polymer-water interactions are stronger than the polymer-polymer interactions. With increasing temperature, the polymer chains collapse due to the enhancements of the hydrophobic interactions and the intra/intermolecular hydrogen bonding, that are in turn caused by the increasing entropic penalty for binding to water. Moving above the phase transition temperature, the polymer-polymer

interactions dominate over the polymer-water interactions, and phase transition takes place. The cooperative effects of hydrophobic interactions and the intra/intermolecular hydrogen bonding contribute to the phase transitions of the grafted amphiphilic copolymers. With the protection of hydrophobic interactions, the intra/intermolecular hydrogen bonding enhances the hydrophobic interactions.

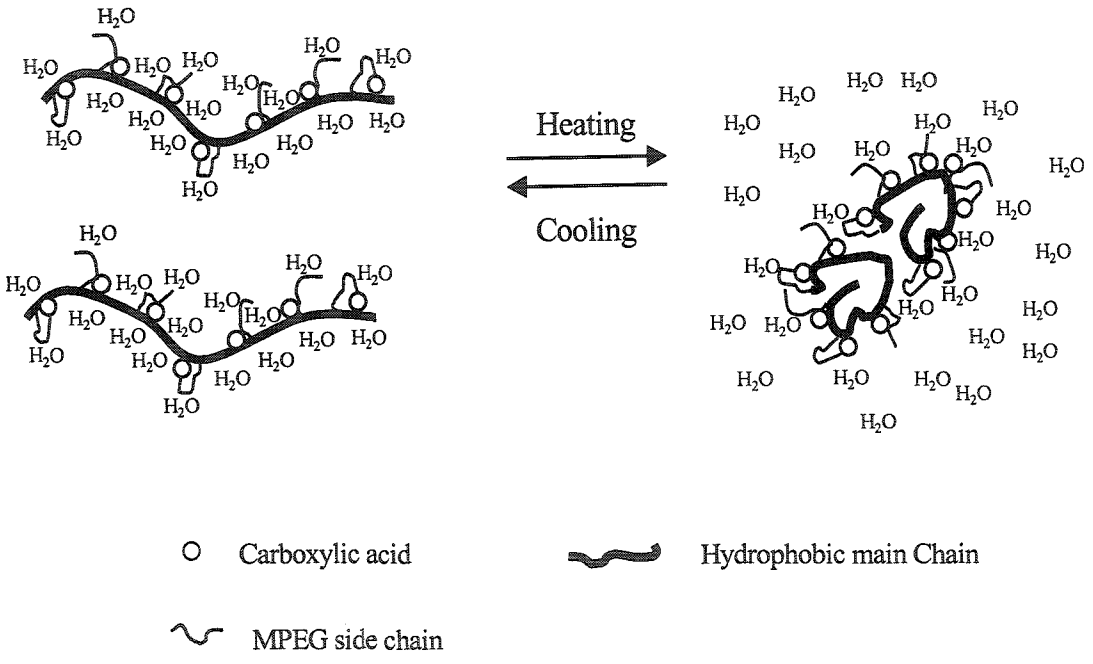


**Figure 2.7** Schematic depiction of the dependence of phase transition on temperature

## 2.3 Conclusion

Five thermosensitive and pH-sensitive amphiphilic graft copolymers based on maleic anhydride copolymers were prepared. Aqueous solutions of these grafted amphiphilic copolymers show phase transition temperatures covering a wide temperature range in response to pH, salinity, additives and polymer compositions. The phase transition temperatures depend on the polymer-polymer and polymer-water interactions, which are related to the cooperative effects of intra/intermolecular hydrogen bonding and hydrophobic interactions of polymers. The grafted amphiphilic copolymers have potential applications as pH/temperature responsive hydrogel and surfactants.

**References**


1. Galaev, I. Y. *Russ. Chem. Rev.* **1995**, *64*, 471- 489.
2. Zhu, P. W.; Napper, D. H. *J. Colloid Interface Sci.* **1994**, *168*, 380-385.
3. Wu, C.; Zhou, S. *Macromolecules* **1995**, *28*, 8381-8387.
4. Zhu, P. W.; Napper, D. H. *Langmuir* **1996**, *12*, 5992-5998.
5. Qiu, X.; Wu, C. *Macromolecules* **1997**, *30*, 7921-7926.
6. Feil, H.; Bae, Y. H.; Feijen, J.; Kim, S. W. *Macromolecules* **1993**, *26*, 2496-2500.
7. Yuk, S. H.; Cho, S. H.; Lee, S. H. *Macromolecules* **1997**, *30*, 6856-6859.
8. Cho, S. H.; Jhon, M. S.; Yuk, S. H. Lee, H. B. *J. Polym Sci., Part B: Polym Phys.* **1997**, *35*, 595-598.
9. Wesslén, B.; Wesslén, K.B. *J. Polym. Sci., Part A: Polym Chem.* **1989**, *27*, 3915-3926.
10. Bo, G.; Wesslén, B.; Wesslén, K.B. *J. Polym. Sci., Part A: Polym Chem.* **1992**, *30*, 1799-1808.
11. Wittgren, B.; Wahlund, K. G.; Dérand, H.; Wesslén, B. *Macromolecules* **1996**, *29*, 268-276.
12. Eckert, A. R.; Webber S. E. *Macromolecules* **1996**, *29*, 560-567.
13. Dubin, P. L.; Strauss, U. P. *J. Phys. Chem.* **1973**, *77*, 427-1431.
14. Chitanu, G.C.; Rinaudo, M.; Desbrières, J.; Milas, M; Carpov A. *Langmuir* **1999**, *15*, 4150-4156.
15. Garnier, G.; Smrckova, M. D.; Vyhnalkova, R.; Ven, T. G. M.; Revol, J. F. *Langmuir* **2000**, *16*, 3757-3763.

16. Maiti, S.; Jayachandran, K. N.; Chatteerji, P.R. *Polymer* **2001**, *42*, 7801-7808.

17. Braun, D.; Sauerwein, R.; Hellmann, G. P. *Macromol. Symp.* **2001**, *163*, 59-66.

18. Claracq, J.; Santos S.; Duhamel, J.; Dumousseaux, C.; Corpart, J. M. *Langmuir* **2002** *18*, 3829-3835.

19. Chen, G.; Hoffman, A. S. *Nature (London)* **1995**, *373*, 49-52.

20. Maeda, Y.; Higuchi, T.; Ikeda, I. *Langmuir* **2000**, *16*, 7503-7509.

21. Klier, J.; Scranton, A.B.; Peppas, N.A. *Macromolecules* **1990**, *23*, 4944-4949.

22. Ilmain, F.; Tanaka T.; Kokufuta, E. *Nature (London)* **1991**, *349*, 400-401.

23. Otake, K.; Inomata, H.; Konno, M.; Saito, S. *Macromolecules* **1990**, *23*, 283-289.

24. Fang, Y.; Qiang, J.; Hu, D.; Wang, M. Cui, Y. *Colloid Polym. Sci.* **2001**, *279*, 14-21.

# Chapter 3 Hydrogel Microspheres Formed by Complex Coacervation of Partially MPEG-Grafted Poly(Styrene-*alt*-Maleic Anhydride) with pDADMAC and Crosslinking with Polyamines


## Abstract

Poly(styrene-*alt*-maleic anhydride) partially grafted with methoxy poly(ethylene glycol) (SMA-*g*-MPEG) was prepared by reacting poly(styrene-*alt*-maleic anhydride) with a stoichiometric amount of MPEG lithium alcoholate. Aqueous solutions of the resulting SMA-*g*-MPEG formed complex coacervates with polydiallyldimethylammonium chloride (pDADMAC). These phase-separated liquid polyelectrolyte complexes were subsequently crosslinked by the addition of two different polyamines to prepare crosslinked hydrogel microspheres. Chitosan served as an effective crosslinker at pH 7.0, while polyethylenimine (PEI) was used as crosslinker under basic conditions (pH 10.5). The resulting coacervate microspheres swelled with increasing salinity, which was attributed mainly to the shielding of the electrostatic association within the polyelectrolyte complex. The morphology of the coacervate microspheres was investigated by environmental scanning electron microscopy. This chapter has been reproduced with permission from *Macromolecules* **2003**, *36*, 8773-8779. Copyright 2003 American Chemical Society.

## 3.0 Introduction

Hydrogel microspheres are being studied for uses in drug delivery, protein separation, and enzyme immobilization.[1,2] They can be prepared by precipitation polymerization or emulsion polymerization,[3-5] though the use of organic solvents in these processes, and the unreacted monomer remaining in the final microspheres, are undesirable for some applications.

In contrast, coacervation is a water-based phase separation process of preformed polymers, and hence offers interesting new routes to hydrogel microparticles.[6,7] Coacervation involves the phase separation of an aqueous polymer solution into two immisible liquid phases, a polymer-rich phase (coacervate phase) and a polymer-lean phase (equilibrium phase).[8,9] Coacervation can be induced either by polyelectrolyte complexation (complex coacervation), or by decreasing the polymer-solvent interactions such as by changing the solvent composition or the temperature (simple coacervation).[10] Both coacervation processes have been widely used for protein separations and for encapsulations.[6,7,11,12]

Coacervates can be dispersed as microdroplets in the equilibrium phase. These microdroplets are not colloidally stable and tend to coalesce, but can be crosslinked by covalent bonds or by physical gelation.

Until now, natural products, such as gelatin/acacia, chitosan/alginate, were the main materials used for preparing microparticles through coacervation,[13-15] and only a few studies have been carried out using synthetic polymers.[16-18] The gelatin/acacia complex coacervates are typically covalently crosslinked with formaldehyde or

glutaraldehyde. In contrast, the ionically crosslinked chitosan/alginate systems, where alginate/calcium gel beads are subsequently coated with the positively charged chitosan, are usually not stable under high salt concentrations.

We describe here a complex coacervate system that combines electrostatic coacervation and covalent crosslinking, based on anhydride-functional polyelectrolytes. Maleic anhydride copolymers have been widely studied as surfactants and materials for biomedical applications such as immobilizing proteins.[19-20] In previous studies, we described the use of oil-soluble styrene-maleic anhydride copolymers in interfacial microencapsulation reactions,[21-22] and investigated the temperature sensitivity and pH-sensitivity of the poly(ethylene glycol) grafted poly(styrene-*alt*-maleic anhydride) in aqueous solutions.[23]

In this study, we use the methoxy poly(ethylene glycol) partially grafted poly(styrene-*alt*-maleic anhydride), as a reactive polyanion to form complex coacervates with polydiallyldimethylammonium chloride. The resulting coacervate microdroplets are subsequently crosslinked using both a synthetic and a natural polyamine to form crosslinked hydrogel microspheres. The swelling of the resulting crosslinked coacervate microspheres at different salt levels has been studied.

## 3.1 Experimental Section

### 3.1.1 Materials

Styrene, maleic anhydride, methoxy poly(ethylene glycol) (MPEG) ($M_n$, 350), butyl lithium (1.60 mol $L^{-1}$ in hexane), polydiallyldimethylammonium chloride

(pDADMAC) (40 wt % aqueous solution), chitosan and polyethylenimine (PEI) (branched, $M_n$, 1800) were purchased from Aldrich. Maleic anhydride was recrystallized in chloroform before use, others were used as received. 2,2'-Azobis(isobutyronitrile) (AIBN) was obtained from American Polymer Standards Laboratories and recrystallized in methanol. Methyl ethyl ketone (MEK), tetrahydrofuran (THF), and anhydrous diethyl ether were obtained from Caledon. THF was dried by refluxing with metallic sodium followed by distillation. The number average molecular weight and the polydispersity index of chitosan were $1.5 \times 10^4$ and 2.5 respectively, measured by aqueous gel permeation chromatography as described below.

### 3.1.2 Preparation of Methoxy Poly(ethylene glycol) Partially Grafted Poly(Styrene-*alt*-Maleic Anhydride) (SMA-*g*-MPEG)

Poly(styrene-*alt*-maleic anhydride) (SMA) was prepared by free radical polymerization as previously reported.[23] The number average molecular weight and polydispersity index of SMA were $1.37 \times 10^4$ and 2.2 respectively. In a typical procedure, a solution of MPEG lithium alcoholate, obtained by reacting 2.46 g ($7.0 \times 10^{-3}$ mol) methoxy poly(ethylene glycol) with 4.4 mL of 1.6 mol $L^{-1}$ butyl lithium ($7.0 \times 10^{-3}$ mol) in 10 mL of THF, was added to a solution of 2.0 g of SMA in 100 mL of THF. The reaction was carried out at room temperature under a nitrogen atmosphere for 24 h. The grafted copolymer was precipitated into 500 mL of diethyl ether, the product was separated by centrifugation and dried under vacuum at 40°C overnight. 4.0 g of product was obtained, corresponding to a yield of 90%.

Several SMA-*g*-MPEG copolymers with different MPEG contents were prepared by adjusting the molar ratio of MPEG alcoholate to succinic anhydride groups in the SMA. Their compositions are summarized in Table 3.1.

SMA-*g*-MPEG copolymers were characterized by FT-IR and $^1$H NMR. FT-IR spectra were measured on a Bio-RAD FTS-40 spectrometer using KBr pellets. $^1$H NMR spectra were recorded on a Bruker AC 200, using DMF-$d_7$ as the solvent.

### 3.1.3 Chitosan

Chitosan of low molecular weight was prepared by a free radical degradation method following a literature procedure:[24] 5.0 g of chitosan was dissolved in 250 g of 2 wt % acetic acid solution. The solution was heated to 80°C and 4.17g of 30 wt % hydrogen peroxide (BDH) was added. The degradation was carried out under a nitrogen atmosphere for 5 h. The reaction mixture was neutralized to pH 7.0 with 1 N NaOH, centrifuged and filtered to obtain a clear solution. The final product was obtained by dialysis against distilled water for one week, using a Spectrum membrane with a molecular weight cut-off of 1000. The solution was freeze-dried to give 2.0 g of degraded chitosan (yield, 40%).

The molecular weight of the degraded chitosan was estimated by a gel permeation chromatograph, consisting of a Waters 515 HPLC pump, three Ultrahydrogel columns (0-3k, 0-5k, 2k-300k Dalton) and a Waters 2414 refractive index detector, with 0.5 mol $L^{-1}$ sodium acetate/0.5 mol $L^{-1}$ acetic acid solution as eluent at a flow rate of 0.8 mL $min^{-1}$, and narrow disperse poly(ethylene glycol) as calibration standards. The $M_n$ and PDI of degraded chitosan were $3.9 \times 10^3$ and 1.2 respectively.

The degree of ionization of chitosan at different pH values was determined by potentiometric titration. 20 mL of 2.0 wt % chitosan solution containing 0.05 mol $L^{-1}$ NaCl, acidified to pH 2.0 with 1.0 N hydrochloric acid, was titrated with 0.1 N NaOH. The degree of ionization is defined as $\alpha = \alpha_N + [H^+]/C_p$, where $\alpha_N$ is the degree of neutralization, $C_p$ is the equivalent concentration of chitosan, $[H^+]$ is the proton concentration and is deduced from the pH of the solution. Titrations were performed on an automatic PC-Titrator (Mandel) at room temperature.

### 3.1.4 Polydiallyldimethylammonium Chloride (pDADMAC)

The molecular weight of commercial pDADMAC was determined by viscometry in 1.0 mol $L^{-1}$ NaCl solution at 30°C using an Ubbelohde viscometer. All stock solutions were filtered through a 0.45 μm PTFE membrane filter prior to measurements. The molecular weight of PDADMAC was calculated to be $2.0 \times 10^4$, using the Mark-Houwink equation $[\eta] = k\,[M]^{\alpha}$, where $k$ is $4.7 \times 10^{-3}$, and $\alpha$ is 0.83.[25]

### 3.1.5 Coacervation

Coacervations were conducted in 0.05 mol $L^{-1}$ NaCl solution. The pH value of the solution was adjusted to the desired values by adding 1 N NaOH or HCl.

In a typical procedure, a solution of 2.0 wt % pDADMAC was prepared in 0.05 M NaCl solution at pH 7.0. 2.8g of this solution was added to 50 g of 0.25 wt % SMA-*g*-MPEG-70% in 0.05 M NaCl solution at pH 7.0 under 600 RPM stirring. The mixture was maintained at pH 7.0 by adding 0.1 N NaOH during this coacervation process. After the coacervate mixture was stirred for 5 min, it was centrifuged at 3000 RPM for 10 min. The

coacervate was separated by decanting the transparent supernatant phase and dried to constant weight at 65°C. 0.070g of dry coacervate was obtained (yield, 38 %).

### 3.1.6 Preparation of Hydrogel Microspheres

Microspheres were prepared using the same coacervation process as described above. After coacervation and while still stirring, 4.2g of 2.0 wt % chitosan in 0.05 mol $L^{-1}$ NaCl solution at pH 7.0 was added to crosslink the coacervate droplets into microspheres. The crosslinking reaction was continued for 3 h. Microspheres were isolated by centrifugation at 500 RPM for 10 min, and were washed with 0.05 M NaCl solution to remove unreacted materials. They are stored in 0.05 M NaCl solution for further studies.

### 3.1.7 Characterization of Hydrogel Microspheres

Optical images of particles were recorded using a scale-calibrated Olympus BH-2 microscope equipped with a Kodak DC 120 Zoom digital camera. The mean diameter of the microspheres was estimated by analyzing about 200 particles using UTHSCSA Image Tool software.

Morphologies of microspheres were examined using a Phillips ElectroScan 2020 environmental scanning electron microscope (ESEM). For the sample preparation, the microspheres were dehydrated using a series of water/acetone mixtures with increasing acetone contents. ESEM samples were prepared by applying a drop of microparticles in acetone suspension to a glass-covered ESEM stub, drying under vacuum and sputter-coating with about 5 nm thick layer of gold.

### 3.1.8 Equilibrium Swelling Studies

The microspheres were incubated in 0.05, 0.1, 0.2, 0.5 and 1.0 M NaCl solutions at pH 7.0 in order to study their swelling response to changes of NaCl concentrations. The microsphere diameters were monitored by optical microscopy, by taking samples at different times and measuring the size of the swollen particles until they reached equilibrium. The average diameters of the swollen particles were estimated using UTHASCA Image Tool software, as described above.

## 3.2 Results and Discussion

### 3.2.1 Synthesis and Characterization of SMA-*g*-MPEG

Several partially methoxy poly(ethylene glycol) grafted poly(styrene-*alt*-maleic anhydride) copolymer (SMA-*g*-MPEG) were prepared by reacting stoichiometric amounts of MPEG lithium alcoholate with poly(styrene-*alt*-maleic anhydride) (SMA). This grafting reaction is quantitative. Figure 3.1 shows FT-IR spectra of both SMA, and SMA-g-MPEG. The spectrum of SMA displays characteristic anhydride peaks at 1780 and 1850 $cm^{-1}$. In spectra of partially grafted copolymers (SMA-*g*-MPEG-55%, 70%, 87%), the anhydride absorptions are still present but much weaker. In addition, these spectra show absorptions characteristic for ester carbonyl at 1730 $cm^{-1}$, ether at 1106 $cm^{-1}$ and carboxylic acid at 1605 $cm^{-1}$. In the spectrum of fully grafted copolymer (SMA-*g*-MPEG-97%), the anhydride peaks have disappeared.

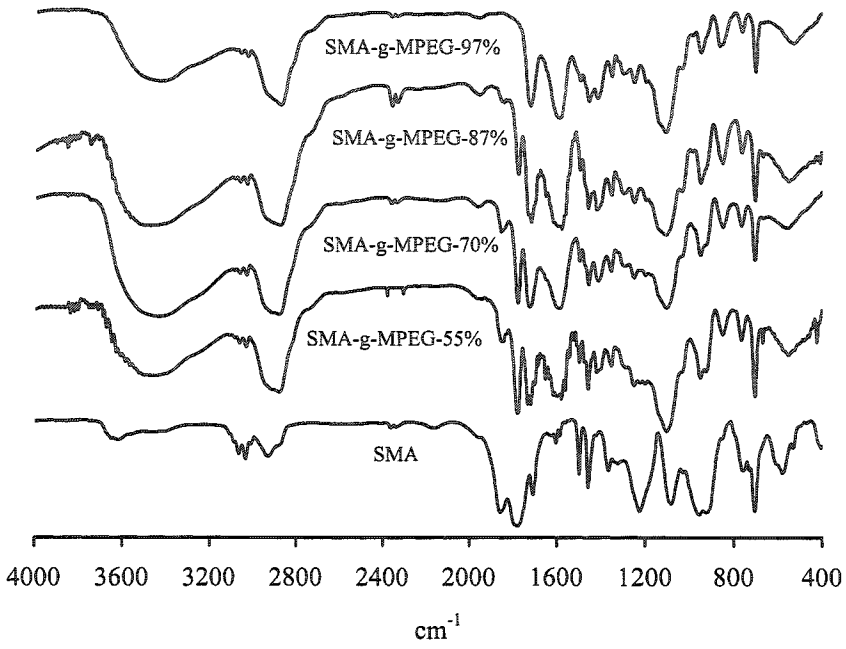


**Figure 3.1** IR spectra of SMA and SMA-*g*-MPEG copolymers.

The amount of MPEG in SMA-*g*-MPEG can be estimated by $^1$H NMR spectroscopy (Figure 3.2). The $^1$H NMR spectrum of SMA-*g*-MPEG reveals a broad aromatic resonance at $\delta = 7.2$ ppm, and peaks at $\delta = 3.56$ and 3.24 ppm, corresponding to the ethylene oxide and methoxy units of the MPEG grafts, respectively. The extent of MPEG reaction with anhydride units in SMA is estimated from the ratio of peak areas for methoxy protons (3H) vs. phenyl protons (5H). The results are shown in Table 3.1.

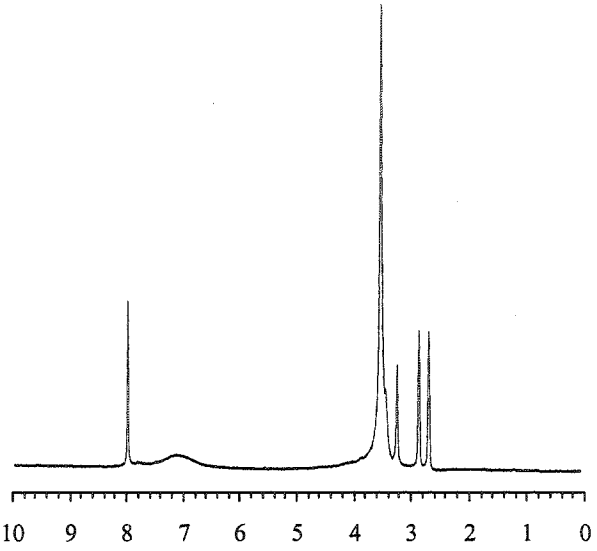


**Figure 3.2** NMR spectrum of SMA-*g*-MPEG-70% copolymer dissolved in DMF-$d_7$. The residual DMF solvent peaks are at around 2.7, 2.9 and 8.0 ppm.

**Table 3.1** The composition of SMA-*g*-MPEG copolymers as estimated from $^1$H NMR.

| Sample | MPEG/styrene unit (mol/mol) |
|---|---|
| SMA-*g*-MPEG-55% | 0.55 |
| SMA-*g*-MPEG-70% | 0.70 |
| SMA-*g*-MPEG-87% | 0.87 |
| SMA-*g*-MPEG-97% | 0.97 |

The primary objective for this research is to use SMA-*g*-MPEG copolymers as reactive polyanions to prepare coacervate microspheres. The SMA-*g*-MPEG backbone contains both carboxylic acid and anhydride groups. The carboxylic acid forms a complex with polycations to induce the coacervation, and the anhydride group can be used to subsequently crosslink the dispersed complex coacervate droplets to prepare microspheres. SMA-*g*-MPEG-55% is only water-soluble under basic conditions, while the content of anhydride groups in SMA-*g*-MPEG-87% is too low for crosslinking reactions. Hence, SMA-g-MPEG-70% is chosen for further studies to prepare coacervate hydrogel microspheres.

### 3.2.2 Complexation of SMA-*g*-MPEG-70% with Reactive Polyamines

In initial experiments, we attempted to crosslink the complex coacervate in-*situ*, by complexing the SMA-MPEG-70% with reactive polycations based on the partially protonated polyamines, chitosan and PEI. These complex coacervations were carried out at pH 7.0 to minimize the hydrolysis of the anhydride groups in SMA-*g*-MPEG-70%. At pH 7.0, the degree of ionization of PEI is about 50%,[26] while that of chitosan is approximately 30% (Figure 3.3).

We found that the addition of a dilute PEI solution at pH 7.0 to the SMA-*g*-MPEG-70% solution resulted not in coacervation, but rather in bulk precipitation of the crosslinked polymer. Similarly, addition of chitosan produced a mixture of some spherical coacervate particles besides much gel precipitate (Figure 3.4).

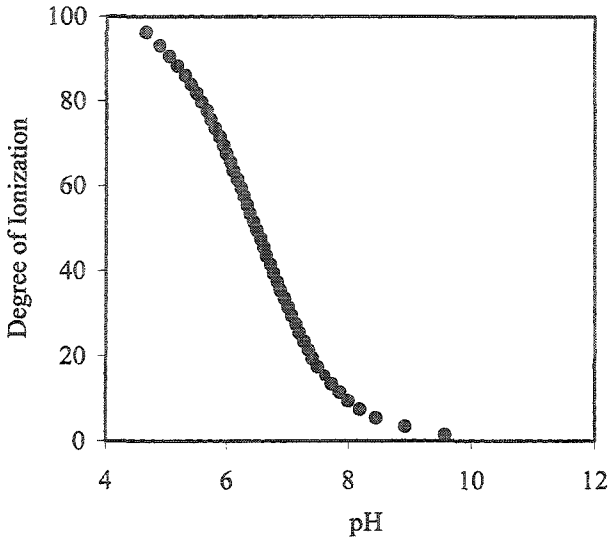


**Figure 3.3** The degree of ionization of chitosan versus pH.

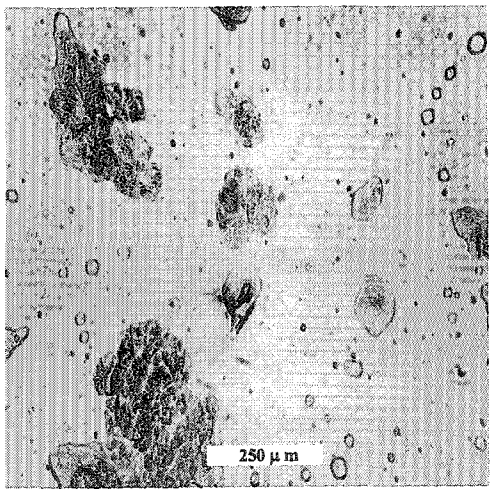


**Figure 3.4** Optical microscope image of uncontrolled phase separation and crosslinking upon reacting SMA-g-MPEG-70% with chitosan at pH 7.0 in 0.05 mol $L^{-1}$ NaCl solution.

Clearly, coacervation and crosslinking compete in these reactions. Significant crosslinking occurring prior to or during the coacervation would lead to macroscopic gelation. Apparently, chitosan and especially PEI react rapidly with the anhydride groups, preventing the formation of distinct coacervate droplets and hence microspheres. In principle, working at a lower pH could reduce the concentration of free amine, and slow the crosslinking reaction. However, an acidic pH would catalyze anhydride hydrolysis,[20] and hence reduce the effective crosslinking achievable.

We describe here another, two-step strategy to form crosslinked complex coacervates from SMA-*g*-MPEG. Specifically, poly(diallyldimethylammonium chloride) (pDADMAC) is used to form an initial complex coacervate with SMA-*g*-MPEG, which is subsequently crosslinked by adding chitosan or PEI.

### 3.2.3 Complex Coacervation between SMA-*g*-MPEG and pDADMAC

Figure 3.5 shows a typical optical microscopy image of complex coacervates of SMA-*g*-MPEG-70% and pDADMAC. The coacervate droplets are not colloidally stable and will coalesce after several minutes without stirring.

The dependence of the coacervate yield on the ratio of pDADMAC to SMA-*g*-MPEG-70% is described in Figure 3.6. The coacervation takes place over a range of pDADMAC/SMA-*g*-MPEG-70% ratios, and the coacervate yield goes through a maximum upon increasing the pDADMAC/SMA-g-MPEG-70% ratio.

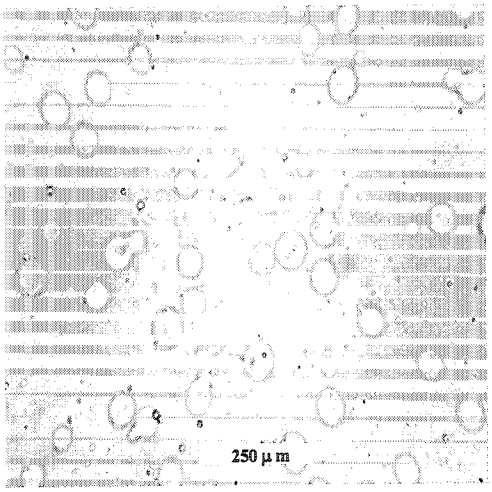


**Figure 3.5** Optical microscopy image of SMA-*g*-MPEG-70%/pDADMAC complex coacervate.

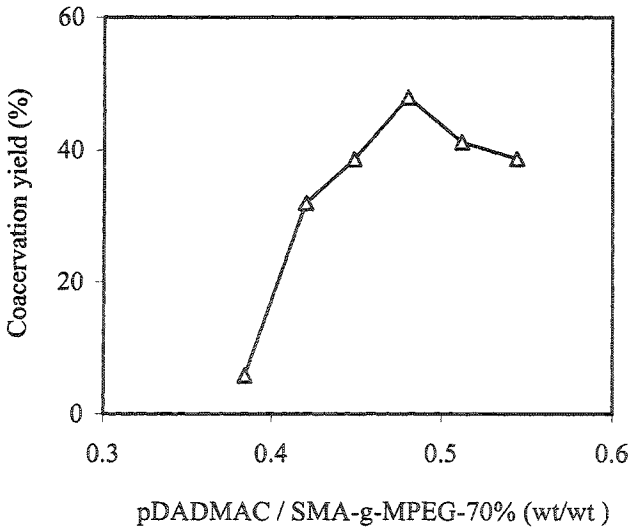


**Figure 3.6** Effect of pDADMAC to SMA-*g*-MPEG-70% ratio on coacervation yield. pH of 7.0 in 0.05 mol $L^{-1}$ NaCl solution. SMA-*g*-MPEG, 0.5 wt %; pDADMAC, 2.0 wt %.

### 3.2.4 Formation of Microspheres by Crosslinking SMA-*g*-MPEG/pDADMAC Coacervates with Chitosan

The results of crosslinking SMA-*g*-MPEG-70%/pDADMAC coacervates with chitosan are listed in Table 3.2. The mass ratios of pDADMAC to SMA-*g*-MPEG-70% used correspond to the coacervation yield shown in Figure 3.6. Under these conditions, the coacervation yield is only about 6% (Figure 3.6) when the mass ratio of pDADMAC to SMA-*g*-MPEG-70% is 0.38. Most of the polymer remains in the solution, and the coacervate droplets are finely dispersed. When chitosan is added in this coacervate mixture, gelation occurs due to the reaction of chitosan with the SMA-*g*-MPEG-70% in the solution. The ESEM microphotograph (Figure 3.7a) reveals some crosslinked coacervate microspheres within the precipitate matrix. The coacervation yield increases with increasing the mass ratio of pDADMAC/SAM-*g*-MPEG-70% to 0.42 and 0.45. When chitosan is added at such conditions, crosslinked coacervate microspheres are obtained. The ESEM images of these microspheres are shown in Figure 3.7b and c.

**Table 3.2** Effect of polymer ratios on crosslinking of SMA-*g*-MPEG-70%/pDADMAC coacervates with chitosan.[a]

| Sample | pDADMAC/ SMA-*g*-MPEG (wt/wt) | Chitosan/ PDADMAC (wt/wt) | Appearance [b] | Mean diameter of particles [c] (μm) |
|---|---|---|---|---|
| SDC-1 | 0.38 | 1.5 | precipitate | — |
| SDC-2 | 0.42 | 1.5 | microspheres | 38 |
| SDC-3 | 0.45 | 1.5 | microspheres | 40 |
| SDC-4 | 0.48 | 1.5 | no crosslinking | — |
| SDC-5 | 0.51 | 1.5 | no crosslinking | — |
| SDC-6 | 0.54 | 1.5 | no crosslinking | — |
| SDC-7 | 0.45 | 1.0 | no crosslinking | — |
| SDC-8 | 0.45 | 2.0 | microspheres | 43 |

[a] The coacervation and crosslinking reaction were carried out at pH 7.0 in 0.05 mol $L^{-1}$ NaCl solution. The concentrations of SMA-*g*-MPEG-70%, pDADMAC and chitosan were 0.5 wt %, 2.0 wt % and 2.0 wt %, respectively. [b] Observed by optical microscopy. [c] In 0.05 mol $L^{-1}$ NaCl solution.

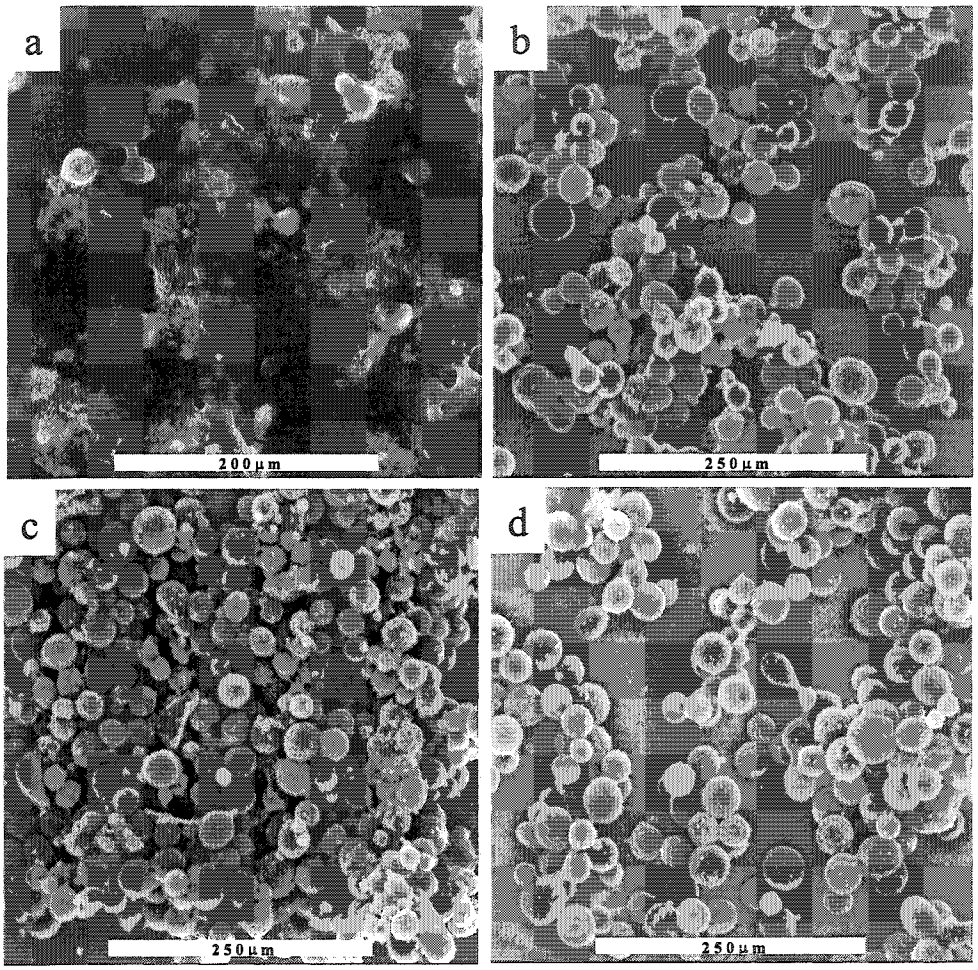


**Figure 3.7** ESEM micrographs of microspheres formed by crosslinking SMA-*g*-MPEG-70%/pDADMAC coacervates with chitosan at pH 7.0 in 0.05 mol $L^{-1}$ NaCl solution. (a) SDC-1, (b) SDC-2, (c) SDC-3, (d) SDC-8.

The coacervation has the highest yield at the mass ratio of 0.48 of pDADMAC/SMA-*g*-MPEG-70% under the studied conditions. However, no crosslinked microspheres are obtained when chitosan is added to this coacervate mixture (Table 3.2).

As described above, coacervation has its maximum yield at the electrostatic neutralization point of the complexed polyelectrolytes. Before the coacervation reaches the maximum yield point, the SMA-*g*-MPEG-70%/pDADMAC coacervates should be partially negatively charged. When chitosan, which is about 30% ionized at pH 7.0, is added, it will penetrate into the coacervate droplets by electrostatic association, and subsequently react with the SMA-*g*-MPEG-70% to crosslink coacervates into microspheres. On the other hand, at the point of maximum coacervate yield, the coacervate is charge-neutral, Hence chitosan is no longer electrostatically attracted into the coacervate, and no crosslinking takes place. These results were confirmed by further increasing the mass ratio of pDADMAC/SMA-*g*-MPEG-70% to 0.51 and 0.54. These coacervates are now positively charged, and again no crosslinking takes places when chitosan is added (Table 3.2).

The amount of chitosan added affects the crosslinking density of the microspheres (SDC-3, SDC-7, and SDC-8 in Table 3.2). At a mass ratio of chitosan to pDADMAC of 1.0, no stable microsphere is observed, indicating that the concentration of chitosan is too low to diffuse into and crosslink the coacervates efficiently. Increasing the addition amount of chitosan, crosslinked coacervate microspheres are obtained. ESEM images of these microspheres are shown in Figure 3.7c and d.

Figure 3.8 shows IR spectra of SMA-*g*-MPEG-70%/pDADMAC coacervate and coacervate microspheres crosslinked with chitosan. The spectrum of the coacervate displays characteristic anhydride peaks at 1780 and 1850 $cm^{-1}$. In the spectrum of crosslinked microspheres, these characteristic absorptions have disappeared.

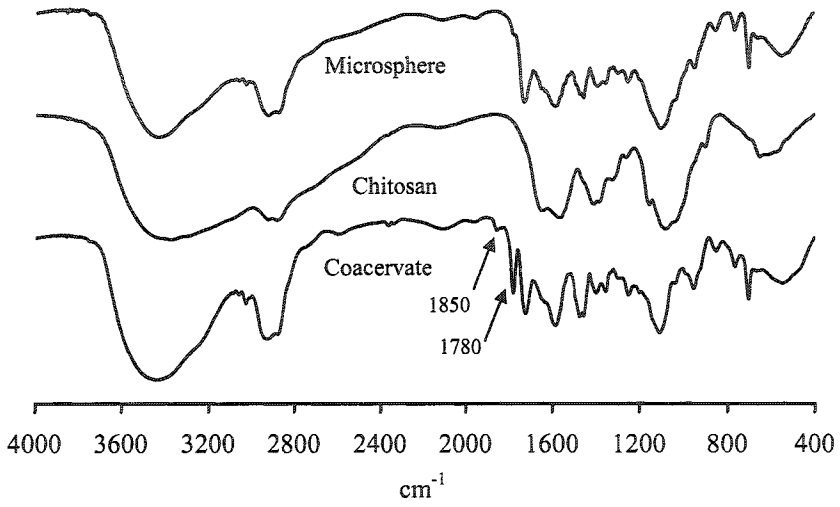


**Figure 3.8** IR Spectra of SMA-*g*-MPEG-70%/pDADMAC coacervates, chitosan and crosslinked microspheres (SDC-3).

### 3.2.5 Formation of Microspheres by Crosslinking SMA-*g*-MPEG/pDADMAC Coacervates with PEI

When PEI is used as the crosslinker at pH 7.0, macroscopic precipitation takes place as soon as the PEI is added into SMA-*g*-MPEG-70%/pDADMAC coacervate mixture under all circumstances.

Compared to chitosan, PEI has both a high charge density and high amine content at pH 7.0.[26] Furthermore, the PEI chain is more flexible. PEI is able to access the coacervate more easily than chitosan. During the accessing process, PEI may substitute pDADMAC from SMA-*g*-MPEG-70%/pDADMAC coacervates. Meanwhile, the crosslinking reaction between amines and anhydrides takes place very quickly, leading to the similar situation as PEI complexing directly with SMA-*g*-MPEG, and gel precipitations.

One solution to prevent the PEI from breaking up SMA-*g*-MPEG-70%/pDADMAC coacervates during the crosslinking process is to reduce the charge density of PEI, making it function only as a crosslinker. We find that PEI is an effective crosslinker for crosslinking coacervates under basic conditions, such as pH 10.5, where PEI is less than 5% ionized.[26]

The results of crosslinking SMA-*g*-MPEG-70%/pDADMAC coacervates with PEI at pH 10.5 are listed in Table 3. ESEM images of these crosslinked microspheres are shown in Figure 3.9.

**Table 3.3** Effects of polymer ratios on the morphology of PEI-crosslinked coacervate microspheres of SMA-*g*-MPEG-70%/pDADMAC [a]

| Sample | pDADMAC/ SMA-*g*-MPEG (wt/wt) | Appearance [b] | Mean diameter of particles [c] (μm) |
|---|---|---|---|
| SDE-1 | 0.45 | agglomerated microspheres | — |
| SDE-2 | 0.51 | agglomerated microspheres | — |
| SDE-3 | 0.58 | agglomerated microspheres | — |
| SDE-4 | 0.70 | microspheres | 38 |
| SDE-5 | 0.78 | microspheres | 36 |

[a] The coacervation and crosslinking reaction were taken at pH 10.5 in 0.05 mol $L^{-1}$ NaCl solution. 1.0g of 2.0 wt % PEI was added after coacervation. The concentrations of SMA-*g*-MPEG-70% and pDADMAC were 0.5 wt% and 2.0 wt %. [b] Observed by optical microscopy. [c] In 0.05 mol $L^{-1}$ NaCl solution.

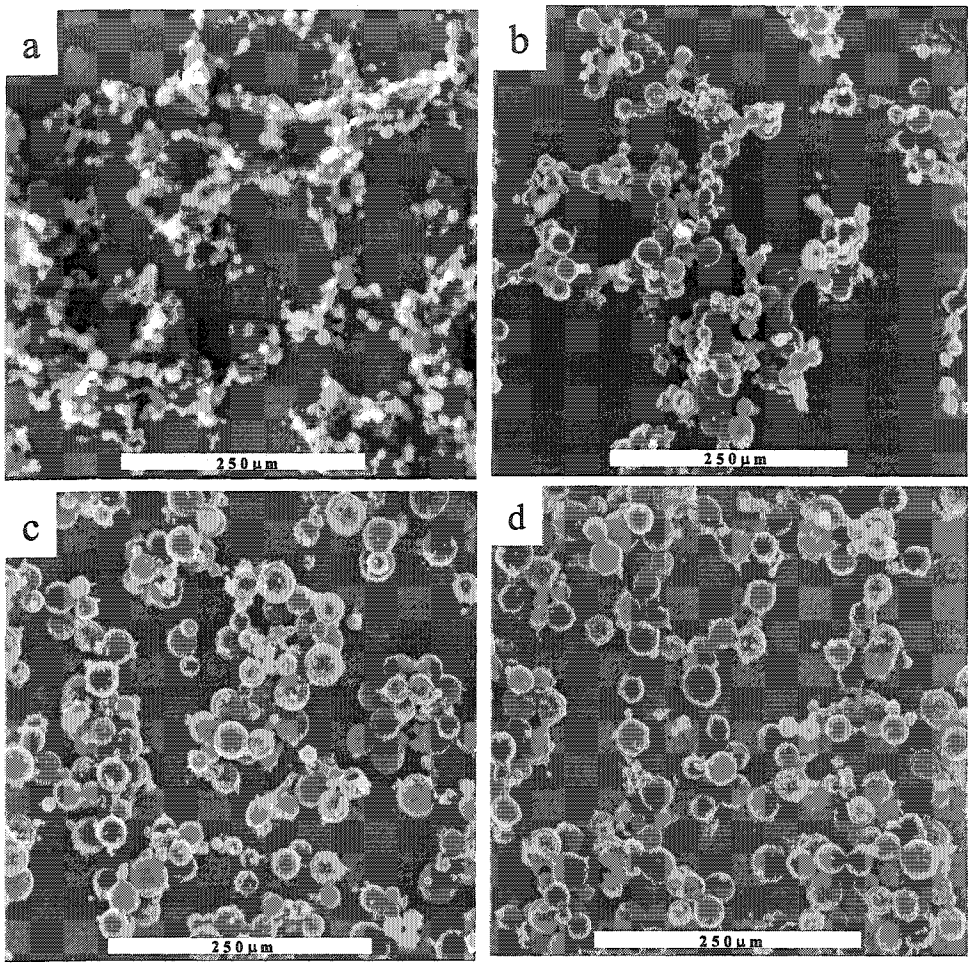


**Figure 3.9** ESEM micrographs of microspheres formed by crosslinking SMA-*g*-MPEG-70%/pDADMAC coacervates with PEI at pH 10.5 in 0.05 mol $L^{-1}$ NaCl solution. (a) SDE-1, (b) SDE-2, (c) SDE-4, (d) SDE- 5.

At basic conditions, even though the hydrolysis of anhydride groups happens during the coacervation and the crosslinking processes, the remaining anhydride groups seem sufficient to be crosslinked by the PEI chains and form stable coacervate microspheres. Morphologies of these crosslinked coacervate microspheres are dependent on the pDADMAC/SMA-*g*-MPEG-70% ratios used. Microspheres aggregate extensively at relatively low mass ratios. As shown in Figure 3.9a and b, these microspheres are clustered and appearing to be joined or welded. Colloidally stable microspheres are obtained at relatively high mass ratios of pDADMAC/SMA-*g*-MPEG-70% (Figure 3.9c and d). Although definitive proof is lacking, it seems very likely that the coacervates have excess anionic charges due to the hydrolysis of anhydride groups. These excess anionic charges play an important role on the accessing of PEI into the coacervates. At low mass ratio of pDADMAC/SMA-g-MPEG-70%, the charge association between PEI and SMA-*g*-MPEG-70% is still relatively strong, causing the PEI to penetrate the coacervates very quickly. A PEI chain may penetrate into several coacervates at the same time, and hence bridge microspheres together, leading to agglomerations. While at high mass ratio of pDADMAC/SMA-g-MPEG-70%, PEI penetrates into the coacervates and crosslinks them smoothly, agglomeration does not take place. As shown in the ESEM image (Figure 3.9), particles obtained at low mass ratios of pDADMAC/SMA-*g*-MPEG-70% have smaller sizes than those obtained at high mass ratios.

### 3.2.6 Independent Swelling Properties of Coacervate Microspheres

The rapid response of hydrogel microspheres to pH, temperature and salinity has attracted much interest in recent years.[30-34] These hydrogel microspheres contain either

anionic polymers, such as polyacrylic acid, or cationic polymers, such as poly(dimethylamino ethyl methacrylate). The swelling of the hydrogel microsphere at different pH and salinity is mainly due to the osmotic pressure, which results from the net difference in concentration of mobile ions between the interior of the microsphere and the exterior bathing solution.[32,33] As a result, the microspheres will shrink with increasing salt concentrations.

Up to now, few studies have studied the salt dependent swelling of microspheres containing both anionic and cationic polymers. Some research has targeted the swelling properties of polyampholyte hydrogels.[35,36] Here, we present the salt dependent swelling of complex coacervate microspheres.

Figure 3.10 describes the sizes of coacervate microspheres at various NaCl solutions. In contrast to the anionic or cationic polyelectrolyte hydrogel microspheres, the coacervate microspheres swell with the increase of salt concentrations. The particle sizes first increase, and then reach a roughly constant value at the studied salt concentrations.

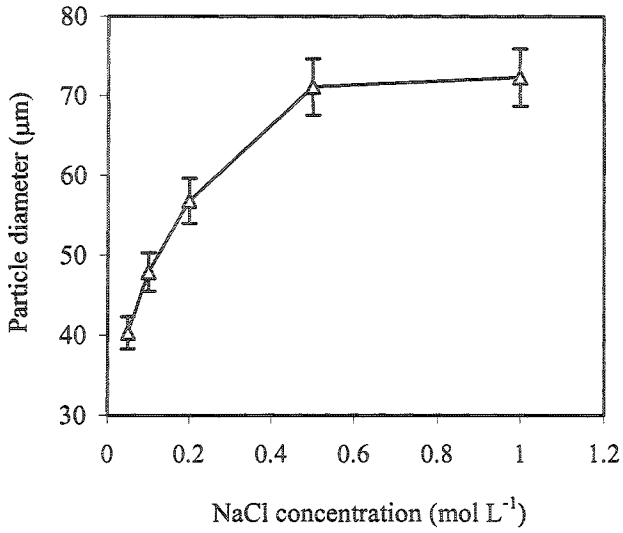


**Figure 3.10** Dependence of swelling properties of the coacervate microspheres upon NaCl concentrations. SDC-3 coacervate microspheres were used.

At low salt concentrations, the polymer chains in complex coacervate microspheres are oppositely charged polyelectrolytes. With the increase of salt concentrations in the bathing medium, the salt ion penetrates into coacervate microspheres, and partially shields intermolecular ionic bonds. The polymer chains expand with the breakage of ionic crosslinking points, leading to the swelling of coacervate microspheres. Hence, the swelling of complex coacervate microspheres upon increasing the salinity is essentially based on the breakage of electrostatic interactions instead of osmotic pressures.

At high NaCl concentrations (above 0.5 mol $L^{-1}$), most of the charge of polyelectrolytes in coacervate microspheres is screened, and the particle sizes remain roughly constant with further increasing salt concentrations.

### 3.3 Conclusion

Due to the rapid crosslinking reaction between anhydride groups and polyamines, directly complexing poly(ethylene glycol) partially grafted poly(styrene-*alt*-maleic anhydride) with charged polyamines results not in coacervate microspheres, but in gel precipitates. Hydrogel microspheres have been successfully prepared by complex coacervations of poly(ethylene glycol) partially grafted poly(styrene-*alt*-maleic anhydride) with polydiallyldimethylammonium chloride, followed by crosslinking with chitosan or polyethylenimine. Chitosan serves as an effective crosslinker at pH 7.0, while polyethylenimine (PEI) is used as crosslinker under basic conditions (pH 10.5). The difference of crosslinking conditions is mainly due to the structure of polyamines, which affects their accessing abilities to coacervates.

Coacervate microspheres swell with increasing salinity in the bath medium. This swelling is mainly due to the interruption of electrostatic associations of complexed polyelectrolytes with the addition of salts.

## References


1. Langer, R. *Acc. Chem. Res.* **2000**, *33*, 94-101.
2. Hoffman, A. S. *Adv.Drug Deliv. Rev.* **2002**, *54*, 3-12.
3. Funke, W.; Okay, O.; Muller, B. J. *Adv. Polym. Sci.* **1998**, *136*,140-234.
4. Robinson, D. N.; Peppas, N. A. *Macromolecules* **2002**, *35*, 3668-3674.
5. Goh, E.; Stöver, H. D. H. *Macromolecules* **2002**, *35*, 9983-9989.
6. Arshady, R.; *Polym. Eng. Sci.* **1990**, *30*, 905-914.
7. Prokop, A.; Hunkeler, D.; DiMari, S.; Haralson, M.; Wang, T.G. *Adv. Polym. Sci.* **1998**, *136*, 1-51.
8. Burgess, D. J. *J. Colloid Interface Sci.* **1990**, *140*, 227-238.
9. Menger, F. M.; Sykes, B. M. *Langmuir* **1998**, *14*, 4131-4137.
10. Menger, F. M.; Peresypkin, A. V.; Caran, K. L.; Apkarian, R. P. *Langmuir* **2000**, *16*, 9113-9116.
11. Wen, Y.; Dubin, P. L. *Macromolecules* **1997**, *30*, 7856-7861.
12. Kaibara, K.; Okazaki, T.; Bohidar, H. B.; Dubin, P. L. *Biomacromolecules* **2000**, *1*, 100-107.
13. Burgess, D. J.; Singh, O. N. *J. Pharm. Pharmacol.* **1993**, *45*, 586-591.
14. Chandy, T; Mooradian, D. L.; Rao, G. H. *J. Appl. Polym. Sci.* **1998**, *70*, 2143-2153.
15. Tiyaboonchai, W.; Woiszwillo, J.; Middaugh, C. R. *J. Pharm. Sci.* **2001**, *90*, 902-914.
16. Cohen, S.; Baño, M. C.; Visscher, K. B.; Chow, M.; Allcock, H. R.; Langer, R. *J. Am. Chem. Soc.* **1990**, *112*, 7832-7833.
17. Wen, S.; Yin, X.; Stevenson, W. T. K. *Biomaterials* **1991**, *12*, 374-384.

18. Andrianov, A. K.; Chen, J.; Payne, L. G. *Biomaterials* **1998**, *19*, 109-115.

19. Chitanu, G. C.; Rinaudo, M.; Desbrières, M. M.; Carpov, A. *Langmuir* **1999**, *15,* 4150-4156.

20. Ladavière, C.; Delair, T.; Domard, A.; Pichot, T.; Mandrand, B. *J. Appl. Polym. Sci.* **1999**, *72*, 1565-1572.

21. Shulkin, A.; Stöver, H.D.H, *J. Membr. Sci.* **2002**, *209*, 421-432.

22. Shulkin, A.; Stöver, H.D.H, *J. Membr. Sci.* **2002**, *209*, 433-444.

23. Yin, X.; Stöver, H. D. H. *Macromolecules* **2002**, *35*, 10178-10181.

24. Bartkowiak, A.; Hunkeler, D. *Chem. Mater.* **1999**, *11*, 2486-2492.

25. Dautzenberg, H.; Gornitz, E.; Jaeger, W. *Marcomol. Chem. Phys.* **1998**, *199,* 1561-1571.

26. Clark, S. L.; Hammond, P. T. *Langmuir* **2000**, *16,* 10206-10214.

27. Veis, A.; Aranyi, C. *J. Phys. Chem.* **1960**, *64,* 1203-1210.

28. Wang, Y.; Kimura K.; Dubin P. L. *Macromolecules* **2000**, *33*, 3324-3331.

29. Tsung, M.; Burgess, D. J. *J. Pharm. Sci.* **1997**, *86*, 603-607.

30. Hooper, H. H.; Baker, J. P.; Blanch, H. W.; Prausnitz, J. M. *Macromolecules* **1990**, *23*, 1096-1104.

31. Sawai, T.; Yamazaki, S.; Ikariyama, Y.; Aizawa, M. *Macromolecules* **1991**, *24*, 2117-2118.

32. Saunder, B. R.; Crowther, H. M.; Vincent, B. *Macromolecules* **1997**, *30*, 482-487.

33. Eichenbaum, G. M.; Kiser, P. F.; Simon, S. A.; Needham, D. *Macromolecules* **1998**, *31*, 5084-5093.

34. Podual, K.; Doyle, F. J.; Peppas, N. A. *Biomaterials* **2000**, *21*, 1439-1450.

35. Baker, J. P.; Stephens, D. R.; Blanch, H. W.; Prausnitz, J. M. *Macromolecules* **1992**, *25*, 1955-1958.

36. Nisato, G.; Munch, J. P.; Candau, S. J. *Langmuir* **1999**, *15*, 4236-4244.

# Chapter 4 Hydrogel Microspheres by Thermally Induced Coacervation of Poly(*N,N*-Dimethylacrylamide-*co*-Glycidyl Methacrylate) Aqueous Solutions


## Abstract

Aqueous solutions of poly(*N,N*-dimethacrylamide-*co*-glycidyl methacrylate) (DMA-*co*-GMA) were shown to undergo liquid-liquid phase separation upon heating. The phase transition temperatures as measured by the cloud point method decreased with increasing levels of the hydrophobic GMA comonomer. The initially formed coacervate microdroplets could be crosslinked by addition of polyamines. The morphology of the resulting hydrogel microspheres depended on both coacervation conditions and crosslinking conditions. Specifically, colloidally stable microspheres were formed at temperatures slightly above the phase transition temperatures, while agglomeration took place at higher temperatures. Low molecular weight polyamines were effective internal crosslinkers for the coacervate droplets, while higher molecular weight polyamines resulted in agglomeration. Addition of sodium dodecyl sulfate increased the phase transition temperatures of polymer solutions dramatically, while addition of poly(vinylpyrrolidone) did not affect the phase separation temperatures, and could be used as a steric stabilizer. This chapter has been reproduced with permission from *Macromolecules* **2003**, *36*, 9817-9822. Copyright 2003 American Chemical Society.

## 4.0 Introduction

Polymer systems that show phase transitions in response to environmental stimuli have potential uses in biotechnology, chemical separation and catalysis.[1] Thermally induced phase separations of aqueous polymer solutions are attractive as they require no additives and are usually reversible. Poly(*N*-isopropylacrylamide) (pNIPAM) undergoes a sharp coil-globule transition at its lower critical solution temperature (LCST) of around 32°C, and precipitates in form of a solid driven by both hydrophobic interactions between its isopropyl groups, and hydrogen bonding between the amide groups.[2-7] Aqueous solutions of poly(*N,N*-dimethylacrylamide) (pDMA), having only two methyl groups and no hydrogen bonding ability, do not show LCST's below 100°C. DMA copolymers with hydrophobic comonomers do exhibit LCST behavior, though unlike pNIPAM solutions, they undergo liquid-liquid phase separations.[8-10] Recently, Akashi's group described similar liquid-liquid phase separations of linear and crosslinked copolymers comprised of *N*-vinylformamide or *N*-vinylacetamide, and vinyl acetate, as respectively the hydrophilic and hydrophobic components.[11] In both cases the phase transition temperature depends on the comonomer ratio. Similar phase separations are known in certain proteins such as elastin, and are being explored for uses in protein separation and tissue engineering.[12,13]

Such liquid-liquid phase separations of aqueous polymer solutions into a polymer-rich coacervate phase and a polymer-lean equilibrium phase are collectively called coacervation,[14-16] and are generally divided into two classes: complex coacervation and simple coacervation. Complex coacervation involves polyelectrolyte complexation, while simple coacervation is caused by changing the solvent composition or the solution

temperature. Both processes have been used for protein separation and for preparing hydrogel microparticles.[17-20] Natural polymers such as gelatin/acacia, and chitosan/alginate, still form the majority of materials used to make microparticles via complex coacervation.[21-23] A few studies have been carried out using synthetic polymers.[24-27]

Recently, our group prepared hydrogel microspheres by a novel two-step process of complex coacervation followed by crosslinking, using reactive polyanions and polyamines, and investigated the thermo-responsive properties of these copolymers.[27, 28] Independently, Tirelli's group developed a similar concept based on Michael-addition self-crosslinking of a mixture of thiolate and acrylate-functional pluronic polymers, both below and above their LCST.[29]

In this paper, we report the thermally induced coacervation of aqueous solutions of poly(*N,N*-dimethylacrylamide-*co*-glycidyl methacrylate) copolymers, and the covalent crosslinking of the resulting coacervate droplets in a second step with polyamines to form hydrogel microspheres. While presently carried out using small polyamines, and aimed at forming microspheres, these processes may also be carried out using chitosan or other bio-compatible polyamines, and hence lead to new crosslinking materials useful in a variety of applications including cell encapsulations, and biomaterial design.

## 4.1 Experimental Section

### 4.1.1 Materials

*N,N*-Dimethylacrylamide (DMA), glycidyl methacrylate (GMA), *N*-isopropylacrylamide (NIPAM), sodium dodecyl sulfate (SDS), poly(vinylpyrrolidone) (PVP) ($M_w$, 40,000), ethylenediamine (EDA), tetraethylenepentamine (TEPA), and polyethylenimine (PEI) of different molecular weights were purchased from Aldrich and used as received. 2,2'-Azobisisobutyronitrile (AIBN) was obtained from American Polymer Standards Laboratories and recrystallized from methanol. Tetrahydrofuran (THF) and anhydrous diethyl ether were obtained from Caledon Laboratories. THF was refluxed over sodium and distilled prior to use.

### 4.1.2 Preparation of Poly(*N,N*–Dimethylacrylamide-*co*-Glycidyl Methacrylate) (DMA-*co*-GMA) Copolymers.

For a typical procedure, 6.57 g of *N,N*-dimethylacrylamide (0.066 mol) and 2.82 g of 95 wt % glycidyl methacrylate (0.019 mol) were dissolved in 100 ml of THF in a 125 ml HDPE plastic screw cap bottle. Oxygen was removed by bubbling nitrogen through the mixture before adding 0.070 g of AIBN ($4.26 \times 10^{-4}$ mol, 0.5 mol % relative to monomers). Polymerization was carried out at 70°C for 1 hour by rolling the bottles in a thermostated reactor fitted with a set of horizontal rollers. The product was precipitated into 500 ml of diethyl ether and dried under vacuum at 40°C to provide 3.0 g of polymer (yield, 32%).

Molecular weights of copolymers were determined using a gel permeation chromatograph consisting of a Waters 515 HPLC pump, three ultrastyragel columns

(500-20k, 500-30k, 5k-600k Daltons) and a Waters 2414 refractive index detector, using THF as solvent at a flow rate of 1 mL $min^{-1}$, and narrow disperse polystyrene as calibration standards.

$^1H$ NMR spectra of the copolymers were recorded on a Bruker AC 200, using chloroform-*d* as the solvent. Compositions of DMA-*co*-GMA copolymers were determined by integration of characteristic peaks.

### 4.1.3 Measurement of Phase Transition Temperatures

Phase transition temperatures of aqueous solutions of DMA-*co*-GMA copolymers were measured using the cloud point method. An automatic PC-Titrator (Mandel) equipped with a temperature probe and with a photometer incorporating a 1 cm path length fiber optics probe (GT-6LD, Mitsubishi) was used to trace the phase transition by monitoring the transmittance of a beam of white light. The turbidity of the solution was recorded as photoinduced voltage (mV). The phase transition temperature was defined as the inflection point of the mV vs. temperature curve, as determined by the maximum in the first derivative. The heating rate was 1.0°C $min^{-1}$ and concentrations of polymer solutions were 0.2, 0.5, 1.0 and 2.0 wt %.

### 4.1.4 Preparation of Hydrogel Microspheres

The DMA-*co*-GMA copolymers were dissolved in deionized water at a temperature below the phase transition temperature. The solutions were stirred, and heated above the phase separation temperature to induce coacervation. After phase equilibration, polyamine was added to crosslink the formed coacervate droplets.

In a typical reaction, 30 g of a 0.5 wt % DMA-*co*-GMA43 solution was stirred at 1000 RPM and heated to 40 °C in a 50 mL jacketed beaker. After the coacervate was equilibrated at 40°C for 5 min, 1.5 ml of 2.0 wt % ethylenediamine was added. The crosslinking reaction was allowed to proceed for 2 hours, and the resulting microspheres were separated by centrifugation at 3000 RPM for 10 min. The microspheres were washed with deionized water to remove unreacted materials and dried in a vacuum at 65°C to provide 0.03g of microspheres (yield, 16.7 %).

### 4.1.5 Characterization of Hydrogel Microspheres

Optical images of the microspheres were recorded at room temperature using an Olympus BH-2 microscope equipped with a Kodak DC 120 Zoom digital camera. Morphologies of the microspheres were examined using a Phillips ElectroScan 2020 environmental scanning electron microscope (ESEM). ESEM samples were prepared by depositing a drop of aqueous microsphere suspension onto a glass-covered ESEM stub, drying under vacuum and sputter-coating with about 5 nm of gold.

## 4.2 Results and Discussion

### 4.2.1 Synthesis and Properties of DMA-*co*-GMA Copolymers

Copolymerization with glycidyl methacrylate (GMA) permits both thermal coacervation and subsequent crosslinking of the resulting coacervate droplets to form hydrogel microspheres. The copolymerization conversions were kept below 30% in order to limit copolymer composition drifts.

$^1$H NMR spectra of DMA and GMA homopolymers, and of a copolymer are shown in Figure 4.1, with peak assignments from the literature.[30,31] Copolymer compositions (Table 4.1) were estimated by comparing the peak area (A) of a GMA methyleneoxy protons (f) at 4.27 ppm, with the total peak area (B) between 2.3 and 3.3 ppm, which includes seven protons (a, b) from DMA and three protons (e, d, d') from GMA. The mole ratio of DMA to GMA in each copolymer is then found as (B-3A)/7A.

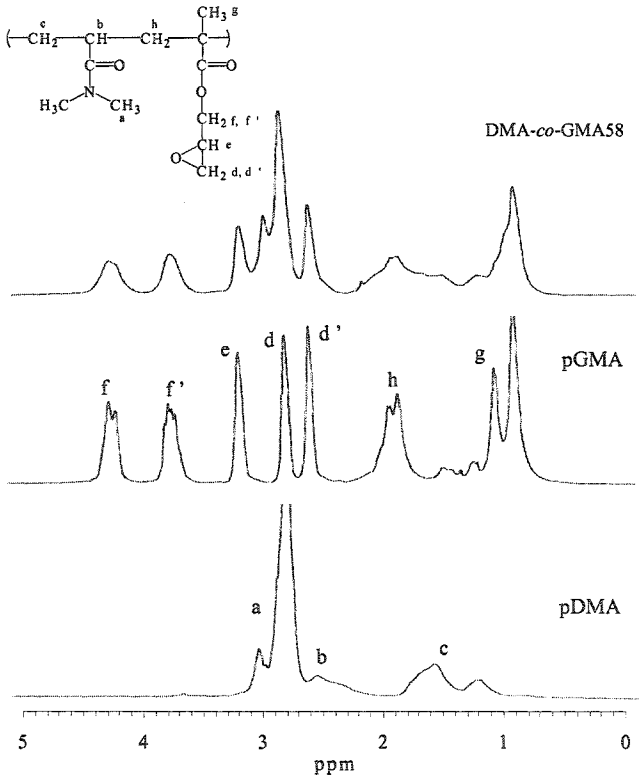


**Figure 4.1** $^1$H NMR Spectra of pDMA and pGMA homopolymers and copolymer DMA-*co*-GMA58 in chloroform-*d*.

The temperature-dependent phase separation of aqueous solutions of different DMA-*co*-GMA copolymers was investigated by turbidimetry. Figure 4.2 shows photo voltage vs. temperature curves for four DMA-*co*-GMA compositions, and for p(NIPAM), with zero volt corresponding to an opaque solution. The compositions and their corresponding phase transition temperatures ($T_p$) are shown in Table 4.1.

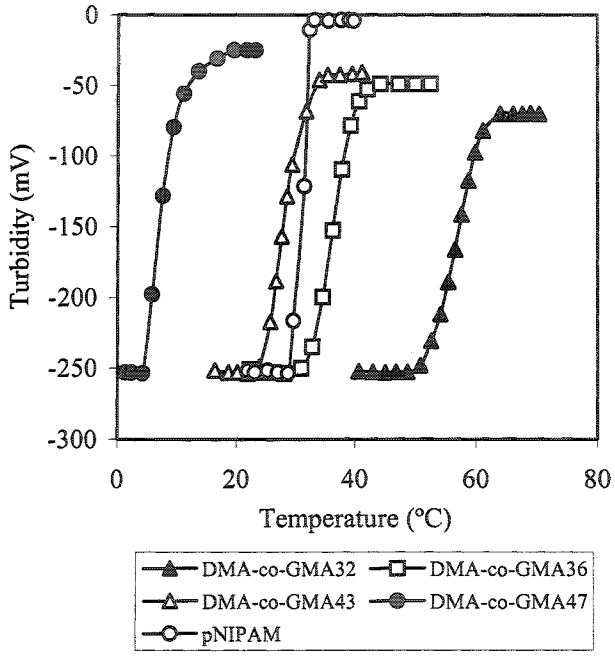


**Figure 4.2** Photovoltaic cloud point curves for 0.5 wt % aqueous solutions of DMA-*co*-GMA and pNIPAM, with -250 mV corresponding to a transparent solution.

**Table 4.1** Compositions and phase transition temperatures of poly(*N,N*-dimethylacrylamide-*co*-glycidyl methacrylate) (DMA-*co*-GMA) copolymers

| DMA-*co*-GMA Copolymer | GMA amount (mol %) in feed | GMA amount (mol %) in polymer [a] | $M_n$ [b] | $M_w/M_n$ [b] | $T_p$ [c] (°C) |
|---|---|---|---|---|---|
| DMA-*co*-GMA12 | 10.0 | 12.2 | $7.3 \times 10^3$ | 1.6 | none [d] |
| DMA-*co*-GMA19 | 16.6 | 19.4 | $7.0 \times 10^3$ | 1.6 | none [d] |
| DMA-*co*-GMA32 | 22.2 | 32.2 | $6.4 \times 10^3$ | 1.8 | 58.7 |
| DMA-*co*-GMA36 | 26.3 | 35.6 | $7.0 \times 10^3$ | 1.8 | 35.4 |
| DMA-*co*-GMA43 | 28.6 | 42.9 | $7.8 \times 10^3$ | 1.9 | 27.6 |
| DMA-*co*-GMA47 | 33.3 | 46.5 | $8.6 \times 10^3$ | 1.9 | 7.6 |
| DMA-*co*-GMA58 | 40.0 | 57.7 | $1.4 \times 10^4$ | 1.7 | not soluble [e] |

[a] Estimated by $^1$H NMR. [b] Determined by GPC. [c] Inflection points of the cloud point curves measured at 0.5 wt % polymer concentration. [d] Below 100°C. [e] Even at 0°C.

The pNIPAM solution shows the characteristically sharp liquid-solid phase transition at about 32°C, with the complete opacity above the LCST due to scattering from the de-solvated pNIPAM particles.

Aqueous solutions of DMA-*co*-GMA copolymers with less than 20 mol % GMA do not show thermal phase transitions (Table 4.1). GMA contents between 30 and 45% result in liquid-liquid phase transition, as indicated by both the finite transmittance above their cloud points (Figure 4.2), and the separation into a viscous polymer-rich bottom

layer and a transparent polymer-poor top layer upon standing. DMA-*co*-GMA copolymers with more than 50% GMA are not soluble in water, even at 0°C.

Figure 4.3 presents an optical microscope image of a 1.0 wt % DMA-*co*-GMA47 solution at room temperature, showing the expected liquid coacervate droplets.

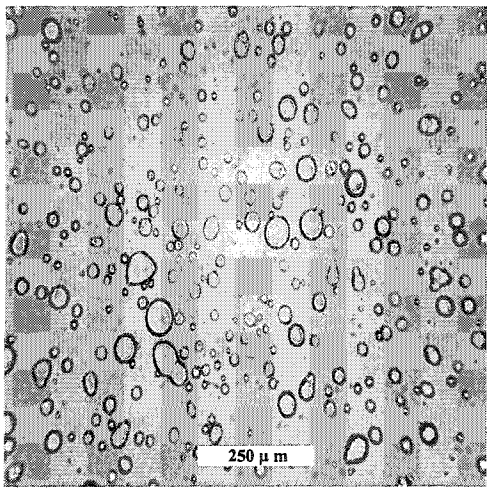


**Figure 4.3** Optical microscope image of coacervate droplets in 1 wt % aqueous DMA-*co*-GMA47 solution at room temperature (25°C).

The phase separation temperatures of these copolymer solutions drop by several degrees as the polymer concentration is increased from 0.2 to 2% (Figure 4.4). It is currently not clear whether this behavior is due to a true shift of the liquid-liquid phase separation temperature with concentration, or an artifact of the cloud point measurement method, where droplet size and refractive index difference may affect the turbidity. Similar concentration dependencies have been reported for the liquid-solid phase

transition of poly(*N,N*-diethylacrylamide), and were attributed to the cloud point method.[32] The phase transition behavior of aqueous solutions of DMA copolymers will be studied by microcalorimetry and light scattering in future studies.

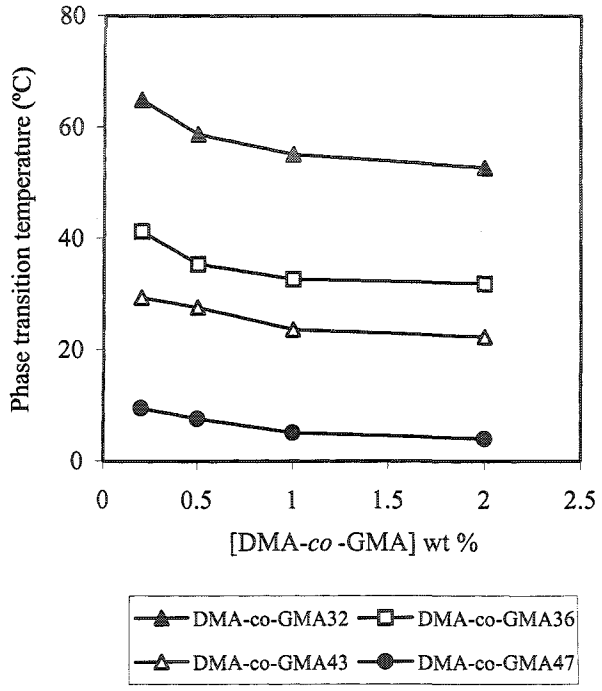


**Figure 4.4** Effects of polymer concentration on the phase separation temperatures of DMA-*co*-GMA solutions as measured by the cloud point method.

Phase transition temperatures of thermally responsive polymer solutions commonly increase with the addition of surfactants up to the critical aggregation concentration, through formation of hydrophilic polymer-surfactant complexes.[33-34] Figure 4.5 shows that adding 0.1 wt % (ca. 3.5 mM) sodium dodecyl sulfate (SDS)

increases the phase transition temperature of a 0.5 wt % DMA-*co*-GMA43 solution by about 37°C, by introducing charges to the copolymer.

In contrast, adding poly(vinyl pyrrolidone) (PVP) does not significantly affect the phase transition temperatures (Figure 4.5), indicating that PVP does not bind to DMA-*co*-GMA copolymers in aqueous solutions, a result similar to that known for pNIPAM.[35]

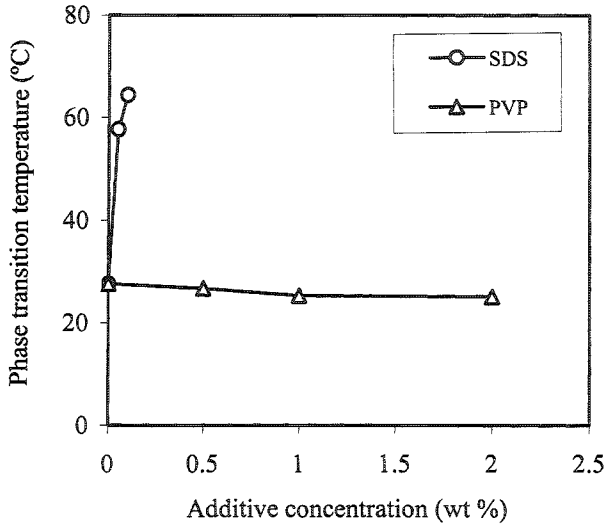


**Figure 4.5** Effects of additives on phase separation temperatures of 0.5 wt % DMA-*co*-GMA43 solutions.

### 4.2.2 Crosslinking of DMA-*co*-GMA Coacervate Droplets

Coacervate microdroplets are inherently unstable and will coalesce into a bulk coacervate phase in absence of a dispersing force. However, they may be crosslinked to form colloidally stable hydrogel microspheres. The thermally induced DMA-*co*-GMA

coacervate droplets described here were designed to be crosslinked by addition of diamines and polyamines to the aqueous phase after phase separation.

Figure 4.6 shows the environmental scanning electron microscopy (ESEM) images of crosslinked hydrogel microspheres prepared by addition of ethylene diamine to DMA-*co*-GMA coacervate droplets. Coacervation and crosslinking were carried out at temperatures slightly above the corresponding phase transition temperatures. Under these conditions, ethylene diamine diffuses into the coacervates and reacts with epoxy groups in the polymer chain. Crosslinking is promoted over simple functionalization by the enrichment of the polymer in the coacervate phase, and no crosslinking or gelation is observed when ethylene diamine is added at temperatures below the phase transition temperature.

The crosslinked microspheres are stable during work-up. The conversion of epoxy groups to hydroxyl groups and the incorporation of amines render the microspheres more hydrophilic and even ionic, and remove their temperature-responsive properties.

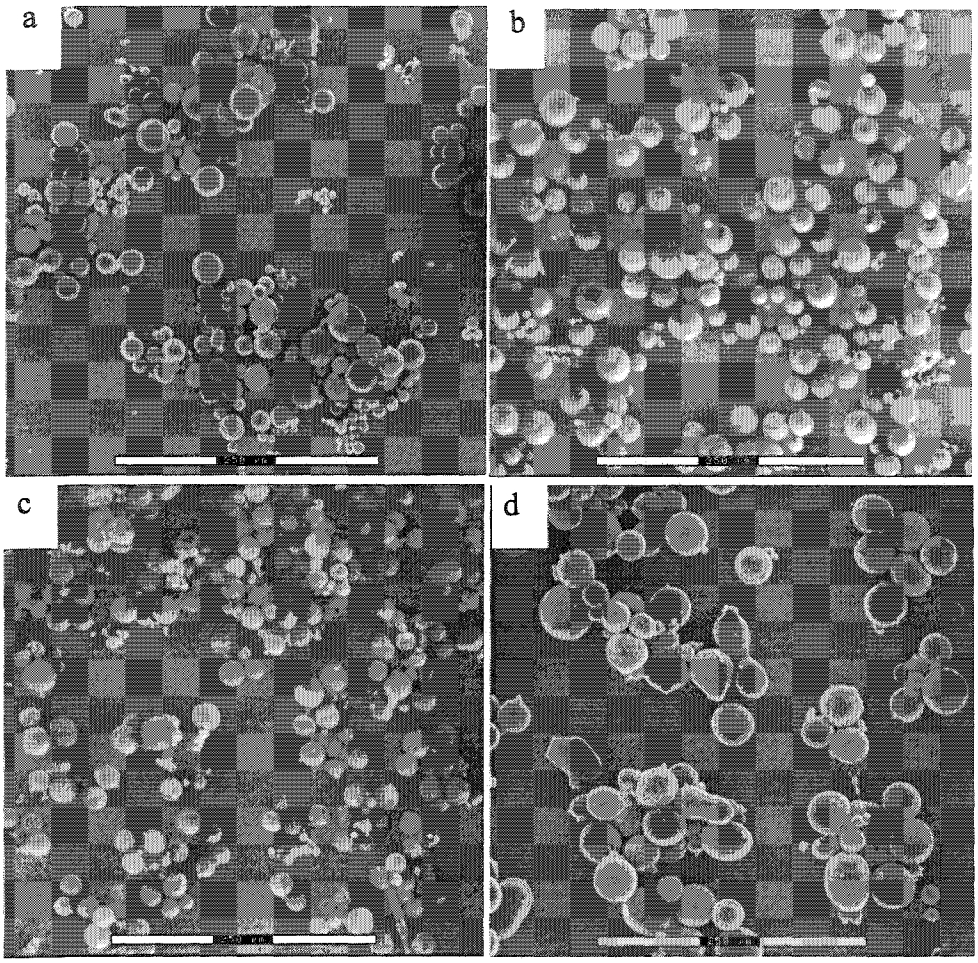


**Figure 4.6.** ESEM images of hydrogel microspheres prepared by crosslinking thermally induced coacervates (30 ml, 0.5 wt%) with ethylene diamine (1.5 ml, 2.0 wt %). (a) DMA-*co*-GMA32 at 60°C, (b) DMA-*co*-GMA36 at 40°C, (c) DMA-*co*-GMA43 at 30°C, (d) DMA-*co*-GMA47 at 20°C. Scale bars are 250 μm.

### 4.2.3 Coacervate and Microsphere Yield

Figure 4.7 shows the yield of crosslinked microspheres as function of crosslinking temperatures. The microsphere yields, which reflect both the coacervate yield and the crosslinking efficiency, increase with increasing crosslinking temperatures.

The phase transition of DMA-*co*-GMA47 aqueous solution occurs below room temperature, which allows us to easily measure the coacervate yield itself. The coacervate yield of a 0.5 wt % DMA-*co*-GMA47 aqueous solution at 25°C is 26%, which roughly corresponds to the microsphere yield in that temperature range (Figure 4.7). This indicates that the microsphere yield mainly depends on the coacervation process, and that crosslinking of the formed coacervate is quite efficient. Hence, the coacervation yield can be estimated through the microsphere yield.

This temperature-dependent coacervation yield is partly due to the compositional distribution of the copolymer. *N,N*-dimethylacrylamide and glycidyl methacrylate monomers have different reactivity ratios, and chains generated at the beginning of the polymerization should contain more GMA, be more hydrophobic and have lower cloud point temperatures than chains generated later in the polymerization. The resulting compositional distribution will broaden the temperature range over which coacervation occurs, even though we limited our polymerizations to about 30% monomer conversion. In future we will explore living/controlled radical copolymerizations to further narrow the compositional distributions of the copolymers. As well, the liquid-liquid phase separations are continuous processes, in contrast to pNIPAM's liquid-solid precipitation. The consequences of this progressive chain collapse will be explored in future work.

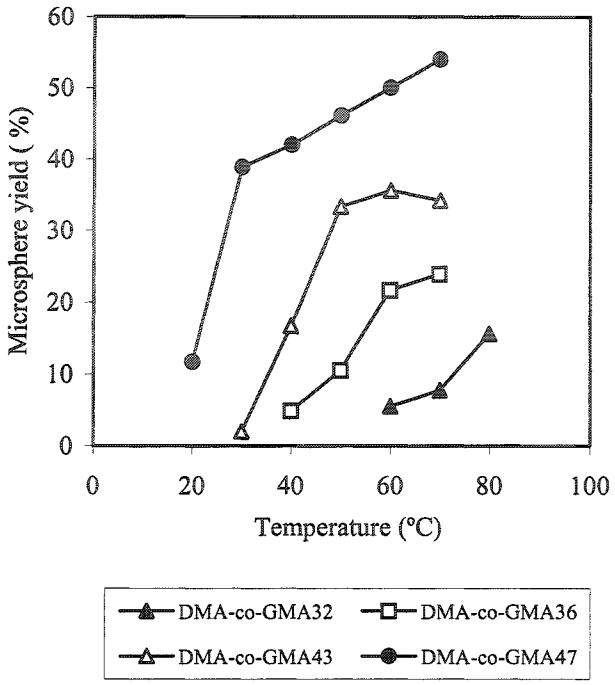


**Figure 4.7** Yields of microspheres obtained by crosslinking at different temperatures. Reaction conditions are those shown in Figure 4.6.

### 4.2.4 Microsphere Morphology

Figure 4.8 presents ESEM micrographs of microspheres prepared from 0.5 wt % DMA-*co*-GMA43 at 40 and 70°C. Compared to the microspheres crosslinked at 30°C shown in Figure 4.6c, crosslinking at these higher temperatures leads to more and larger microspheres, but with less colloidal stability. This is expected, given the same dispersing force but a higher yield of more viscous and more hydrophobic coacervates. In addition, the more efficient crosslinking at higher temperature may cause more particles inter-bonded, which would contribute to the observed aggregation.

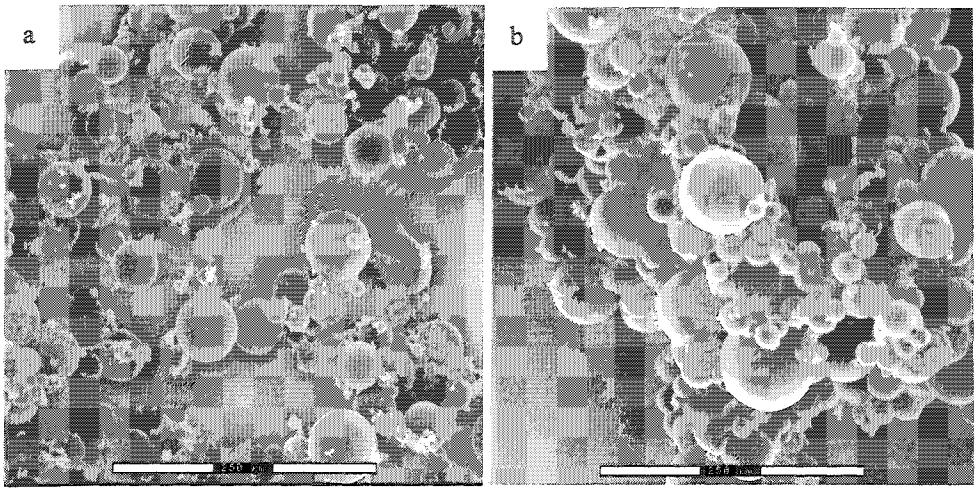


**Figure 4.8** ESEM images of hydrogel microspheres prepared by crosslinking DMA-*co*-GMA43 coacervates with ethylene diamine at (a) 40°C and (b) 70°C. Reaction conditions are those in Figure 4.6. Scale bars are 250μm.

Figure 4.9 presents the effect of polyamine length on the morphologies of crosslinked coacervate microspheres. Colloidally stable microspheres are obtained upon crosslinking with the small amines such as ethylene diamine or tetraethylenepentamine (Figure 4.9). Using linear PEI 432 leads to more aggregation, and branched PEI 1800 gives microspheres that appear more fused, plausibly due to enhanced bridging between microspheres.

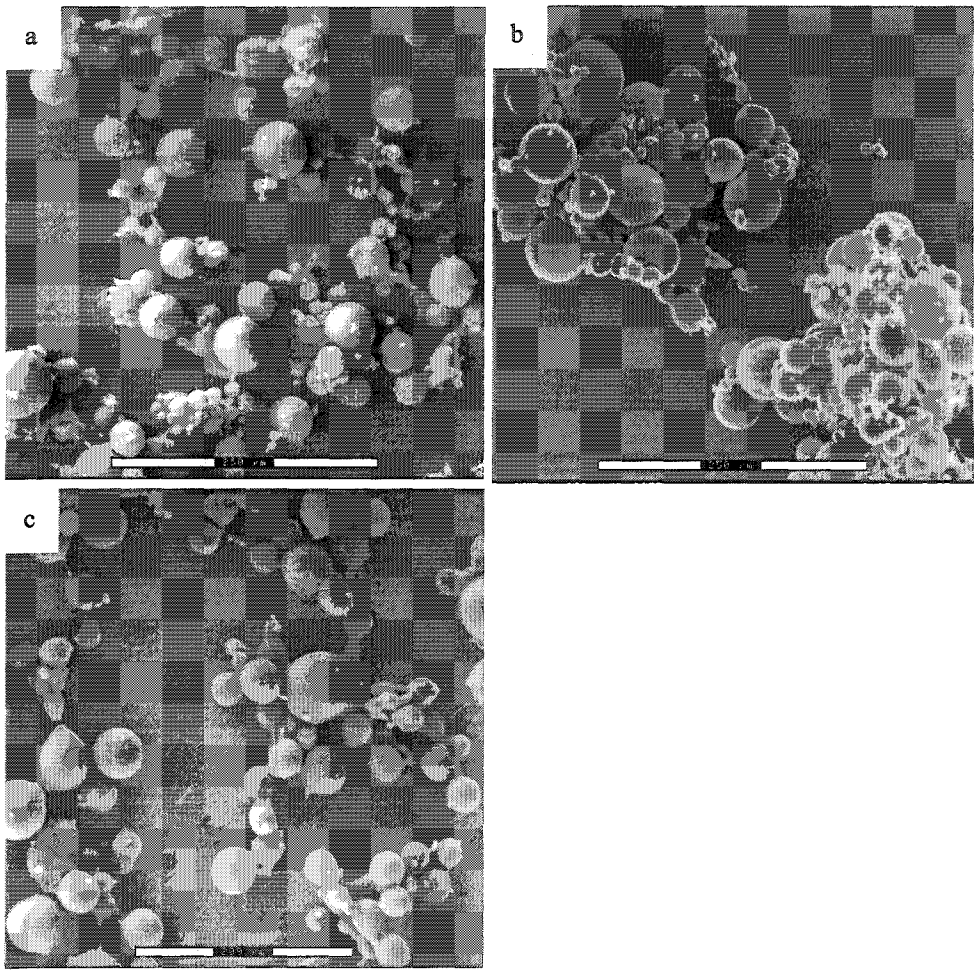


**Figure 4.9** ESEM images of hydrogel microspheres prepared by crosslinking DMA-*co*-GMA43 coacervates at 40°C with (a) TEPA, (b) linear PEI 423, (c) branched PEI 1800. Reaction conditions are those shown in Figure 4.6. Scale bars are 250 μm.

Increasing the polymer concentration increases both the amount of coacervate dispersed in the continuous medium and the viscosity. In turn, this leads to larger particle sizes and broader size distributions (Figures 4.10).

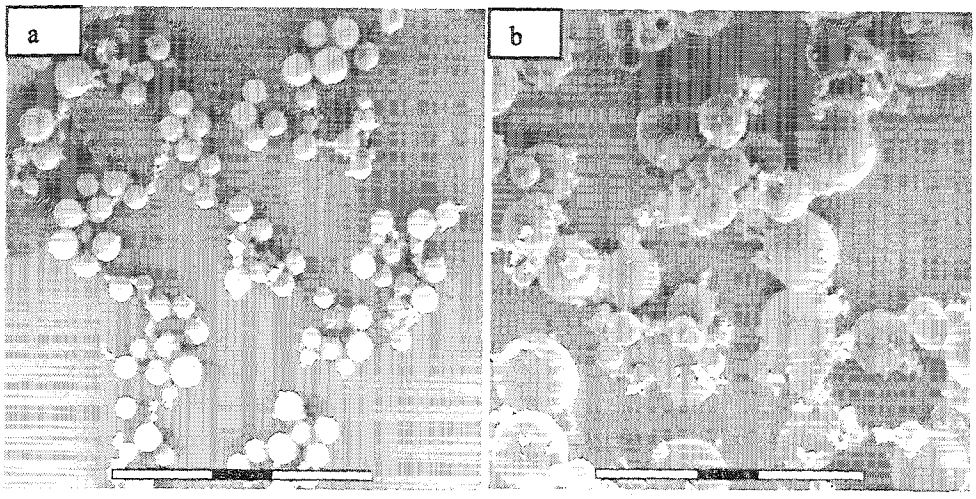


**Figure 4.10** ESEM images of hydrogel microspheres prepared at 40°C from 30 mL of (a) 0.2 wt % (b) 2.0 wt% DMA-*co*-GMA43 solutions and ethylene diamine. Amine to polymer ratio was held constant, and reaction conditions are those shown in Figure 4.6. Scale bars are 250 μm.

### 4.2.5 Effect of adding PVP

As discussed above, PVP has no significant effect on the phase transition temperature of DMA-*co*-GMA solutions, and hence apparently does not bind to the copolymer below its cloud point. However, PVP may bind to the more hydrophobic

coacervate, and hence may provide some steric stabilization to the droplets, and to the crosslinked microspheres. Figure 4.11 shows that addition of 1 wt % PVP reduces the particle size and the degree of aggregation, compared to Figure 4.8a.

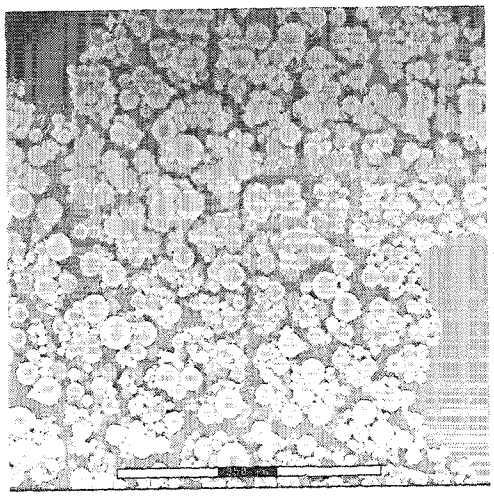

**Figure 4.11** ESEM images of hydrogel microspheres prepared from DMA-*co*-GMA43 coacervates in presence of 1 wt % PVP at 40°C. Reaction conditions are same as described in Figure 4.8a. Scale bar is 250 μm.

## 4.3 Conclusion

Poly(*N,N*-dimethacrylamide-*co*-glycidyl methacrylate) (DMA-*co*-GMA) copolymers have been prepared by free radical copolymerizations. The thermal phase separation of DMA-*co*-GMA aqueous solutions is a coacervation process, and the phase transition temperature decreases with increasing GMA content.

The DMA-*co*-GMA coacervate droplets can be crosslinked by adding diamines and small polyamines. The yield, size and size distribution of the resulting hydrogel microspheres increases with increasing reaction temperature and polymer concentration. The size and aggregation of the microspheres can be reduced by addition of PVP.

**References**


1. Pelton, R. *Adv. Colloid Interface Sci.* **2000**, *85*, 1-33.
2. Zhu, P. W.; Napper, D. H. *J. Colloid Interface Sci.* **1994**, *168*, 380-385.
3. Wu, C.; Zhou, S. *Macromolecules* **1995**, *28*, 8381-8387.
4. Zhu, P. W.; Napper, D. H. *Langmuir* **1996**, *12*, 5992-5998.
5. Qiu, X; Wu, C. *Macromolecules* **1997**, *30*, 7921-7926.
6. Maeda, Y.; Higuchi, T.; Ikeda, I. *Langmuir* **2000**, *16*, 7503-7509.
7. Maeda, Y.; Nakamura, T.; Ikeda, I. *Macromolecules* **2001**, *34*, 1391-1399.
8. Mueller, K. F. *Polymer* **1992**, *33*, 3470-3476.
9. Miyazaki, H.; Kataoka, K. *Polymer* **1996**, *37*, 681-685.
10. Shibanuma, T.; Aoki, T.; Sanui, K.; Ogata, N.; Kikucji, A.; Sakurai, Y., Okano, T. *Macromolecules* **2000**, *33*, 444-450.
11. Yamamoto, K.; Serizawa, T.; Akashi, M. *Macromol. Chem. Phys.* **2003**, *204*, 1027-1033.
12. Yang, G.; Woodhouse, K. A.; Yip, C. M. *J. Am. Chem. Soc.* **2002**, *124*, 10648-10649.
13. Betre, H.; Setton, L. A.; Meyer, D. E.; Chilkoti A. *Biomacromolecules* **2002**, *3*, 910-916.
14. Burgess, D. J. *J. Colloid Interface Sci.* **1990**, *140*, 227-238.
15. Menger, F. M.; Sykes, B. M. *Langmuir* **1998**, *14*, 4131-4137.
16. Menger, F. M.; Peresypkin, A. V.; Caran, K. L.; Apkarian, R. P. *Langmuir* **2000**, *16*, 9113-9116.
17. Arshady, R.; *Polym. Eng. Sci.* **1990**, *30*, 905-914.

18. Prokop, A.; Hunkeler, D.; DiMari, S.; Haralson, M.; Wang, T.G. *Adv. Polym. Sci.* **1998**, *136*, 1-51.

19. Wen, Y.; Dubin, P. L. *Macromolecules* **1997**, *30*, 7856-7861.

20. Kaibara, K.; Okazaki, T.; Bohidar, H. B.; Dubin, P. L. *Biomacromolecules* **2000**, *1*, 100-107.

21. Burgess, D. J.; Singh, O. N. *J. Pharm. Pharmacol.* **1993**, *45*, 586-591.

22. Chandy, T; Mooradian, D. L.; Rao, G. H. *J. Appl. Polym. Sci.* **1998**, *70*, 2143-2153.

23. Tiyaboonchai, W.; Woiszwillo, J.; Middaugh, C. R. *J. Pharm. Sci.* **2001**, *90*, 902-914.

24. Cohen, S.; Baño, M. C.; Visscher, K. B.; Chow, M.; Allcock, H. R.; Langer, R. *J. Am. Chem. Soc.* **1990**, *112*, 7832-7833.

25. Wen, S.; Yin, X.; Stevenson, W. T. K. *Biomaterials* **1991**, *12*, 374-384.

26. Andrianov, A. K.; Chen, J.; Payne, L. G. *Biomaterials* **1998**, *19*, 109-115.

27. Yin, X.; Stöver, H. D. H. *Macromolecules,* **2003**, *36*, 8773-8779.

28. Yin, X.; Stöver, H. D. H. *Macromolecules* **2002**, *35*, 10178-10181.

29. Cellesi, F.; Tirelli, N.; Hubbell, J.A. *Macromol. Phys. Chem.* **2002**, *203*, 1466-1472.

30. Miron, Y.; Morawetz, H. *Macromolecules* **1969**, *2*, 162-165.

31. Virtanen, J.; Tenhu, H. *J. Polym. Sci. Part A: Polym. Chem.* **2001**, *39*, 3716-3725.

32. Idziak, I.; Avoce, D.; Lessard, D.; Gravel, D.; Zhu, X. X. *Macromolecules* **1999**, *32*, 1260-1263.

33. Schild, H. G.; Tirrell, D. A. *Langmuir* **1991**, *7*, 665-671.

34. Lee, L.; Cabane, B. *Macromolecules* **1997**, *30*, 6559-6566.

35. Subotic, D. V.; Wu, X. Y. *Ind. Eng. Chem. Res.* **1997**, *36,* 1303-1309.

# Chapter 5 Temperature-Sensitive Hydrogel Microspheres Formed by Liquid-Liquid Phase Transitions of Aqueous Solutions of Poly(*N,N*-dimethylacrylamide-*co*-Allyl Methacrylate)


## Abstract

Poly(*N,N*-dimethylacrylamide-*co*-allyl methacrylate) (DMA-*co*-AMA) copolymers were prepared by copolymerizing DMA with the hydrophobic comonomer AMA. The methacryloyl group of AMA reacted preferentially, resulting in pendant allyl groups along the copolymer chains. Aqueous solutions of these DMA-*co*-AMA copolymers were thermo-responsive, and showed liquid-liquid phase transitions at temperatures depending on the AMA content. Hydrogel microspheres were prepared from these thermally phase-separated liquid microdroplets by free radical crosslinking of the pendant allyl groups. The resulting microspheres retained some of the thermo-responsive properties of their precursor polymers. The morphologies of microspheres as a function of reaction temperature and amount of initiator were described. This chapter has been reproduced with permission from *J. Polym. Sci., Part A: Polym. Chem.*, submitted for publication. Copyright 2004 John Wiley &Sons.


## 5.0 Introduction

Polymer hydrogels that undergo phase transitions in response to changes in temperature, pH and solvency are gaining attention as media for separation,

immobilization and controlled delivery of proteins.[1,2] Such hydrogels may be prepared either by crosslinking stimuli-responsive polymers directly,[3] or by immobilizing the polymer onto a substrate.[4]

The most widely studied responsive polymer hydrogels are those based on alkylacrylamide polymers, especially poly(*N*-isopropylacrylamide) (pNIPAM). pNIPAM hydrogels undergo a volume transition in water upon heating above 32°C, wherein the hydrophilic extended coils collapse into hydrophobic globules,[5] causing the gels to shrink and expel most of the absorbed water. This reversible process allows pNIPAM hydrogels to bind proteins through hydrophobic interaction at high temperatures, followed by release at low temperatures.[6-8]

As there is some concern that the liquid-solid precipitation of pNIPAM solution may cause some protein denaturation, liquid-liquid polymer phase separations may offer a milder approach to protein separation.[9,10] One example is the thermally induced liquid-liquid phase separation of elastin-like polypeptide solutions used for purifying proteins from the cell lysates.[11,12]

The term coacervation describes the liquid-liquid phase separations of aqueous polymer solutions into a polymer-rich coacervate phase and a polymer-lean equilibrium phase.[13-15] Complex coacervation is induced by complexation between oppositely charged polyelectrolytes, while simple coacervation is based on changing the solvent composition or the solution temperature. The coacervate phase usually contains more than 60% water, while the equilibrium phase is 99+% aqueous. Proteins will partition between these two immiscible aqueous phases according to their hydrophilicity, and the

high water content of both phases reduces the risk of protein denaturation or precipitation during the separation process. The current bottleneck in using coacervation for industrial protein purification lies in the separation of the target protein from the coacervate polymer. Such problems may be addressed by crosslinking the liquid coacervate into hydrogels.[16]

Recently, our group has developed hydrogel microspheres using both polyelectrolyte complexation and thermally induced simple coacervation.[17,18] The hydrogel microspheres formed upon crosslinking the thermally induced coacervate of poly(*N,N*-dimethylacrylamide-*co*-glycidyl methacrylate) (DMA-*co*-GMA) copolymers using amines were colloidally stable, but had lost their thermo-responsive properties due to the presence of amines in the polymer networks.[18]

The present hydrogel microspheres are designed to be crosslinked without changing the hydrophilic/hydrophobic balance of the polymer in order to retain their thermosensitive properties. Specifically, we prepare the copolymers of DMA with allyl methacrylate (AMA), where AMA units serve both to increase the hydrophobicity of the copolymer to permit thermally induced phase separation, and to allow covalent post-crosslinking of the coacervate by a free radical reaction.

## 5.1 Experimental

### 5.1.1 Materials

*N,N*-Dimethylacrylamide (DMA, 99w%), allyl methacrylate (AMA, 98 wt %), and *N, N, N',N'*-tetramethylethylenediamine (TEMED) were obtained from Aldrich.

2,2'-azobis(2,4-dimethyl valeronitrile) (ADVN) was obtained from Polysciences Inc., and ammonium persulfate (APS) was obtained from BDH. Tetrahydrofuran (THF), acetone, and pentane were obtained from Caledon Laboratories. All chemicals were used as received.

**5.1.2 Preparation of Poly(*N,N*–Dimethylacrylamide-*co*-Allyl Methacrylate) (DMA-*co*-AMA) Copolymers.**

For a typical procedure, *N,N*-dimethylacrylamide (8.0 g, 0.08 mol) and allyl methacrylate (0.02mol, 2.57 g) were dissolved in 90 mL of THF in a 125 mL HDPE plastic screw cap bottle. ADVN (0.138g, 0.5mmol, 0.5 mol % relative to monomers) was added. Polymerizations were carried out at 55°C for 1 hour by rolling the bottles in a thermostated reactor fitted with a set of horizontal rollers. The polymer solution was precipitated into 300 mL of pentane. The product was redissolved in acetone and reprecipitated into pentane, and dried under vacuum at 40°C to provide 2.5 g of polymer (yield, 24%).

Molecular weights of copolymers were determined using a gel permeation chromatograph consisting of a Waters 515 HPLC pump, three ultrastyragel columns (500-20k, 500-30k, 5k-600k Daltons) and a Waters 2414 refractive index detector, using THF as solvent at a flow rate of 1 mL $min^{-1}$, and narrow disperse polystyrene as calibration standards.

$^1H$ NMR spectra of the copolymers were recorded on a Bruker AC 200, using chloroform-*d* as the solvent.

### 5.1.3 Cloud Point Measurement

The cloud points of aqueous solutions of DMA-*co*-AMA copolymers were measured using an automatic PC-Titrator (Mandel) equipped with a temperature probe and with a photometer incorporating a 1 cm path length fiber optics probe (GT-6LD, Mitsubishi). The turbidity of the solution was recorded as photoinduced voltage (mV). The phase transition temperature was defined as the inflection point of the mV vs. temperature curve, as determined by the maximum in the first derivative. The heating rate and the concentration of polymer solutions were 1.0°C $min^{-1}$ and 0.5 wt % respectively.

### 5.1.4 Preparation of Hydrogel Microspheres

The DMA-*co*-AMA copolymers were dissolved in distilled water at a temperature below the phase transition temperature. The solutions were stirred, and heated above the phase separation temperature to induce coacervation. After phase equilibration, APS and TEMED solutions were added to initiate the crosslinking of coacervates.

In a typical reaction, 100 g of 0.5 wt % DMA-*co*-AMA-28 solution was stirred at 500 RPM and 30°C in a 100 mL Buchi Miniclave Drive glass reactor. After addition of APS (1.0 mL, 1.0 mol $L^{-1}$) and TEMED (1.0 mL, 1.0 mol $L^{-1}$), the system was stirred for another 2 hours. The resulting microspheres were separated by centrifugation at 4500 RPM for 5 min and washed 3 times with distilled water. The products were dried in a vacuum at 65°C to provide 0.09 g of microspheres (yield, 18 %).

### 5.1.5 Characterization of Hydrogel Microspheres

Optical images of the microspheres were recorded at room temperature using an Olympus BH-2 microscope equipped with a Kodak DC 120 Zoom digital camera. The mean diameter of the microspheres was estimated by analyzing about 200 particles using UTHSCSA Image Tool software.

Electron micrographs of the microspheres were obtained using a Phillips ElectroScan 2020 environmental scanning electron microscope (ESEM). ESEM samples were prepared by depositing a drop of aqueous microsphere suspension onto a glass-covered ESEM stub, drying under vacuum and sputter-coating with an about 5 nm thick layer of gold.

Transmission electron microscope (TEM) images of microspheres were obtained using a JEOL 1200EX microscope, the microspheres were embedded in Spurr epoxy resin and microtomed to about 100 nm thickness.

Solid state $^{13}C$ cross-polarization magic angle spinning (CP-MAS) NMR spectroscopy was carried out on a Bruker AC 300 at 10 kHz spinning rate.

## 5.2 Results and Discussion

### 5.2.1 Synthesis and Thermoresponsive Properties of DMA-*co*-AMA Copolymers

Poly(*N,N*-dimethylacrylamide-*co*-allyl methacrylate) (DMA-*co*-AMA) copolymers were prepared by copolymerizing DMA with AMA in THF at 55°C.

Conversions were kept below 30% to keep the copolymer compositions close to the comonomer ratios, as well as to prevent crosslinking through the pendant allyl groups.

Figure 5.1 shows a typical $^1$H NMR spectrum of a DMA-*co*-AMA copolymer, with peak assignments made according to literature.[18-20] The peak areas for the protons *g, h, f, e* of the AMA units scale according to 1:2:2:3, confirming that the allyl groups of AMA remain almost unreacted during the copolymerization process.

The copolymer compositions shown in Table 5.1 were estimated from the ratio of peak areas for protons *g* of the AMA units (1H) vs. protons *a* plus *c* of the DMA units (7H).

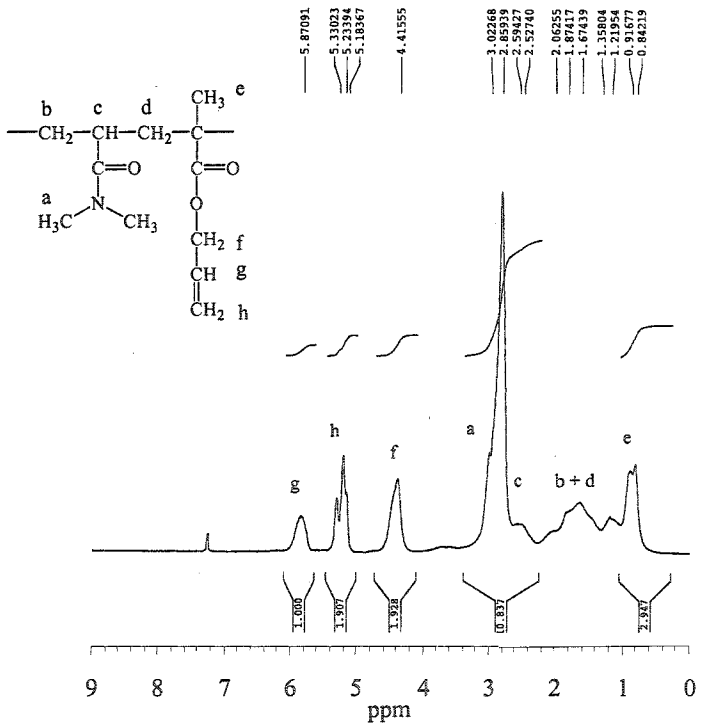


**Figure 5.1** $^1$H NMR spectrum of DMA-*co*-AMA-40 obtained in chloroform-*d*

**Table 5.1** Preparation and phase transition temperatures ($T_p$) of poly(DMA-*co*-AMA).

| DMA-*co*-AMA Copolymer | mol % AMA in feed | mol % AMA in polymer [a] | Yield (wt %) | $M_n$ [b] | $M_w/M_n$ [b] | $T_p$ [c] (°C) |
|---|---|---|---|---|---|---|
| DMA-*co*-AMA-14 | 11.1 | 14 | 32 | $9.2 \times 10^3$ | 1.9 | 72.0 |
| DMA-*co*-AMA-19 | 14.3 | 19 | 29 | $1.0 \times 10^4$ | 2.2 | 54.0 |
| DMA-*co*-AMA-21 | 16.7 | 21 | 26 | $1.2 \times 10^4$ | 2.3 | 40.6 |
| DMA-*co*-AMA-23 | 18.2 | 23 | 24 | $1.3 \times 10^4$ | 2.2 | 29.4 |
| DMA-*co*-AMA-28 | 20.0 | 28 | 24 | $1.3 \times 10^4$ | 2.3 | 23.1 |
| DMA-*co*-AMA-30 | 22.2 | 30 | 21 | $1.2 \times 10^4$ | 2.1 | 15.7 |
| DMA-*co*-AMA-40 | 28.6 | 40 | 18 | $1.4 \times 10^4$ | 2.3 | not soluble |

[a] Estimated by $^1$H NMR. [b] Determined by GPC. [c] Measured by the cloud point method with 0.5 wt% aqueous polymer solutions.

While aqueous solutions of DMA homopolymer are not thermo-responsive, their copolymers with hydrophobic comonomers such as AMA cause their solutions to undergo thermally induced phase separation. Figure 5.2 shows the phase transitions of dilute DMA-*co*-AMA solutions upon heating, with the corresponding phase transition temperatures shown in Table 5.1. For example, a 0.5 wt % solution of DMA-*co*-AMA-14 containing 14 mol% AMA shows a phase transition temperature ($T_p$) of 72°C. The $T_p$ decreases with increasing AMA content, with DMA-*co*-AMA-30 having a $T_p$ of 15.7°C, and DMA-*co*-AMA-40 not being water-soluble even at 0°C.

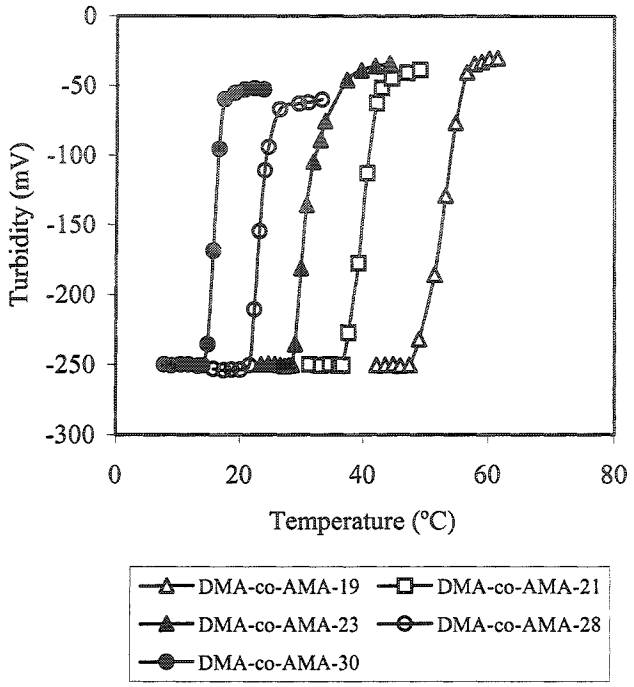


**Figure 5.2** Phase transition curves for 0.5 wt% DMA-*co*-AMA aqueous solutions as measured by the cloud point method. The vertical axis shows the photo-induced voltage due to 180° transmitted light, with -250 mV corresponding to a transparent solution.

As previously discussed,[18,21] the thermally induced phase transition of aqueous solutions of such DMA copolymers is a liquid-liquid coacervation. Figure 5.3 shows an optical microscope image of a 0.5 wt % DMA-*co*-AMA-30 solution at room temperature, showing the corresponding liquid coacervate droplets. These droplets are not colloidally stable and coalesce within several minutes in the absence of stirring. The phase transition is reversible upon cooling.

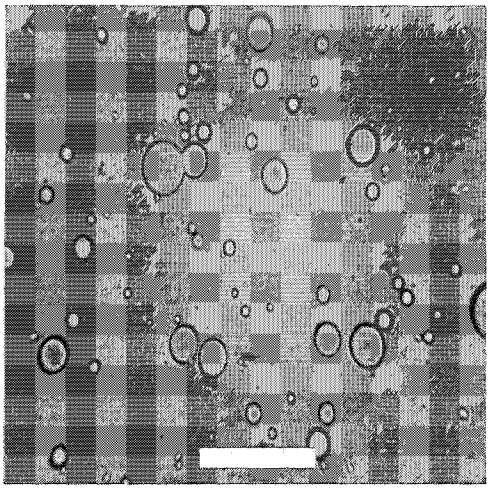

**Figure 5.3** Optical microscope image of coacervate droplets formed from 0.5 wt % DMA-*co*-AMA-30 solution ($T_p$, 15.7°C) at room temperature. Scale bar is 250 μm.

### 5.2.2 Preparation of Coacervate Hydrogel Microspheres

Hydrogel microspheres were formed by free radical crosslinking of the thermally induced DMA-*co*-AMA coacervate droplets through the pendant allyl groups. This crosslinking can involve addition of radicals to allylic double bonds, or coupling to allylic radicals.[22, 23]

The redox initiation system of ammonium persulfate/*N, N, N',N'*-tetramethylethylenediamine was chosen since it can be used to generate radicals over a

wide temperature range. Typical optical micrographs of the formed crosslinked microparticles are shown in Figure 5.4A, and the results are summarized in Table 5.2.

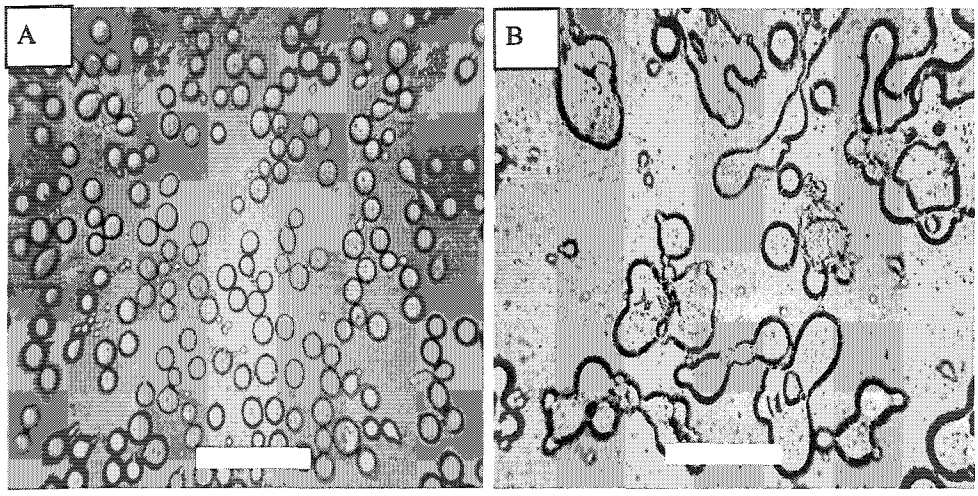


**Figure 5.4** Optical microscope images of particles prepared by crosslinking 100g of 0.5 wt% DMA-*co*-AMA-28 ($T_p$, 23.1°C) coacervate mixture with APS (1.0 mL, 1.0 mol $L^{-1}$) and TEMED (1.0 mL, 1.0 mol $L^{-1}$) at 30°C (A), and 40°C (B). The images were recorded at room temperature, while wet. Scale bars are 250 μm.

**Table 5.2** Free radical crosslinking of thermally induced DMA-*co*-AMA coacervates. [a]

| DMA-*co*-AMA Copolymer | $T_p$ of polymer (°C) | Reaction temp. (°C) | Yield [b] (wt %) | Mean diameter [c] (μm) |
|---|---|---|---|---|
| DMA-*co*-AMA-19 | 54.0 | 60 | 8.8 | 18 ± 6 |
| DMA-*co*-AMA-19 | 54.0 | 70 | 22 | 30 ± 9 |
| DMA-*co*-AMA-19 | 54.0 | 80 | 25 | 72 ± 26 |
| DMA-*co*-AMA-21 | 40.6 | 45 | 13 | 14 ± 4 |
| DMA-*co*-AMA-21 | 40.6 | 55 | 18 | 33 ± 9 |
| DMA-*co*-AMA-21 | 40.6 | 65 | 29 | 50 ± 11 |
| DMA-*co*-AMA-21 | 40.6 | 75 | 44 | Gel precipitate |
| DMA-*co*-AMA-23 | 29.5 | 35 | 8.2 | 19 ± 5 |
| DMA-*co*-AMA-23 | 29.5 | 45 | 25 | 60 ± 15 |
| DMA-*co*-AMA-23 | 29.5 | 55 | 29 | Gel precipitate |
| DMA-*co*-AMA-28 | 23.1 | 30 | 18 | 35 ± 6 |
| DMA-*co*-AMA-28 | 23.1 | 40 | 26 | Gel precipitate |
| DMA-*co*-AMA-30 | 15.7 | 20 | 15 | 34 ± 5 |
| DMA-*co*-AMA-30 | 15.7 | 30 | 28 | 61 ± 14 |
| DMA-*co*-AMA-30 | 15.7 | 40 | 32 | Gel precipitate |

[a] 100 g of 0.5 wt % polymer solution was used and was crosslinked with APS (1.0 mL, 1.0 mol $L^{-1}$) and TEMED (1.0 mL, 1.0 mol $L^{-1}$). [b] Calculated from the weight percentage of particles over polymers used. [c] Particles were suspended in water at room temperature.

Radical crosslinking at temperatures below the $T_p$ of 0.5 wt % copolymer solutions did not result in noticeable gelation. Hydrogel microspheres were formed by crosslinking the thermally induced coacervates of all tested copolymer compositions at temperature just above the $T_p$. Figure 5.4A illustrates the hydrogel microspheres formed from DMA-*co*-AMA-28 at 30°C. The coacervate phase is a highly concentrated polymer solution and the polymer chains are severely entangled, allowing for efficient radical crosslinking.

As shown in Figure 5.4B and Table 5.2, heating the coacervate to temperatures much above their $T_p$ led to gel precipitation, and subsequent radical crosslinking as larger, irregular particles. These results indicate that aqueous solutions of DMA-*co*-AMA copolymers first separate as liquid coacervates, and dehydrate further to form gel precipitates with increasing temperature.

The DMA-*co*-GMA copolymer reported earlier did not show such gel precipitation upon heating above their $T_p$, but instead only liquid-liquid phase separations even at elevated temperatures.[18] It appears that the more hydrophobic allyl methacrylate promotes further desolvation and collapse of the copolymer chain upon heating.

In analogy to these earlier DMA-*co*-GMA copolymers,[18] the microsphere yields increase with crosslinking temperatures (Table 5.2). This is again attributed to the composition distribution of the copolymer and to the loss of some copolymer to the equilibrium phase. Due to the different reactivity ratios of DMA and AMA, chains formed early during the polymerization contain more AMA, and are hence more hydrophobic, than chains formed later. This compositional distribution would broaden the

temperature range over which coacervation occurs. The fairly broad molecular weight distribution will also influence the phase transition temperature and the efficiency of phase transitions.[24] In a forthcoming paper, we will investigate the thermally induced coacervation of DMA copolymers with tailored composition distribution and molecular weight distribution, prepared using living/controlled radical polymerizations.

The microsphere size and size distribution increase with reaction temperature (Table 5.2), likely due to loss of colloidal stability of the coacervate.

### 5.2.3 Morphologies of Coacervate Microspheres

The crosslinked coacervate microspheres maintain their spherical shapes in aqueous suspension even upon cooling below the phase transition temperature of the corresponding copolymers. Figure 5.5A and B show room temperature optical images of wet and dry crosslinked coacervate microspheres prepared from DMA-*co*-AMA-19 ($T_p$, 54°C).

Environmental scanning electron microscope (ESEM) image of these dry microspheres show raisin-like shapes (Figure 5.5C), indicating that the particles surfaces are more crosslinked than their cores. Preferential crosslinking at the surface is in agreement with the hydrophilic APS and TEMED residing mainly in the aqueous equilibrium phase, and with the fact that diffusion of radicals into the coacervate would become more difficult as the crosslinking proceeds. The dried particles can regain their spherical shape when redispersed in water.

Transmission electron microscopy (TEM) was used to study the internal structure of the coacervate microspheres. The crosslinked particles were extracted with distilled

water at low temperature to remove any uncrosslinked copolymers. The TEM images (Figure 5.5D) show smooth, resin-swollen interiors. A slightly darker line of the particle surface may correspond to higher crosslinking density. This will be studied in future using scanning transmission X-ray Microscopy (STXM).

Crosslinking the DMA-*co*-AMA-19 coacervate at 70 and 80°C leads to larger raisin-shaped microspheres, as shown in Figure 5.6.

The amount of APS/TEMED added affects the crosslinking efficiency of the coacervates. No stable microspheres are observed upon adding 0.5 mL of 1.0 mol $L^{-1}$ APS/TEMED, indicating that the concentration of initiators is too low to diffuse into and crosslink the coacervates efficiently. Rather, the microspheres coalesce upon drying (Figure 5.7A). Microspheres prepared at higher initiator concentrations show spherical shapes, and a smoother surface upon drying, in agreement with higher crosslinking efficiency (Figure 5.7 B). Increasing the reaction time from 2 to 4 and 24 hrs did not affect microsphere morphology significantly (Figure 5.7 B-D).

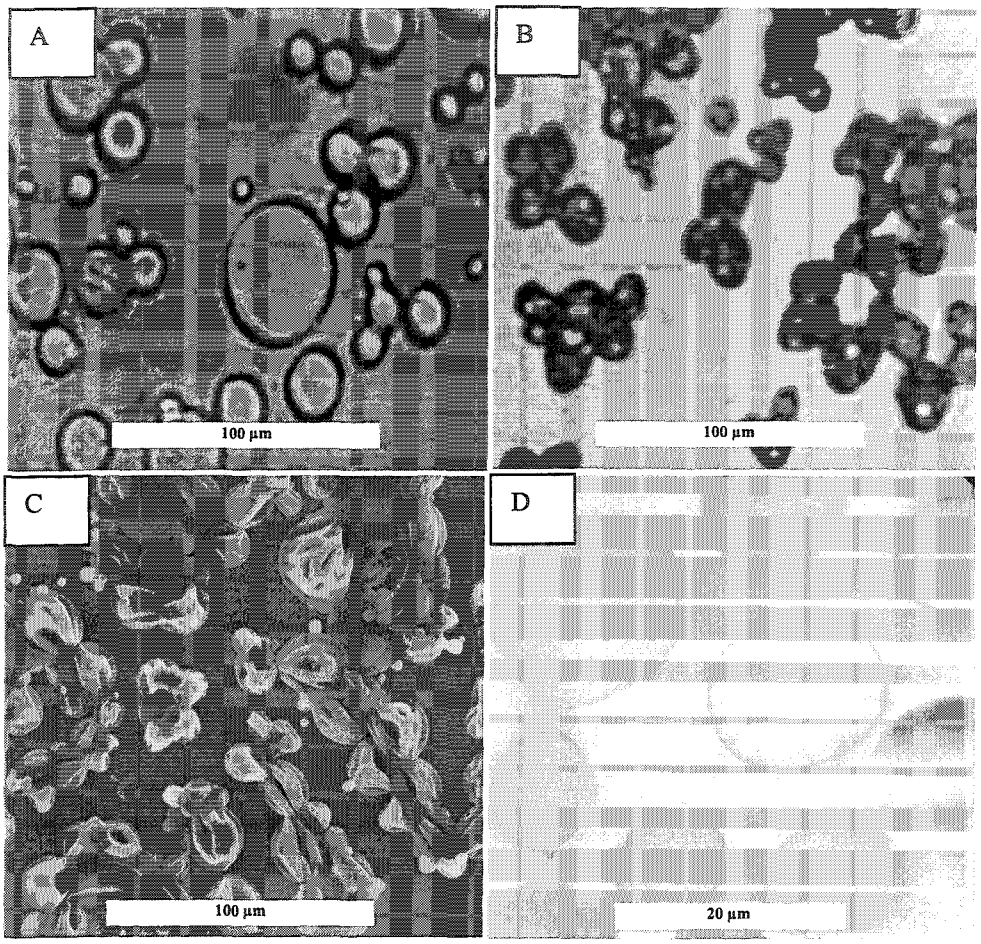


**Figure 5.5** Microscope images of particles prepared by crosslinking DMA-*co*-AMA-19 ($T_p$, 54°C) coacervate with APS (1.0 mL, 1.0 mol $L^{-1}$) and TEMED (1.0 mL, 1.0 mol $L^{-1}$) at 60°C for 2hrs. (A) Optical micrograph of wet particles, (B) Optical micrograph of dry particles, (C) ESEM image of dry particles, (D) TEM image of particles embedded in Spurr epoxy.

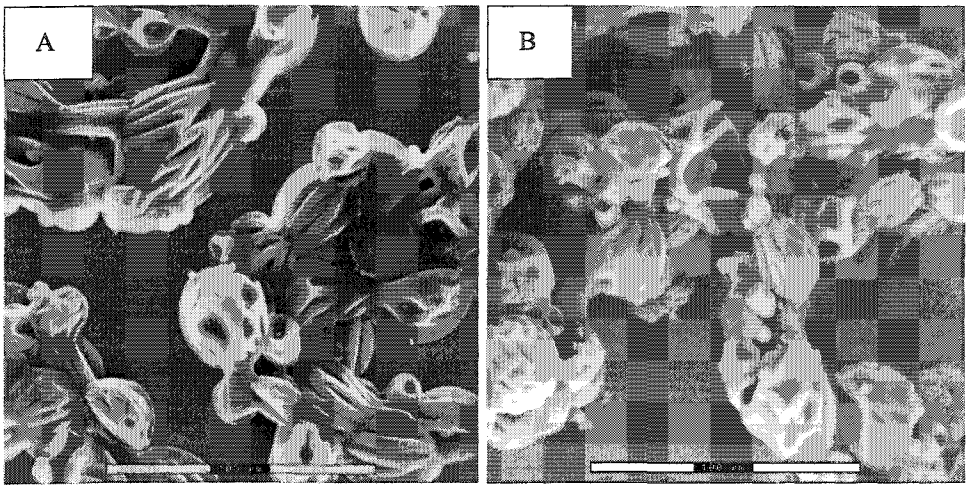


**Figure 5.6** ESEM images of microspheres formed by crosslinking DMA-*co*-AMA-19 ($T_p$, 54°C) coacervate mixture with APS (1.0 mL, 1.0 mol $L^{-1}$) and TEMED (1.0 mL, 1.0 mol $L^{-1}$) at 70°C (A), and 80°C (B). Scale bars are 100 μm.

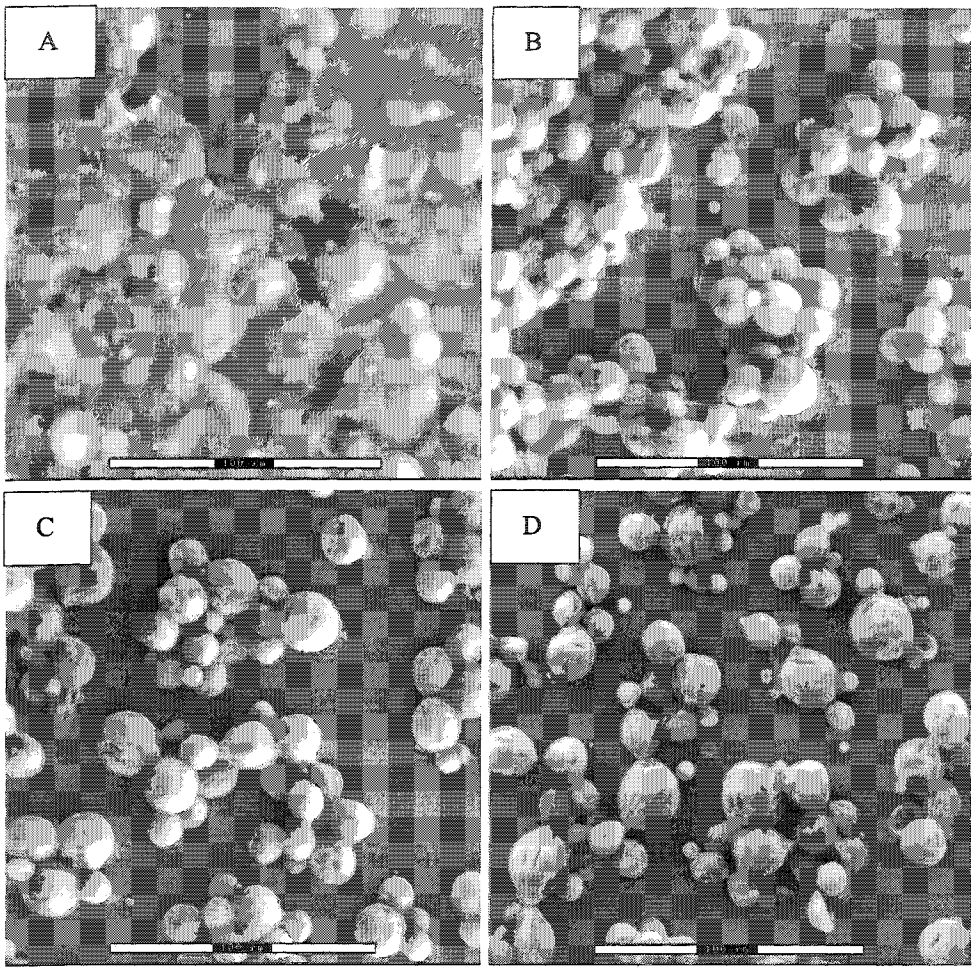


**Figure 5.7** ESEM micrographs of microspheres formed by crosslinking DMA-*co*-AMA-19 ($T_p$, 54°C) coacervate mixtures at 60°C with (A) 0.5 mL of 1.0 mol $L^{-1}$APS/TEMED for 2 hrs, (B) 4.0 mL of 1.0 mol $L^{-1}$APS/TEMED for 2 hrs, (C) 4.0 mL of 1.0 mol $L^{-1}$ APS/TEMED for 4 hrs, and (D) 4.0 mL of 1.0 mol $L^{-1}$APS/TEMED for 24 hrs. Scale bars are 100 μm.

### 5.2.4 Characterization of Coacervate Microspheres

$^{13}C$ CP-MAS NMR spectroscopy was used to characterize the crosslinked microspheres formed from DMA-*co*-AMA-19, and specifically to try to determine the conversion of allyl groups during the crosslinking reaction. Figure 5.8 shows the spectrum of the crosslinked microspheres formed by reacting DMA-*co*-AMA-19 coacervate with 4 mL of 1.0 mol L-1 APS/TEMED at 60°C for 2 hrs. The carbonyl carbons of the ester and amide groups appear at 175ppm, the vinyl carbons at 133 and 119 ppm, and the methylene oxy carbon of AMA at 66 ppm. The peak areas for the allyl double bond carbons and the allylic methylene carbon have decreased by roughly 40% and 15%, respectively, relative to the precursor copolymer. Reaction with less APS/TEMED resulted in correspondingly lower allyl group conversions. We cannot currently determine which fraction of allyl groups have formed actual crosslinks, as opposed to having simply been subjected to a radical reaction.

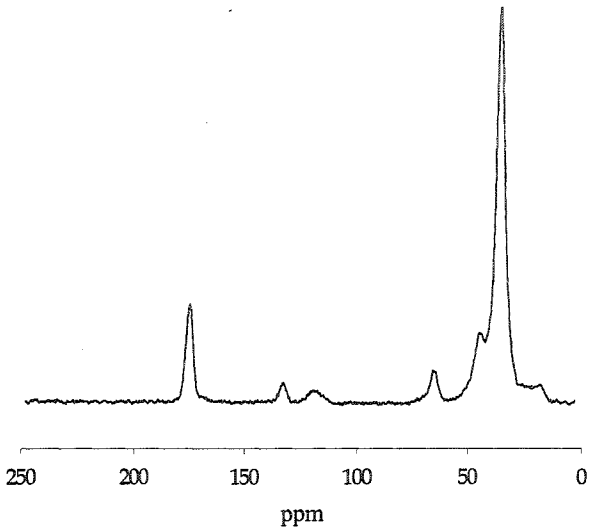


**Figure 5.8** $^{13}C$ CP-MAS NMR spectrum of crosslinked coacervate microspheres prepared from DMA-*co*-AMA-19 copolymer according to the conditions in Figure 5.7B.

It is well known that the thermal response of pNIPAM hydrogel can be detected by conventional thermal analysis such as differential scanning calorimetry (DSC).[25] DSC has also been applied to study the liquid-liquid phase transition of elastin-like polypeptide.[26] However, we cannot detect the phase transitions of both DMA-*co*-AMA aqueous solution and coacervate microspheres by conventional DSC measurements, even with 10 wt % of copolymer solutions. Besides the relatively small enthalpy changes of the liquid-liquid phase transition, the broad distribution of polymer composition due to the free radical copolymerization should also broaden the DSC signal.

Packing the crosslinked coacervate microspheres into a glass tube permits observation of a reversible volume transition upon changing the temperature. The volume of the coacervate microspheres prepared from DMA-*co*-AMA-28 ($T_p$, 23.1°C) at 30°C shrinks by about 20% upon increasing the temperature from 20 to 30°C, and coacervate microspheres prepared from DMA-*co*-AMA-30 ($T_p$, 15.7 °C) at 20°C show a 15% volume change between 10 and 20°C. These volume changes are temperature-reversible. In contrast to pNIPAM microgels,[3] the relatively small macroscopic volume transition of the present microspheres is anticipated, given the liquid-liquid phase transition as well as their inhomogeneous crosslink distribution.

## 5.3 Conclusion

Aqueous solutions of poly(*N,N*-dimethacrylamide-*co*-allyl methacrylate) (DMA-*co*-AMA) copolymers prepared by free radical polymerizations show continuous solution/coacervate/gel precipitate phase transitions upon heating. The polymer first separates from the solution as a liquid coacervate at temperatures slightly above the corresponding transition temperatures, and forms gel precipitates at high temperatures. The phase transition temperature depends on the AMA content in the copolymers.

Novel thermo-sensitive hydrogel microspheres were prepared by thermally induced coacervation of DMA-*co*-AMA aqueous solution followed by radical crosslinking. The size and size distributions of the microspheres increase with increasing reaction temperatures, which are attributed to the increase in the coacervate amount, and a decrease in the colloidal stability of the coacervate droplets. The amount of initiator added affects the crosslinking efficiency, and hence the morphology of the microspheres. The formed coacervate microspheres are thermo-responsive indicating that such materials may find applications in protein separation and protein delivery.

**References:**


1. Kost, J.; Langer, R. *Adv. Drug Deliv. Rev.* **2001**, *46*, 125-148.
2. Ding, Z.; Fong, R. B.; Long, C. J.; Stayton, P. S.; Hoffman, A. S. *Nature (London)* **2001**, *411*, 59-62.
3. Pelton, R. *Adv. Colloid Interface Sci.* **2000**, *85*, 1-33.
4. Nath, N.; Chilkoti, A. *Adv. Mater.* **2002**, *14*, 1243-1247.
5. Wu, C.; Zhou, S. *Macromolecules* **1995**, *28*, 8381-8387.
6. Sassi, A. P.; Shaw, A. J.; Han, S.; Blanch, H. W.; Prausnitz, J. M. *Polymer* **1996**, *37*, 2151-2164.
7. Kobayashi, J.; Kikuchi, A.; Sakai, K.; Okano, T. *Anal. Chem.* **2003**, *75*, 3244-3249.
8. Cunliffe, D.; Alarcón, C. D. L. H.; Peters, V.; Smith, J. R.; Alexander, C. *Langmuir* **2003**, *19*, 2888-2899.
9. Johansson, H. O.; Persson, J.; Tjerneld, F. *Biotechnol Bioeng.* **1999**, *66*, 247-257.
10. Pietruszka, N.; Galaev, I. Y.; Kumar, A.; Brzozowski, Z. K.; Mattiasson, B. *Biotechnol. Prog.* **2000**, *16*, 408-415.
11. Meyer, D. E.; Chilkoti, A. *Nature Biotechnol.* **1999**, 17, 1112.
12. Meyer, D. E.; Carlson, K. T.; Chilkoti, A. *Biotechnol. Prog.* **2001**, *17*, 720-728.
13. Burgess, D. J. *J. Colloid Interface Sci.* **1990**, *140*, 227-238.
14. Menger, F. M.; Sykes, B. M. *Langmuir* **1998**, *14*, 4131-4137.
15. Menger, F. M.; Peresypkin, A. V.; Caran, K. L.; Apkarian, R. P. *Langmuir* **2000**, *16*, 9113-9116.
16. Gehrke, S. H.; Vaid, N. R.; Mcbride, J. F. *Biotechnol Bioeng.* **1998**, *58*, 416-427.

17. Yin, X.; Stöver, H. D. H. *Macromolecules* **2003**, *36*, 8773-8779.

18. Yin, X.; Stöver, H. D. H. *Macromolecules* **2003**, *36*, 9817-9822.

19. Matsumoto, A.; Ishido, H.; Oiwa, M. *J. Polym. Sci.: Polym. Chem. Ed.***1982**, *20*, 3207-3217.

20. Liu, F.; Liu, G. *Macromolecules* **2001**, *34*, 1302-1307.

21. Miyazaki, H.; Kataoka, K. *Polymer* **1996**, *37*, 681-685.

22. Higgins, J. P. J.; Weale, K. E. *J. Polym. Sci.: Part A-1,* **1968**, *6*, 3007-3013.

23. Wolk, S. K.; Eisenhart, E. *Macromolecules* **1993**, *26*, 1086-1090.

24. Rao, G. V. R.; Balamurugan, S.; Meyer, D. E.; Chilkoti, A.; López, G. P. *Langmuir* **2002**, *18*, 1819-1824.

25. Otake, K.; Inomata, H.; Konno, M.; Saito, S. *Macromolecules* **1990**, *23*, 283-289.

26. Urry, D. W. *J. Phys. Chem. B* **1997**, *101*, 11007-11028.

# Chapter 6 Probing The Influence of Polymer Architecture on Liquid-Liquid Phase Transitions of Aqueous Poly(*N,N*-Dimethylacrylamide) Copolymer Solutions


## Abstract

Thermosensitive poly(*N,N*-dimethylacrylamide-*co*-*N*-phenylacrylamide) (DMA-*co*-PhAm) copolymers were prepared by atom transfer radical polymerization (ATRP) in methanol/water mixtures at room temperature with methyl 2-chloropropionate as the initiator and CuCl/$Me_6$TREN as the catalyst. The resultant DMA-*co*-PhAm copolymers had tailored compositions and controlled molecular weights, and their aqueous solutions underwent liquid-liquid phase separations upon heating. These phase transition temperatures, measured by the cloud point method, were dependent on polymer concentrations, compositions and molecular weights. The efficiency of the thermally induced liquid-liquid phase transition, i.e. the yield of phase separated polymer, increased with increasing solution temperature. This suggested that the thermally induced liquid-liquid phase transition was a continuous process, and the solubility of polymers in the equilibrium phase decreased with increasing temperatures beyond the onset of phase separation. The efficiency of phase separation could be enhanced by adding NaCl to the solution. This chapter has been reproduced with permission from *Macromolecules*, submitted for publication. Copyright 2004 American Chemical Society.

## 6.0 Introduction

The liquid-liquid phase transitions of aqueous polymer solutions have been widely used in biochemistry and biotechnology for purifications of amino acids, proteins, nucleic acids and cells.[1-3] Due to the high water content in both phases, the liquid-liquid phase transition provides a mild approach to separate biomaterials without denaturation. The traditional systems for such applications are dextran/polyethylene glycol and polyethylene glycol/salts.[4-6] Recently, the liquid-liquid phase transition of thermally responsive polymers has gained increasing attention since the phase transition is readily reversible simply by changing the temperature.[7,8] The thermo-responsive polymers separate from the solutions at temperatures above their lower critical solution temperatures (LCST).

Thermally induced liquid-liquid phase transitions are commonly seen in biomacromolecules such as elastin-like polypeptides, and have been explored to purify recombinant proteins from the cell lysate.[9-11] The most studied thermo-responsive polymer is poly(*N*-isopropylacrylamide) (pNIPAM), which undergoes a liquid-solid phase transition at its LCST of around 32°C.[12] In contrast to pNIPAM, aqueous solutions of the analogous poly(*N,N*-dimethylacrylamide) (pDMA) do not have an LCST. However, aqueous solutions of DMA copolymers containing hydrophobic groups, which can enhance the polymer-polymer interactions, are thermo-responsive. Unlike pNIPAM, many of these DMA copolymer solutions undergo liquid-liquid phase transitions, with phase transition temperatures depending on the amount of hydrophobic comonomer.[13-15]

We have studied the thermally induced liquid-liquid phase transitions of aqueous solutions of pDMA copolymers, and used the liquid-liquid phase transition to prepare crosslinked hydrogel microspheres.[16,17] We found that the yield of phase-separated polymers was less than 10% at the onset of phase separations, and increased with increasing temperatures. Despite extensive studies on thermo-responsive polymers, there is little published information available on the efficiency of phase separation. The efficiency of phase separation will mainly depend on 1) the microstructure of the copolymers, such as the average composition and the compositional distribution, as well as molecular weight and the molecular weight distribution, and 2) the mechanism of thermally induced phase transitions. Most thermo-responsive polymers studied to date were prepared by conventional radical polymerization, which does not enable fine control of the structural features of polymers, such as molecular weight and composition.

Controlled/living radical polymerization, in particular atom transfer radical polymerization (ATRP), has been extensively used to prepare well-defined polymers.[18] For example, the architecture of the polymer (comb, star, dendritic), and composition of the polymer backbone (random, gradient, blocky) can all be readily designed using ATRP. In the present work, we report the synthesis of well-defined pDMA random copolymers by ATRP, and their aqueous solution properties. Specifically, ATRP was used to prepare copolymers of DMA with *N*-phenylacrylamide (PhAm), where the PhAm units serve to increase the hydrophobicity of the copolymer to permit thermally induced phase separations. The primary objective for this research is to probe the mechanism of

the thermally induced liquid-liquid phase transition using copolymers with well-defined structures.

## 6.1 Experimental Section

### 6.1.1 Materials

*N,N*-Dimethylacrylamide (DMA), aniline (99%), acryloyl chloride (96%), triethylamine (99%), tris(2-aminoethyl)amine, methyl 2-chloropropionate (MCP) (97%), copper (I) chloride (>99%), and silica gel (100-200 mesh, column chromatography grade) were purchased from Aldrich. Methanol (HPLC grade), water (HPLC grade), tetrahydrofuran (THF), dimethylformamide (DMF), methylene chloride, and anhydrous diethyl ether were obtained from Caledon Laboratories. DMA was purified by vacuum distillation, while other materials were used as received. Tris(2-(dimethylamino)ethyl)amine ($Me_6$TREN) was synthesized according to the reported procedure.[19]

### 6.1.2 Synthesis of *N*-Phenylacrylamide (PhAm)

Aniline (36.9 mL, 0.4 mol) and triethylamine (84.5 mL, 0.6 mol) were dissolved in 200 mL of methylene chloride. Acryloyl chloride (25.4 mL, 0.3 mol) dissolved in 15 mL of methylene chloride was added dropwise to this well stirred solution at 0°C. The mixture was then warmed to room temperature and stirred for another 4 hours. The reaction solution was filtered, extracted 3 times with water, and dried over anhydrous magnesium sulfate. The solvent was removed on a rotary evaporator to yield a deep

yellow solid that was recrystallized from acetone and dried under vacuum to afford 22.0 g of PhAm (yield, 50%).

### 6.1.3 ATRP of DMA and PhAm

DMA, methanol, and water were purged with nitrogen for 30 min before use. In a typical procedure, a 50 mL flask was first flushed with nitrogen for about 1 hour. A solution comprised of 7.83 g of DMA (0.079 mol), 3.38 g of PhAm (0.023 mol), 8.97 g of methanol, 2.24 g of water, and 25.3 mg of copper (I) chloride ($2.55 \times 10^{-4}$ mol) was transferred to the flask under nitrogen. 68 μL of $Me_6TREN$ ($2.55 \times 10^{-4}$ mol) was added with a syringe and the flask was placed into a water bath. After stirring the mixture for 10 min, 30.7 μL of MCP ($2.55 \times 10^{-4}$ mol) was added. The polymerization was carried out at room temperature. During the polymerization, 1.0 mL samples were withdrawn at different times with a degassed syringe for molecular weight and conversion measurements. The molecular weight of the polymers was measured directly after passing 0.2 mL of sample through the silica column to remove the catalyst. Conversion was determined gravimetrically by precipitating 0.8 mL of sample solution into 20 mL of diethyl ether. The polymer was isolated by centrifugation and dried under vacuum at 65°C.

Samples for the phase transition study were prepared in a similar procedure. After polymerization, the solution was diluted with THF and passed through a silica column to remove the catalyst. The product was precipitated into diethyl ether, redissolved in acetone and reprecipitated into diethyl ether, and then dried under vacuum at 65°C.

### 6.1.4 Characterization of Copolymers

Molecular weights of copolymers were determined using a gel permeation chromatograph consisting of a Waters 515 HPLC pump, three ultrastyragel columns (500-20k, 500-30k, 5k-600k Daltons) and a Waters 2414 refractive index detector, using THF as solvent at a flow rate of 1 mL $min^{-1}$, and narrow-disperse polystyrene as calibration standards. $^1H$ NMR spectra of the copolymers were recorded on a Bruker AC 200, using methylene chloride-$d_2$ as the solvent.

### 6.1.5 Measurement of Phase Transition Temperatures

Phase transition temperatures of aqueous solutions of DMA-*co*-PhAm copolymers were measured using the cloud point method. A Cary 100 Bio UV-visible spectrophotometer, coupled with a temperature controller, was used to trace the phase transition by monitoring the transmittance at 500 nm. The phase transition temperature was defined as the inflection point of the transmittance vs. temperature curve, as determined by the maximum in the first derivative. The polymer concentration and the heating rate were 1 wt % and 1.0°C $min^{-1}$, respectively.

### 6.1.6 The Liquid-liquid Phase Transition of DMA-*co*-PhAm Copolymer Solutions

Optical images of polymer solutions at temperatures above or below the phase transition temperature were recorded using an Olympus BH-2 microscope equipped with a Kodak DC 120 Zoom digital camera.

To measure the efficiency of the phase separation, 20 g of a 2.0 wt % aqueous solution of DMA-*co*-PhAm22, containing 22 mol % PhAm, was prepared in a 24 mL

glass vial. The solution was incubated in a temperature-controlled water bath at 25°C for 30 min. The resulting two-phase mixture was then separated by centrifugation at 3500 RPM for 1 min into a viscous coacervate bottom phase and a transparent supernatant, which were then isolated by decanting the supernatant into a pan. Both phases were dried to constant weight at 65°C.

## 6.2 Results and Discussion

### 6.2.1 ATRP of DMA in Methanol Solution

The controlled polymerization of DMA using ATRP is difficult, plausibly due to 1) the deactivation of the ATRP catalyst by binding to the amide groups of pDMA, 2) the substitution of halide from the polymer chain end by amide groups, and 3) the low values of the ATRP equilibrium constant.[20,21] Such challenges in the ATRP of DMA were addressed by using stronger ATRP coordinating ligands, and more stable alkyl chlorides as initiators.[22,23] The best system reported to date uses the powerful ATRP catalyst CuCl/$Me_6$TREN and methyl 2-chloropropionate (MCP) as initiator, however, high monomer conversions (up to 70%) were only obtained with high catalyst to initiator ratios (2/1 or 3/1).[23]

Our initial studies concentrated on further improving the ATRP of DMA by exploring the effects of solvents on the polymerization. With CuCl/$Me_6$TREN as the catalyst and MCP as the initiator in a 1:1:1 ratio, the polymerization proceeded initially very rapidly in ethyl acetate, THF, and DMF, but stopped within 5-10 min at room temperature at less than 20% monomer conversions. The polymerization proceeded more

slowly in toluene to reach about 40% monomer conversion after 20 hours. In ethyl acetate, THF and toluene, blue precipitates were formed during the polymerization. In all cases, the molecular weight distributions of prepared polymers were below 1.1, indicating the polymerizations were well controlled. In addition, the polymerizations continued upon adding fresh catalyst. It hence appears that catalyst deactivation is still a major problem in ATRP of DMA, even with CuCl/$Me_6$TREN as the catalyst. The amide groups of pDMA may displace chloride ligands from the copper-based ATRP catalyst, especially when the latter is in its higher oxidation state. In principle, using a hydrogen-bonding solvent such as an alcohol, which would bind to the amide groups, may prevent the coordination of catalysts by the polymers and/or the monomers. Similar approaches have been used in the ATRP of the strongly coordinating monomer, vinylpyridine.[24]

Figures 6.1 and 6.2 depict typical curves for monomer conversion vs. time and molecular weight vs. conversion, for the ATRP of DMA in methanol at room temperature with CuCl/$Me_6$TREN as the catalyst and MCP as the initiator (1:1:1). Polymerizations were carried out in a water bath to improve the heat transfer. The polymerization is rapid at the beginning, leading to 50% monomer conversion within 30 min, and 80% after 4 hours, while maintaining good control over the molecular weight distributions ($M_w/M_n$ < 1.1). In addition, no catalyst precipitates during the polymerization. These results support the hypothesis that H-bonding solvents are suitable reaction media for the controlled ATRP of DMA.

The molecular weights of polymers determined by GPC shown in Figure 6.2 deviate from the target molecular weight, presumably due to the calibration method,

which is based on polystyrene standards in THF solutions. The molecular weights of pDMA from GPC are underestimated by a factor of around 3.

While this work was being carried out, Matyjaszewski's group disclosed results on the ATRP of DMA in methanol solution with the addition of Lewis acids to control the stereo-structure of polymers.[25] Under their conditions, the monomer conversion was less than 50% in presence of Lewis acid.

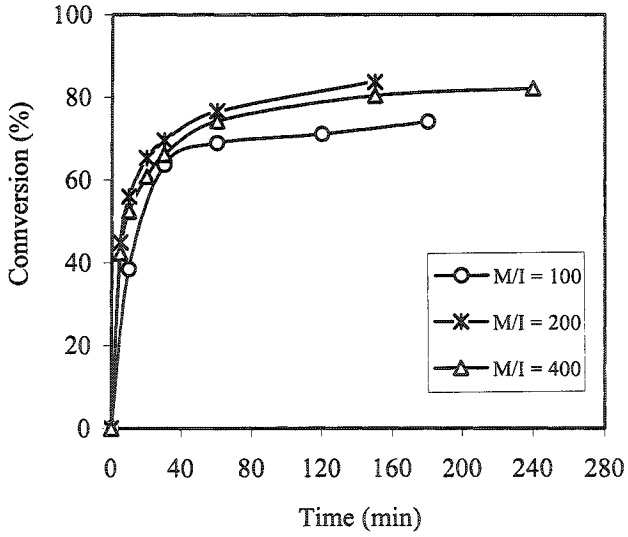


**Figure 6.1** Conversion vs. time curves for the ATRP of DMA in methanol at room temperature at three different monomer/initiator (M/I) ratios. Monomer/solvent = 1/2 (wt/wt), [CuCl]/[$Me_6$TREN]/[MCP] = 1/1/1. The solid lines connecting the data points are only to guide the eye.

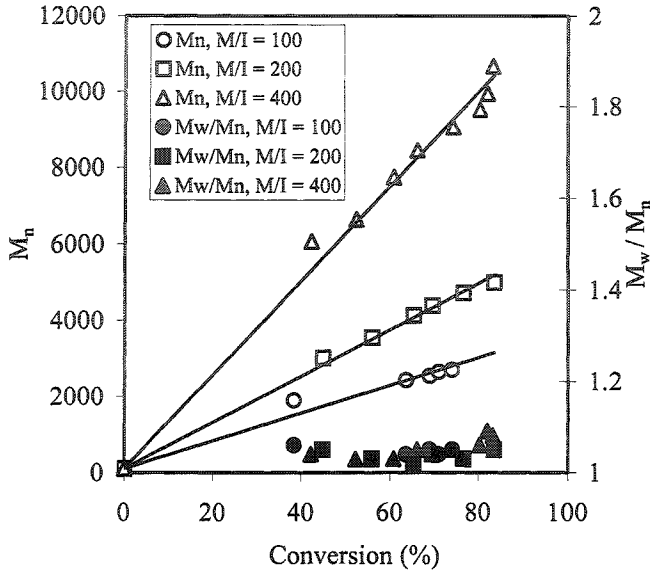


**Figure 6.2** Plots of molecular weight, $M_n$ (GPC), and molecular weight distribution, $M_w/M_n$, vs. monomer conversion for the polymerization of DMA in methanol at room temperature at three different monomer/initiator (M/I) ratios. Monomer/solvent = 1/2 (wt/wt), [CuCl]/[$Me_6$TREN]/[MCP] = 1/1/1. The solid lines are 1$^{st}$ order trendlines.

### 6.2.2 ATRP of DMA and PhAm in Methanol/Water Mixture

After developing the ATRP of DMA, the investigation turned to the copolymerization of DMA with PhAm in methanol solutions under the same conditions described above for DMA homopolymerization. However, the monomer conversion dropped to 57% upon the addition of 9.8 mol % PhAm to the monomer feeds (Table 6.1-I and Figure 6.3-I). Obviously, PhAm lowers the catalyst activity either by changing the

solvency of the reaction medium and/or by coordinating to the catalyst. In order to increase the catalyst activity, the copolymerization was performed in methanol/water mixtures. As previously reported,[26, 27] the activity of ATRP catalysts is particularly high when the polymerization is carried out in presence of water.

The monomer conversion increases to 69% in 90/10 (wt/wt) methanol/water mixtures (Table 6.1-II and Figure 6.3-II), and further to 82% using a 1/1 (wt/wt) monomer/solvent mixture as polymerization medium (Table 6.1-III and Figure 6.3-III). Under the same conditions, the conversion drops to 60% when increasing PhAm to 12.7 mol % (Table 6.1-IV and Figure 6.3-IV), but increases back to 80% upon changing the polymerization medium to 80/20 (wt/wt) methanol/water (Table 6.1-V and Figure 6.3-V). Several other DMA-*co*-PhAm copolymers with different compositions and different molecular weights were prepared by ATRP in 80/20 (wt/wt) methanol/water mixtures (Table 6.1 and 6.2). All polymers have narrow molecular weight distributions, indicating that water both improves the conversion and enhances the control over molecular weight. It is currently not clear that such enhancement of catalyst activity is due to water changing the catalyst structure,[26] and/or due to water reducing the coordination of catalyst to the *N*-phenylacrylamide groups.

**Table 6.1** Synthesis of poly(DMA-*co*-PhAm) via ATRP at room temperature under different conditions [a]

| Entry | Solvent [b] | Monomer /solvent [c] | mol % PhAm in feed | mol % PhAm in polymer [d] | Conv (%) | $M_n$ [e] | $M_w/M_n$ [e] |
|---|---|---|---|---|---|---|---|
| I | MeOH | 2/1 | 9.8 | 9.9 | 56.9 | 6,800 | 1.07 |
| II | MeOH/$H_2O$ (9/1) | 2/1 | 9.8 | 9.8 | 68.8 | 8,200 | 1.07 |
| III | MeOH/$H_2O$ (9/1) | 1/1 | 9.8 | 9.6 | 82.0 | 9,700 | 1.07 |
| IV | MeOH/$H_2O$ (9/1) | 1/1 | 12.7 | 12.2 | 60.1 | 7,900 | 1.07 |
| V | MeOH/$H_2O$ (4/1) | 1/1 | 12.7 | 12.0 | 80.0 | 10,100 | 1.09 |
| VI | MeOH/$H_2O$ (4/1) | 1/1 | 16.7 | 15.9 | 75.9 | 10,200 | 1.07 |
| VII | MeOH/$H_2O$ (4/1) | 1/1 | 22.5 | 21.7 | 70.0 | 8,600 | 1.07 |

[a] [monomer]/[MCP]/[CuCl]/[$Me_6$TREN] = 400/1/1/1.Reaction time, 4h. [b,c] The ratios are by weight. [d] Measured by NMR. [e] Measured by GPC.

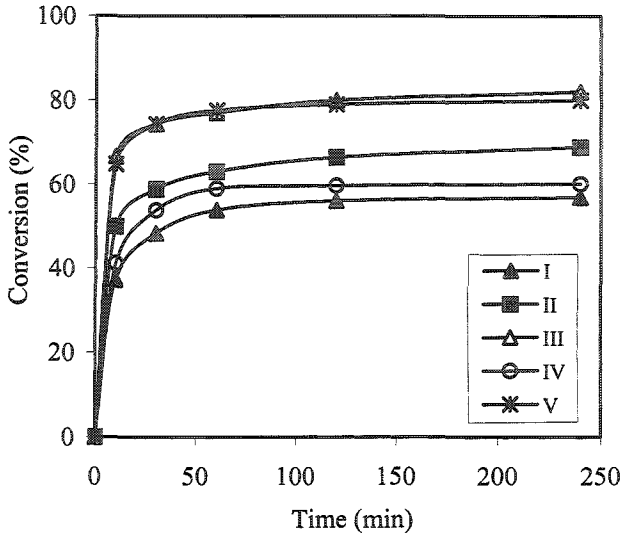


**Figure 6.3** Conversion vs. time curves for the ATRP of DMA and PhAm in methanol/water mixture at room temperature. Reaction conditions are those in Table 6.1. The solid lines connecting the data points are only to guide the eye.

**Table 6.2** Synthesis of poly(DMA-*co*-PhAm) with different molecular weights via ATRP in 80/20 (wt/wt) methanol/water mixtures at room temperature [a]

| [Monomer] /[MCP] | mol % PhAm in feed | mol % PhAm in polymer [b] | Conv (%) | $M_n$ [c] | $M_w/M_n$ [c] | Cloud point [d] (°C) |
|---|---|---|---|---|---|---|
| 60/1 | 16.7 | 15.9 | 89.4 | 2,000 | 1.08 | 39.3 |
| 100/1 | 16.7 | 16.2 | 84.1 | 3,500 | 1.06 | 40.2 |
| 200/1 | 16.7 | 16.3 | 76.5 | 4,700 | 1.05 | 39.1 |
| 400/1 | 16.7 | 15.9 | 75.9 | 10,200 | 1.07 | 43.5 |
| 100/1 | 22.5 | 21.8 | 80.3 | 3,200 | 1.07 | 16.3 |
| 200/1 | 22.5 | 21.7 | 72.5 | 4,600 | 1.07 | 17.2 |
| 400/1 | 22.5 | 21.7 | 70.0 | 8,600 | 1.07 | 20.1 |
| 600/1 | 22.5 | 22.0 | 61.3 | 10,600 | 1.07 | 20.1 |

[a] [CuCl]/[$Me_6$TREN]/[MCP] = 1/1/1. Monomer/solvent = 1/1 (wt/wt). Reaction time, 4h. [b] Measured by NMR. [c] Measured by GPC. [d] 1.0 wt % polymer solution.

A typical $^1$H NMR spectrum of DMA-*co*-PhAm copolymer is presented in Figure 6.4. The copolymer composition was determined by comparing the peak area of the phenyl protons (5 H) from PhAm, with the total peak area between 2.3 and 3.3ppm, which includes seven protons (a, c) from DMA and one proton (e) from PhAm. The results are illustrated in Table 6.1 and 6.2. On the basis of the free radical reactivity ratios of DMA and PhAm reported in the literature,[14] it is expected that the monomer units are randomly distributed in the polymer chains. As shown in Table 6.1 and 6.2, the

compositions of copolymers are close to the monomer feed ratio at all monomer conversions.

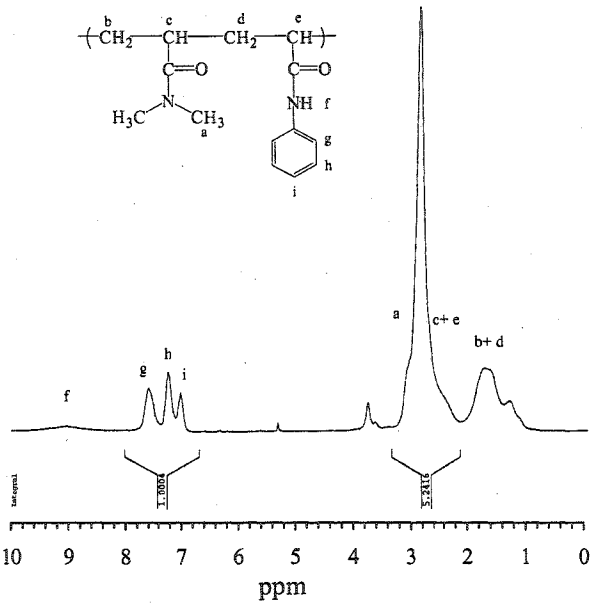


**Figure 6.4** $^1$H NMR spectrum of DMA-*co*-PhAm22 in methylene chloride-$d_2$.

### 6.2.3 Thermally Induced Liquid-Liquid Phase Transitions of DMA-*co*-PhAm Copolymer Solutions

The temperature-dependent phase separation of aqueous solutions of DMA-*co*-PhAm copolymers was investigated by the cloud point method. Figure 6.5 shows the transmittance vs. temperature curves for three DMA-*co*-PhAm copolymers with different compositions. The copolymer characteristics and their corresponding phase transition temperatures are given in Table 6.3.

The phase transition temperature of thermo-responsive polymers is strongly influenced by changes in the hydrophilic/hydrophobic nature of the polymer. Aqueous solutions of DMA-*co*-PhAm copolymers with less than 10 mol % PhAm do not show phase transitions. With increasing content of the hydrophobic PhAm, the phase transition temperatures decrease drastically (Table 6.3). It is thought that LCST behavior of such polymers is caused by the hydration of hydrophobic groups in the polymer chains.[28, 29] At low temperatures, strong H-bonding interactions between hydrophilic groups and water lead to good solubility of the polymer, which results in the hydration of hydrophobic groups. The water surrounding the hydrophobic groups is highly organized, leading to a high entropic penalty. Above the phase transition temperature, the unfavorable entropic contribution dominates, leading to a negative free energy change upon de-mixing. An increase in hydrophobicity of the polymer leads to larger entropic penalty from the oriented water structure and a lower enthalpy gain from H-bonding interactions, and hence a lower LCST.

The thermally induced phase separation observed in aqueous DMA-*co*-PhAm copolymer solution is a liquid-liquid transition process. Figure 6.6 presents an optical microscope image of the liquid coacervate droplets formed from a 1.0 wt % aqueous DMA-*co*-PhAm22 solution. In absence of stirring, these droplets will coalesce into a bulk layer after several minutes.

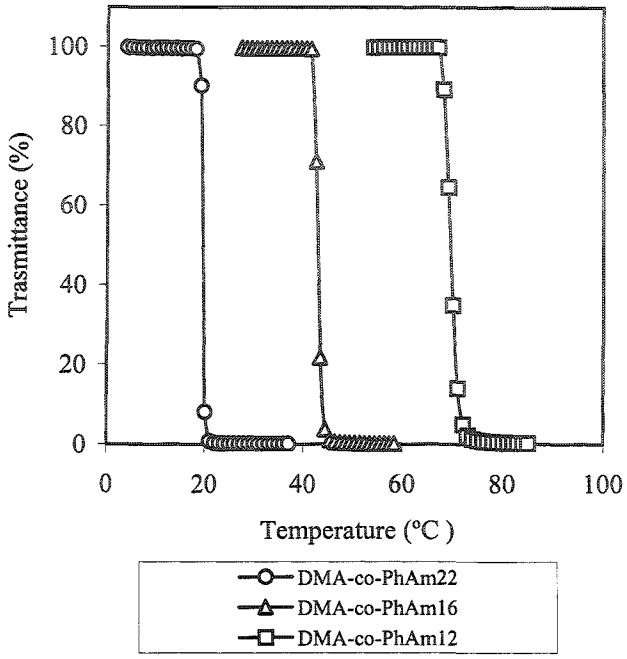


**Figure 6.5** Cloud point curves for 1.0 wt % aqueous solutions of DMA-*co*-PhAm copolymers with different compositions.

**Table 6.3** Compositions and phase transition temperatures of DMA-*co*-PhAm

| Polymer | PhAm in polymer [a] (mol %) | $M_n$ [b] | $Mw/M_n$ [b] | Cloud point [c] (°C) |
|---|---|---|---|---|
| DMA-co-PhAm10 | 9.6 | 9,700 | 1.07 | — |
| DMA-co-PhAm12 | 12.0 | 10,100 | 1.09 | 70.1 |
| DMA-co-PhAm16 | 15.9 | 10,200 | 1.07 | 43.5 |
| DMA-co-PhAm22 | 21.7 | 8,600 | 1.07 | 20.1 |

[a] Estimated by NMR. [b] Measured by GPC. [c] Measured by the cloud point method with 1.0 wt % polymer solution

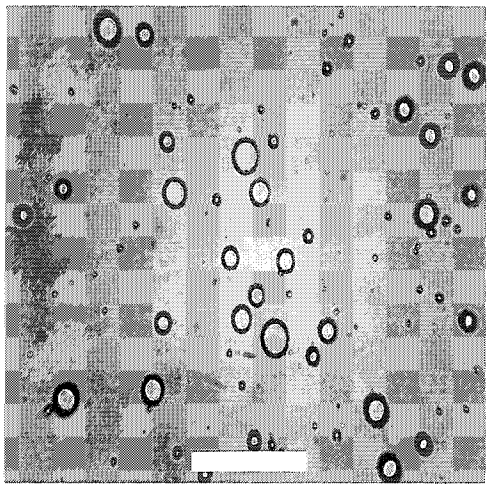

**Figure 6.6** Optical microscope image of liquid droplets formed from the phase transition of 1 wt % DMA-*co*-PhAm22 solution at 25°C. Scale bar is 250 μm.

Due to the difficulty in obtaining thermo-responsive polymers with narrow molecular weight distributions, the dependence of LCST on the molecular weight of polymers has not been systematically studied. Fujishige et al. reported the chain length independent LCST of pNIPAM with molecular weights larger than 50,000,[30] while Schild and Tirrell showed that the LCST of pNIPAM was influenced by the molecular weight but no trend was evident.[31] The pNIPAM used in both studies was prepared by conventional radical polymerization and had broad molecular weight distributions. By studying two fractionated pNIPAMs with narrow molecular weight distributions, Tong et al. found that the pNIPAM with higher molecular weight showed higher LCST.[32]

Figure 6.7 illustrates the effect of molecular weight on the cloud point of two series of DMA-*co*-PhAm copolymers, containing 16% and 22% PhAm, respectively. The

phase transition temperatures first increase slightly with increasing molecular weight, and then become constant (Figure 6.7B). The polymers with lower molecular weights show phase transitions over relatively broad temperature ranges. This may be due small compositional variations, or due to the influence of the initiating group. Both of these effects would be more pronounced at lower molecular weights. This will be the subject of future studies.

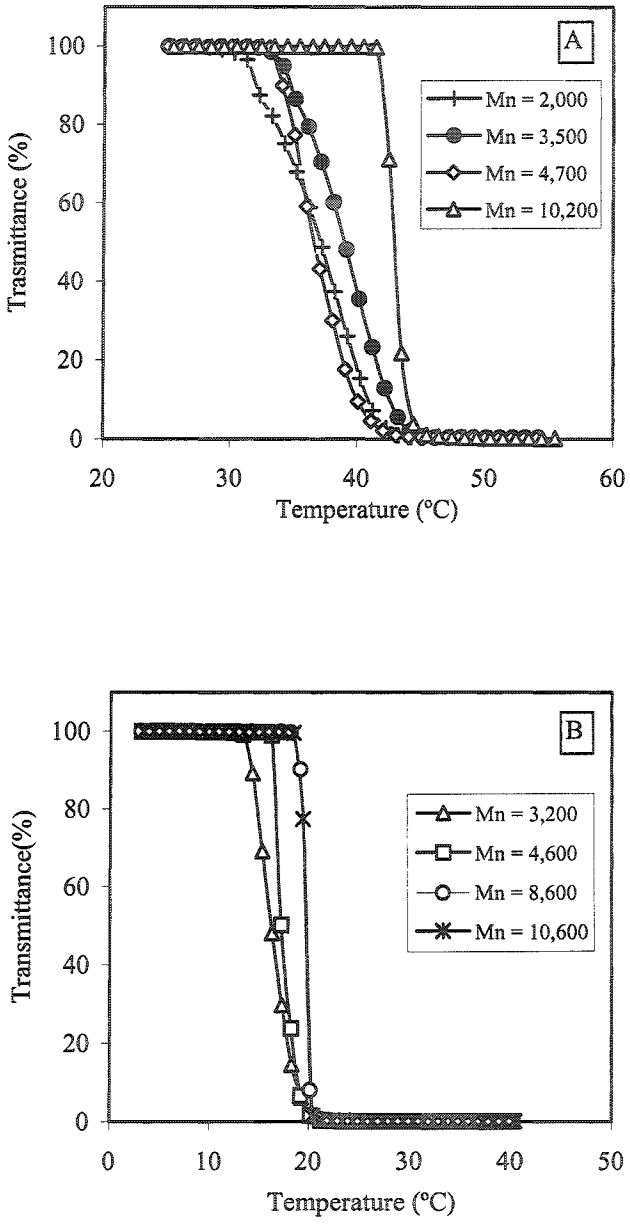


**Figure 6.7** Effect of polymer molecular weight on the phase transition temperature of 1.0 wt % DMA-*co*-PhAm copolymer solutions. The PhAm content in the copolymer is about A) 16 mol %, and B) 22 mol %. The molecular weights indicated are results from GPC. See Table 6.2 for the characteristics of the copolymers.

### 6.2.4 Effects of Polymer Concentration and added NaCl on The Phase Transition Temperatures

Figure 6.8 shows the cloud point curves for DMA-*co*-PhAm22 solutions with different concentrations, and the effect of polymer concentration on the phase transition temperatures is illustrated in Figure 6.9. The phase transition temperatures first decrease with increasing polymer concentrations and become constant at concentrations above 1.0 wt % (Figure 6.9). At low polymer concentration (0.05 wt %), the phase transition occurs over a broad temperature range (Figure 6.8). The thermally induced phase separation of aqueous polymer solutions is believed to take place in two stages:[33] the polymer chains first form primary aggregates through intra-chain interactions, which then further aggregate by inter-chain interactions to cause the phase transition. The intra-chain interactions dominate at low polymer concentrations and the formed primary aggregates require longer times and higher temperatures before further aggregating to complete the phase transition. At higher polymer concentrations, the intra-chain interaction and inter-chain interactions take place simultaneously, causing the transition to occur at a lower temperature. Compared to the liquid-solid phase transition of pNIPAM solution,[32,34] the effect of polymer concentration on the phase transition temperature of DMA-*co*-PhAm solution is more pronounced. Similar results were reported for the liquid-liquid phase transition of elastin-like polypeptide solutions.[35, 36]

It is well known that the effect of salts on the LCST is mainly due to the changes to the structure of water caused by the added salts.[31, 37] As shown in Figure 6.10, the phase transition temperature of DMA-*co*-PhAm solutions decreases with the addition of

NaCl. NaCl is considered as a water-structure maker, and hence shows a "salting-out" effect, which can effectively enhance the hydrophobic interaction and promote the collapse of polymer chains.

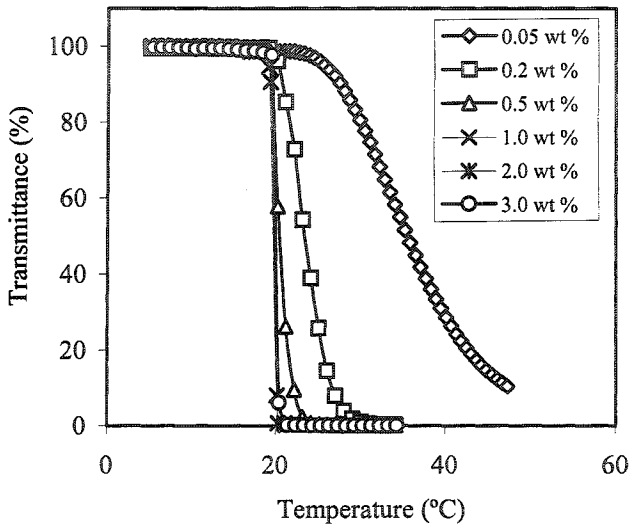


**Figure 6.8** Cloud point curves for aqueous solutions of DMA-*co*-PhAm22 with different concentrations.

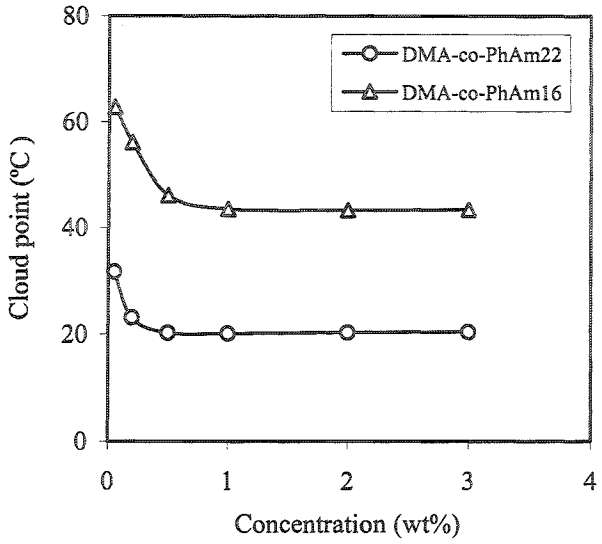


**Figure 6.9** Effect of polymer concentration on the phase separation temperature of DMA-*co*-PhAm solutions as measured by the cloud point method.

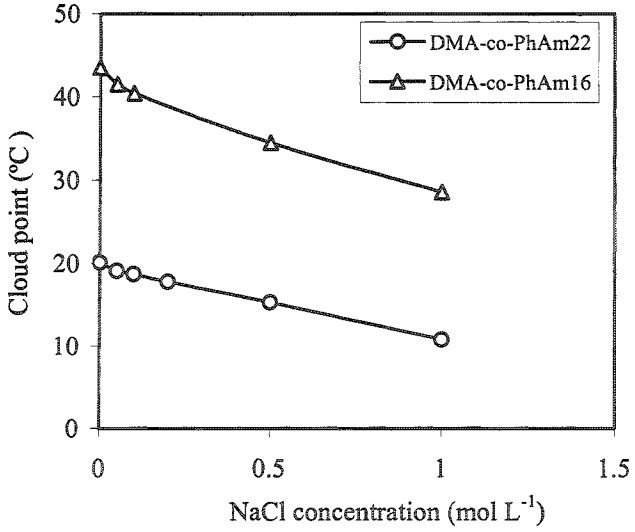


**Figure 6.10** Effect of NaCl concentration on the phase separation temperature of 1.0 wt% DMA-*co*-PhAm solutions as measured by the cloud point method.

### 6.2.5 The Efficiency of Phase Separation

The efficiency of the thermally induced liquid-liquid phase transitions were investigated by determining the yield of polymer recovered from the coacervate phase upon the phase transitions. As presented in Figure 6.11, the percentage of the polymer found in the coacervate phase increases with increasing solution temperature. Compared to the previously studied DMA copolymer systems,[16,17] the yields of phase-separated polymers are much higher near the onset of phase transition. The polymers used in previous works were prepared by conventional radical polymerization and subsequently were broad ranges of both polymer compositions and polymer molecular weights. The present results indicate that the efficiency of phase transitions can be improved by tailoring the polymer structures. Furthermore, the temperature-dependent efficiency of phase separation confirms that the thermally induced liquid-liquid phase transition is a continuous equilibrium process. In this process, the polymer is partially dehydrated upon reaching the critical temperature, and the solubility of polymers in the equilibrium phase decreases with increasing the temperatures, leading to more polymers driven from the equilibrium phase to the coacervate phase.

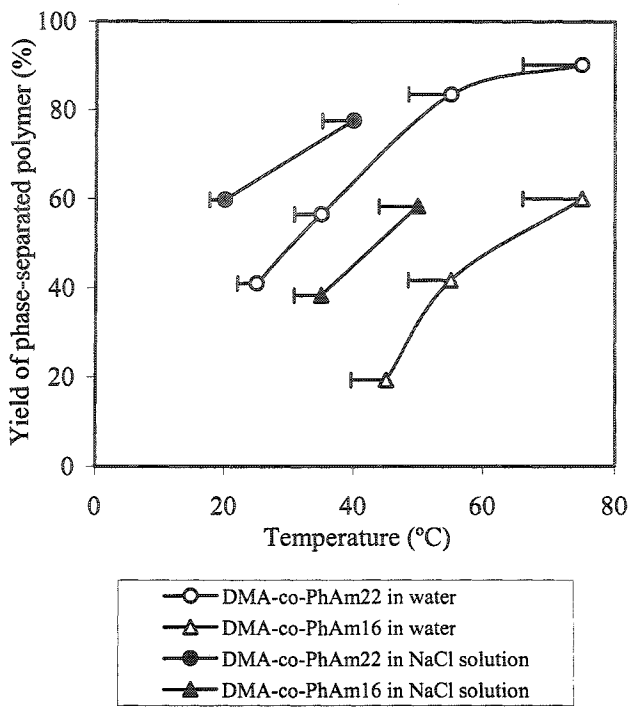


**Figure 6.11** Effect of temperature on the yield of phase-separated polymer from 2.0 wt% DMA-*co*-PhAm copolymer aqueous solutions and in 1.0 mol $L^{-1}$ NaCl solutions. The symbols indicate the equilibrium temperature and the error bars show the decrease of temperature during centrifugation.

Figure 6.12 gives the concentration of DMA-*co*-PhAm22 in the two separated phases as a function of temperature. The temperature changes do not affect the volume of the two separated phases. Hence, the concentrations of polymer in the coacervate phase increase with increasing temperatures. The water content in the coacervate phase is more than 60% even at 75°C.

The polymers recovered from both separated phases were characterized by GPC and NMR, and were found to have similar compositions and molecular weights.

As discussed above, the phase transition temperatures decrease with the addition of NaCl in the solutions. Also illustrated in Figure 6.11 is the effect of NaCl addition on the efficiency of the phase separation. During the polymer recovery, it was assumed that NaCl has the same affinity in both the equilibrium phase and the coacervate phase. With the addition of NaCl, the volume of both separated phases does not change, while the efficiency of phase separations is enhanced.

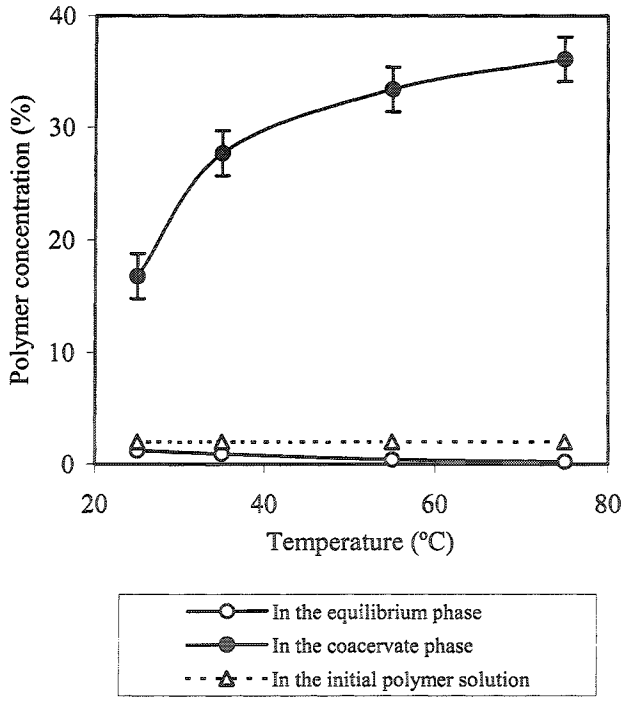


**Figure 6.12** The concentrations of DMA-*co*-PhAm22 in the two separated phases at different temperatures.

## 6.3 Conclusions

pDMA homopolymer and DMA-*co*-PhAm copolymers were synthesized by ATRP using MCP/CuCl/$Me_6$TREN as the initiator and the catalyst at room temperature with H-bonding solvents – methanol and methanol/water mixtures as the reaction media. The polymerizations were well controlled, leading to the production of DMA-*co*-PhAm copolymers with well-defined structures.

Aqueous solutions of DMA-*co*-PhAm copolymers undergo liquid-liquid phase separations at temperatures dependent on the content of hydrophobic PhAm. The phase transition temperatures are also found to be dependent on polymer concentrations and the molecular weights of polymers. The efficiency of the thermally induced liquid-liquid phase transition was studied by measuring the yield of phase-separated polymers, which increased with increasing solution temperature. The temperature-dependent efficiency of phase separation showed that the thermally induced liquid-liquid phase transition was a continuous equilibrium process. The polymer was partially dehydrated upon reaching the critical temperature, and the solubility of polymers in the equilibrium phase decreased with increasing temperature, leading to more polymer driven from the equilibrium phase to the coacervate phase. The addition of NaCl was found to enhance the efficiency of phase separations.

## References


1. Albertsson, P-Å. *Partition of Cell Particles and Macromolecules*, 3rd ed.; J. Wiley & Sons: New York, 1986.
2. Li, M; Zhu, Z. Q.; Mei, L. H. *Biotechnol. Prog.* **1997**, *13*, 105-108.
3. Johansson, H.-O.; Karlström, G.; Tjerneld, F.; Haynes, C. A. *J. Chromatogr., B* **1998**, *711*, 3-17.
4. Abbott, N. L.; Blankschtein, D.; Hatton, T. A. *Macromolecules* **1991**, *24*, 4334-4348.
5. Carlsson, M.; Linse, P.; Tjerneld, F. *Macromolecules* 1993, *26*, 1546-1554.
6. Persson, J.; Nyström, L.; Ageland, H.; Tjerneld, F. *J. Chromatogr. B* **1998**, *711*, 97-109.
7. Johansson, H.-O.; Karlström, G.; Tjerneld, F. *Macromolecules* **1993**, *26*, 4478-4483.
8. Johansson, H.-O.; Persson, J.; Tjerneld, F. *Biotechnol. Bioeng.* **1999**, *66*, 247-257.
9. Urry, D. W. *J. Phys. Chem. B* **1997**, *101*, 11007-11028.
10. Meyer D. A.; Chilkoti, A. *Nature Biotechnol.* **1999**, *17*, 1112-1115.
11. Zhang, Y; Mao, H; Cremer, P. S. *J. Am. Chem. Soc.* **2003**, *125*, 15630-15635.
12. Schild, H. G. *Prog. Polym. Sci.* **1992**, *17*, 163-249.
13. Mueller, K. F. *Polymer* **1992**, *33*, 3470-3476.
14. Miyazaki, H.; Kataoka, K. *Polymer* **1996**, *37*, 681-685.
15. Shibanuma, T.; Aoki, T.; Sanui, K.; Ogata, N.; Kikucji, A.; Sakurai, Y., Okano, T. *Macromolecules* **2000**, *33*, 444-450.
16. Yin, X.; Stöver, H. D. H. *Macromolecules* **2003**, *36*, 9817-9822.
17. Yin, X.; Stöver, H. D. H. *J. Polym. Sci., Part A: Polym. Chem.* Submitted.

18. Matyjaszewski, K.; Xia, J. *Chem. Rev.* **2001**, *101*, 2921-2990.

19. Ciampolini, M.; Nardi, N. *Inorg. Chem.* **1966**, *5*, 41-44.

20. Teodorescu, M; Matyjaszewski, K. *Macromolecules* **1999**, *32*, 4826-4831.

21. Rademacher, J. T.; Baum, M.; Pallack, M. E.; Brittain, W. J.; Simonsick, W. J. *Macromolecules* **2000**, *33*, 284-288.

22. Teodorescu, M.; Matyjaszewski, K. *Macromol. Rapid Commun.* **2000**, *21*, 190-194.

23. Neugebauer, D.; Matyjaszewski, K. *Macromolecules* **2003**, *36*, 2598-2603.

24. Xia, J.; Zhang, X.; Matyjaszewski, K. *Macromolecules* **1999**, *32*, 3531-3533.

25. Lutz, J.; Neugebauer, D.; Matyjaszewski, K. *J. Am. Chem. Soc.* **2003**, *125*, 6986-6993.

26. Wang, X. S.; Armes, S. P. *Macromolecules* **2000**, *33*, 6640-6647.

27. Robinson, K. L.; Khan, M. A.; de Paz Báñez; M. V.; Wang, X. S.; Armes, S. P. *Macromolecules* **2001**, *34*, 3155-3158.

28. Feil, H.; Bae, Y. H.; Feijen, J.; Kim, S. W.; *Macromolecules* **1993**, *26*, 2496-2500.

29. Shibayama M.; Mizutani, S.; Nomura, S. *Macromolecules* **1996**, *29*, 2019-2024.

30. Fujishige, S.; Kubota, K.; Ando, I. *J. Phys. Chem.* **1989**, *93*, 3311-3313.

31. Schild, H. G.; Tirrell, D. A. *J. Phys. Chem.* **1990**, *94*, 4352-4356.

32. Tong, Z.; Zeng, F.; Zheng, X.; Sato, T. *Macromolecules* **1999**, *32*, 4488-4490.

33. Qiu, X; Wu, C. *Macromolecules* **1997**, *30*, 7921-7926.

34. Otake, K.; Inomata, H.; Konno, M.; Saito, S. *Macromolecules* **1990**, *23*, 283-289.

35. Nagarsekar, A.; Crissman, J.; Crissman, M.; Ferrari, F.; Cappello, J.; Ghandehari, H. *Biomacromolecules* **2003**, *4*, 602-607.

36. Yamaoka, T.; Tamura, T.; Seto, Y.; Tada, T.; Kunugi, S.; Tirrell, D. A. *Biomacromolecules* **2003**, *4*, 1680 –1685.

37. Park, T. G.; Hoffman, A. S. *Macromolecules* **1993**, *26*, 5045-5048.

# Chapter 7 Summary and Future Work for Liquid-Liquid Phase Transitions of Aqueous Polymer Solutions

## 7.1 Summary

Liquid-liquid phase transitions of aqueous polymer solutions provide a novel method to design hydrogel microspheres. In this thesis, hydrogel microspheres were developed from liquid-liquid phase transitions of polyelectrolyte complexes and thermally induced phase transitions of non-ionic amphiphilic copolymers. The mechanisms for the liquid-liquid phase transition were described using well-defined synthetic polymers. The resulting contributions are summarized as follows:

1. Amphiphilic copolymers based on maleic anhydride copolymers were prepared by grafting methoxy polyethylene glycol (MPEG) on the polymer backbones. The thermosensitivity and pH-sensitivity of fully MPEG grafted anhydride copolymers were studied. The phase transition behavior was interpreted on the basis of the concept of polymer-polymer and polymer-water interactions, including the cooperative effects of intra/intermolecular hydrogen bonding and hydrophobic interactions. Following the study of solution properties of completely MPEG-grafted maleic anhydride copolymers, analogous partially MPEG grafted poly(styrene-*alt*-maleic anhydride) copolymers were used to prepare hydrogel microspheres by complex coacervation with pDADMAC and subsequent crosslinking with polyamines. The results showed that the two-stage procedures, coacervation followed by crosslinking reaction, were efficient for preparing hydrogel microspheres. Directly complexing the partially MPEG grafted poly(styrene-

*alt*-maleic anhydride) with charged polyamines resulted not in coacervate microspheres, but in gel precipitates.

2. Aqueous solutions of poly(*N,N*-dimethacrylamide-*co*-glycidyl methacrylate) (DMA-*co*-GMA) and poly(*N,N*-dimethylacrylamide-*co*-allyl methacrylate) (DMA-*co*-AMA) copolymers were shown to undergo liquid-liquid phase separation upon heating. The initially formed coacervate microdroplets could be crosslinked to form hydrogel microspheres. DMA-*co*-GMA hydrogel microspheres lost their thermo-responsive properties after the coacervates were crosslinked by polyamines, which was attributed to the increase of hydrophilicity during the crosslinking process. In contrast, DMA-*co*-AMA hydrogel microspheres were thermosensitive since the coacervate droplets were crosslinked by a radical reaction without changing the hydrophilic/hydrophobic balance of the polymer. The resulting hydrogel microspheres may find applications in protein separation and protein encapsulation.

3. Well-defined poly(*N,N*-dimethylacrylamide) homopolymer and poly(*N,N*-dimethylacrylamide-*co*-*N*-phenylacrylamide) (DMA-*co*-PhAm) copolymers were synthesized by atom transfer radical polymerization (ATRP) using hydrogen-bonding solvents – methanol and methanol/water mixtures as the reaction media. The efficiency of the thermally induced liquid-liquid phase transition was studied with the well-defined DMA-*co*-PhAm copolymers. The temperature-dependent efficiency of phase transition indicated that the thermally induced liquid-liquid phase transition was a continuous equilibrium process. The polymer was only partially dehydrated upon reaching the critical temperature, and the solubility of polymers in the equilibrium phase decreased

with increasing temperatures, leading to more polymer driven from the equilibrium phase to the coacervate phase.

## 7.2 Future Work

### 7.2.1 ATRP of Poly(*N*-isopropylacrylamide) in H-bonding Solvents

Due to the difficulty in obtaining thermo-responsive polymers with narrow molecular weight distributions, the dependence of the lower critical solution temperature on the molecular weight of polymers and end groups has not been systematically studied. During the study of thermally induced phase transitions of DMA-*co*-PhAm solutions, it was found that the phase transition temperatures first increased slightly with increasing molecular weights of polymers, and then became constant. This phenomenon could also be due to the small composition drifts of the copolymers. In order to further address this issue, well-defined poly(*N*-isopropylacrylamide) (pNIPAM) homopolymers will be prepared by ATRP and the effect of molecular weights and end groups on the phase transition temperature will be studied.

Up to now, NIPAM has only been successfully polymerized in a controlled/living manner by the reversible addition-fragmentation transfer polymerization (RAFT).[1-3] ATRP has been used to graft pNIPAM on latex particles.[4] The definitive proof of living/controlled ATRP for NIPAM is still missing in the literature despite a recent communication reporting some success in the preparation of pNIPAM with very low molecular weights.[5] Our research has shown that H-bonding solvents such as alcohols are suitable for the living/controlled ATRP of DMA. Similar approaches will be extended to

the ATRP of NIPAM. With the successful ATRP of NIPAM, the influence of molecular weight, polymer architecture (comb, star, dendritic) and polymer composition (random, gradient, blocky) on the thermoresponsive properties of polymers can be explored.

### 7.2.2 Designing Coavervate Hydrogel Microspheres for Protein Separation and Purification with Aqueous Chromatography

Due to the high water content in both separated phases, the liquid-liquid phase transitions of aqueous polymer solutions have been widely studied in protein separation and protein purification. The current bottleneck of this application in industry is the separation of targeted proteins from the phase-forming polymer, and the recycling of the polymer. Such problems can likely be addressed by converting the polymer into hydrogels, or further into hydrogel microspheres with large surfaces. However, the results from poly(*N,N*-dimethylacrylamide-*co*-allyl methacrylate) coacervate microspheres indicated that the thermal response of directly crosslinked coacervate microspheres was limited. The crosslinking limits the swelling-deswelling properties of hydrogel microspheres and would hence reduce the efficiency of protein binding and release. This can be improved by grafting polymers that show thermally induced liquid-liquid phase transition, from the surface of microspheres. Extensive studies have been carried out on the modification of chromatography resins with thermoresponsive polymers for biomaterial separations.[6]

The linear polymer chains tethered on the microsphere surfaces should have similar thermo-responsive properties as polymer chains in solutions. The modified

microspheres can then be used for protein separations and purifications in bulk or in aqueous chromatography.

Hydrophilic silica microspheres or glass beads, which have been extensively applied in aqueous chromatography, can be selected as the microsphere substrates. The ATRP of DMA copolymer developed above can be further extended to grafting DMA copolymers with precise control of chain length and functionality on the microspheres. The thermally induced liquid-liquid phase transition of the grafted polymer chains on the particle surface will also provide interesting interfacial properties.

**References**


1. Ganachaud, F.; Monteiro, M. J.; Gilbert, R. G.; Dourges, M. A.; Thang, S. H.; Rizzardo, E. *Macromolecules* **2000**, *33*, 6738-6745.
2. Schilli, C.; Lazendorfer, M. G.; Müller, A. H. E. *Macromolecules* **2002**, *35*, 6819-6827.
3. Ray, B.; Isobe, Y.; Matsumoto, K.; Habaue, S.; Okamoto, Y.; Kamigaito, M.; Sawamoto, M. *Macromolecules* **2004**, *37*, 1702-1710.
4. Kizhakkedathu, J. N.; Norris-Jones, R.; Brooks, D. E. *Macromolecules* **2004**, *37*, 734-743.
5. Giancarlo, M; Laura, G; Vittorio, C. *Macromol. Rapid Commun.* **2004**, *25*, 559 – 564.
6. Kikuchi, A.; Okano, T. *Prog. Polym. Sci.* **2002**, *27*, 1165-1193.